Dendrimeric Light-Harvesting System

KULJIT KAUR DYAL

PhD Thesis

May 2015

SUPERVISOR

Dr L J TWYMAN

Dendrimeric Light-harvesting system

Kuljit Kaur Dyal

A thesis submitted for the degree of Doctor of Philosophy

Department of Chemistry, The University of Sheffield
Sheffield, S3 7HF
England

For my family

Acknowledgements

Firstly, I would like to express my deepest gratitude to my supervisor Dr Lance Twyman for the guidance, encouragement and advice, he has provided throughout my research.

Special thanks also go to Susan Bradshaw for the help with NMR, Melanie Hannah for all the technical help, Harry Adam for the help with X-Ray, Simon Thorpe for Mass Spectroscopy and Denise Richard, Louise Brown-Leng, Pete Farran, Nick Smith for their help in orders, chemical collections in the department. In addition to this, I would like to extend my thanks to each and every member of Twyman group and all the members of F-floor, who gave me comfortable environment throughout my research. I would also like to convey my sincere appreciation to my friends Dr Georgia Mann, Devanshi Singh, Alaa Kadhim, and Greg Clixby. I would also like to acknowledge Dawn Shambley for reading my thesis with patience.

Finally, I would like to acknowledge with gratitude, the support and love of my family- mum, dad and specially my mother-in-law, father-in-law, my sister-in-law Samrita Mahal, my husband and my son Baltej Singh Dyal. Thank you for everything and I am so blessed to have such a lovely, encouraging and supportive family. They all kept me going and this thesis would not have been possible without them.

Abbreviations

ATP……....Adenosine triphosohate

A……..Acceptor

^{13}C-NMR……Carbon Nuclear Magnetic Resonance Spectroscopy

DNA……....Deoxyribonucleic Acid

DCM……Dichloromethane

D……..Donor

d-$CDCl_3$……...Deuterated chloroform

D_2O……..Deuterated Deuterium Oxide

EDA…….Ethylene diamine

GPC…….Gel Permeation Chromatography

G……..Generation

Gd……Gadolinium

^{1}H-NMR……...Proton Nuclear Magnetic Resonance Spectroscopy

IR……..Infrared Spectroscopy

LHS……...Light-Harvesting system

MALDI-TOF-MS……Matrix-assisted laser desorption ionization - time of flight – mass spectrometer

PAMAM……..Poly(amido amine)

ppm……..Parts per million

RC……Reaction centre

$SnPc(Cl)_2$……Tin(IV) phthalocyanine dichloride

TPP……..Tetraphenylporphyrin

$TPPSn(Cl)_2$……Tin(IV) tetraphenylporphyrin dichloride

$TPPSn(OH)_2$……..Tin(IV) tetraphenylporphyrin dihydroxy

TLC……....Thin layer chromatography

THF…….Tetrahydrofuran

UV/Vis……Ultraviolet/visible light Spectrophotometry

NMR Abbreviations

Ar……..aryl

br…….broad

bm…….broad multiplest

dd……..doublet of doublets

d……doublet

dt……..doublet of triplets

dm……doublet of multiplets

m……..multiplet

mm……..multiplet of multiple

m-……meta

o-……..ortho

p-……..para

s……singlet

s……sharpe

t……..triplet

tt……..triplet of triplets

w……..weak

Table of Contents

Chapter 1- Introduction……10
1.1 Dendritic polymers...……..11
1.1.1 Dendrimeric structure and topology……14
1.1.2 Dendrimeric polymer properties……..15
1.1.3 Synthesis of dendrimers……...17
1.2 Applications of dendrimers……19
1.3 Light harvesting dendritic models……..23
1.3.1 Natural light-harvesting systems……23
1.3.2 Artificial dendrimeric light-harvesting systems……..25
1.3.2.1 Dendrimers as scaffold in light-harvesting systems……27
1.3.2.2 Dendrimers as chromophore in light-harvesting system……28
1.3.2.3 Electron transfer in dendrimeric light-harvesting system……...32
1.3.2.4 Energy transfer in the self-assembled host-guest light-harvesting system……..34

Chapter-2 Aims……37
2.1 Selection of the polymer scaffold……..39
2.2 Selection of chromophores as donor and acceptor……40
2.3 Self-assembly of dendron and chromophores……....40

Chapter-3 Results and discussion……44
3.1 Dendritic macromolecule as scaffold…….....45
3.1.1 Synthesis of ester terminal dendrons……48
3.1.1.1 Characterisation and purification of half generation dendrons……..48
3.1.2 Synthesis of amine terminated dendrons……...50
3.1.2.1 Characterisation and purification of amine terminated dendrons…...51
3.2 Chromophores (acceptor and donor unit)……...53
3.2.1 Synthesis of tetraphenylporphyrin (TPP)……..55
3.2.2 Synthesis of tin(IV) (5,10,15,20-tetraphenylporphyrin) dihydroxy (acceptor unit)……..58
3.2.3 Synthesis of tin(IV)(5,10,15,20-tetraphenylporphyrin) diacetoxy……60
3.2.4 Synthesis of tin(IV)(5,10,15,20-tetraphenylporphyrin) dibenzoxy……62

3.3 Self-assembly of dendrons with the acceptor unit…….64
3.3.1 Self-assembly of dendron G-0.5 with tin(IV) (5,10,15,20-tetraphenylporphyrin) dihydroxy…….66
3.4 Self-assembly of dendron with donor unit…….70
3.4.1 Synthesis of zinc tetraphenylporphyrin (ZnTPP)……..72
3.4.2 Binding interactions between primary and tertiary amines with ZnTPP using UV/Vis Spectroscopy…...……74
3.4.3 UV titrations for half and whole generation dendrons……...79
3.5 Self-assembly between acceptor, dendron and donor unit…….81
3.6 Synthesis of zinc porphyrin dimer……..84
3.6.1 Synthesis of nitro tetraphenylporphyrin…….....86
3.6.2 Reduction of nitro tetraphenylporphyrin……....87
3.6.3 Synthesis of porphyrin dimer…….88
3.6.4 Synthesis of zinc porphyrin dimer……..90
3.6.5 Binding of zinc porphyrin dimer with dendrons……....90
3.7 Synthesis of flexible zinc porphyrin dimer (ZnFPD)…….93
3.8 Synthesis of tin phthalocyanine (acceptor unit)…….97
3.9 Self-assembly between tin(IV) phthalocyanine dichloride and ester terminated dendrons……...99
3.9.1 Self-assembly of tin(IV) phthalocyanine dichloride with G-0.5 dendron...100
3.9.2 Self-assembly of tin(IV) phthalocyanine dichloride, dendrons and acceptor unit……..103
3.10 Light harvesting experiments…….105
3.10.1 Light harvesting studies……...106
3.10.2 Quantum yield calculations……..109

Chapter- 4 Conclusion and future work…….114

Chapter-5 Experimental section…….118
5.1 General Experimental Conditions……119
5.2 Synthesis Procedure…….121
Chapter-6 References…….152
Appendix……158

Abstract

Energy is an important term in our daily life. The modern economy is mostly dependent upon non-renewable energy sources such as fossil fuels. However, dependence on fossil fuels generating some severe issues related to energy security and greenhouse gas emissions. This fossil fuel dependence could be avoided by designing light-harvesting systems. Therefore, this thesis describes the synthesis of dendrimeric light-harvesting model systems, which can efficiently transfer light energy from each of its donor molecules on the surface, to a single acceptor unit. In our system, dendron acted as a scaffold to hold the acceptor and the donor unit at a specific distance.

The first part of this thesis describes the synthesis of dendrons up to G-4.0 and different chromophores. Preliminary studies towards light-harvesting was carried out using tin(IV) porphyrin as an acceptor and zinc porphyrin as donor units. The ester terminated dendrons were chosen for self-assembly studies, as these dendrons showed stronger interactions than amine terminated dendrons. The successful self-assembly between an acceptor ($SnTPP(OH)_2$), ZnTPP and ester terminated dendrons was achieved. However, the light-harvesting could not be achieved for this acceptor-donor pair because of the similar absorption and emission spectrum of this pair. Then, a different acceptor $SnPc(Cl)_2$ (tin(IV) phthalocyanine dichloride) was chosen. To achieve light-harvesting at a lower concentration range ZnTPP donor unit was not found good enough. Therefore, it was decided to use zinc porphyrin dimer, which was synthesised using mono-nitrated tetraphenylporphyrin. The found binding constant K_a results were $9x10^3$ M^{-1}(G-1.5), $15x10^3$ M^{-1} (G-2.5), $16x10^3$ M^{-1} (G-3.5). These results once again were not good enough to perform the light-harvesting test at lower concentrations range. Therefore, flexible zinc porphyrin dimer (ZnFPD) was synthesised and the found binding constant K_a results at concentration (10^{-5}-10^{-6} M) were $1.95x10^5$ M^{-1}(G-1.5), $1.28x10^5$ M^{-1} (G-2.5), $1.72x10^5$ M^{-1} (G-3.5) and were used to perform the LH studies. Finally a self-assembly was achieved using $SnPc(Cl)_2$, ester terminated dendrons and ZnFPD. The confirmation of the self-assembly was achieved using the ^1H NMR technique. After observing the successful self-assembly the light-harvesting test was performed for the synthesised dendritic light-harvesting models. The G-0.5 light-harvesting model showed the successful LH behaviour. However, the bigger generation dendron models were failed to show the LH behaviour. This behaviour was assumed due to the inter-quenching within the model systems through PET (photoinduced electron transfer) process via internal tertiary amines. To stop this inter-quenching TFA (10^{-4} M) solution was used for the protonation of the dendron internal tertiary amines. After the addition of TFA, the bigger generation dendrons showed successful LH behaviour. The calculated quantum yields for the LH complexes of different generation dendrons were 0.07, 0.05, 0.03 and 0.01.

Chapter 1

Introduction

Dendritic Polymers

The main purpose of this chapter is to supply the reader with the necessary information to understand the subject specific concept, employed in this area of research. This review is not an extensive account and for this the reader is directed to a number of recommended reviews in the literature.[1-6]

1.1 Dendritic polymers

In polymer chemistry, dendritic polymers are known as the fourth class of the major macromolecule family. This fascinating polymer class was introduced by Tomalia, Vogtle and Newkone. Tomalia synthesised the first class of a dendrimer family named Polyamidoamine (PAMAM) dendrimer.[7] PAMAM dendrimers are also known as starburst dendrimers. The term “starburst” is a trademark of the Dow chemical company. PAMAM dendrimer consists of alkyl-diamine core and tertiary amine branches. The discovery of PAMAM dendrimers fascinated polymer scientists, and as a result of this various new dendrimer families were constructed.[8-10] There are a variety of different types of dendritic polymers; random hyperbranched polymers, dendrigrafted polymers, dendrons and dendrimers. Major macromolecular architectures are shown in **(Figure 1.1)**. This chapter is mainly focusing on the dendrimers, as they are used in upcoming chapters.

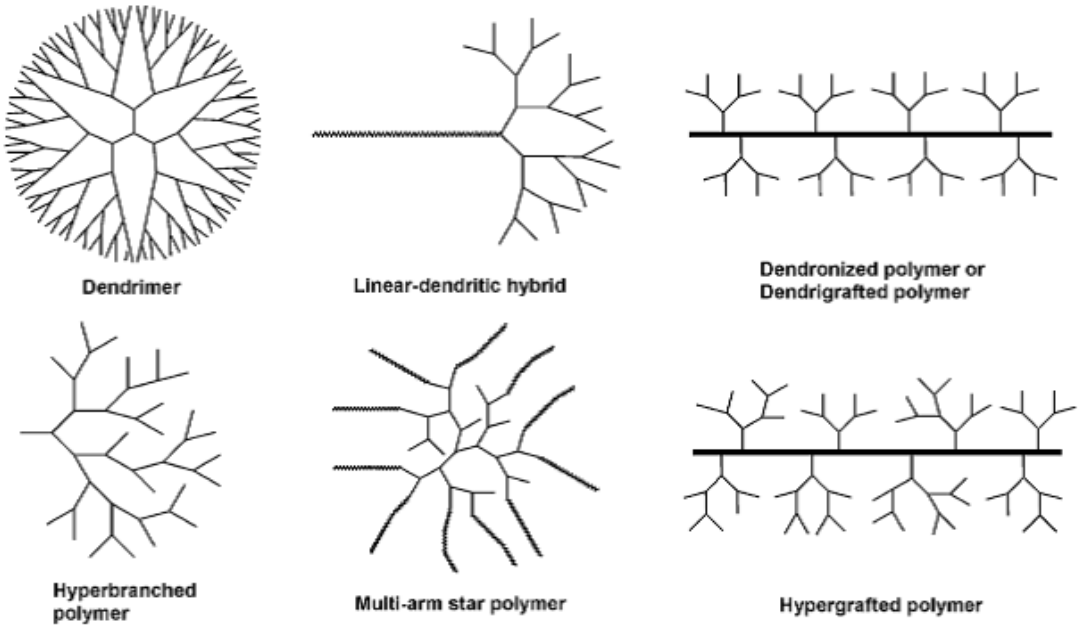

Figure 1.1 Figure illustrating the major macromolecular classes. (Gao, C.; Yan, D.; ***Polym.Sci***, 2004, 29,183)

There are two main types of dendritic architecture, dendrimeric and hyperbranched. These structures are distinguished by the branching units. Dendrimeric structures display perfect branching and layered growth, where as, hyperbranched polymers have imperfect branching and less well defined structure i.e. random growth. **Figure 1.2** shows structures of a dendrimer and a hyperbranched polymer. In addition, dendrimers exhibiting a randomly or perfectly branched structure and can either be constructed entirely from a monomer unit or be attached to a central core. For the perfectly branched dendrimeric polymers, there are two types of substructures which are classified as dendron and dendrimer respectively **(Figure 1.3)**.

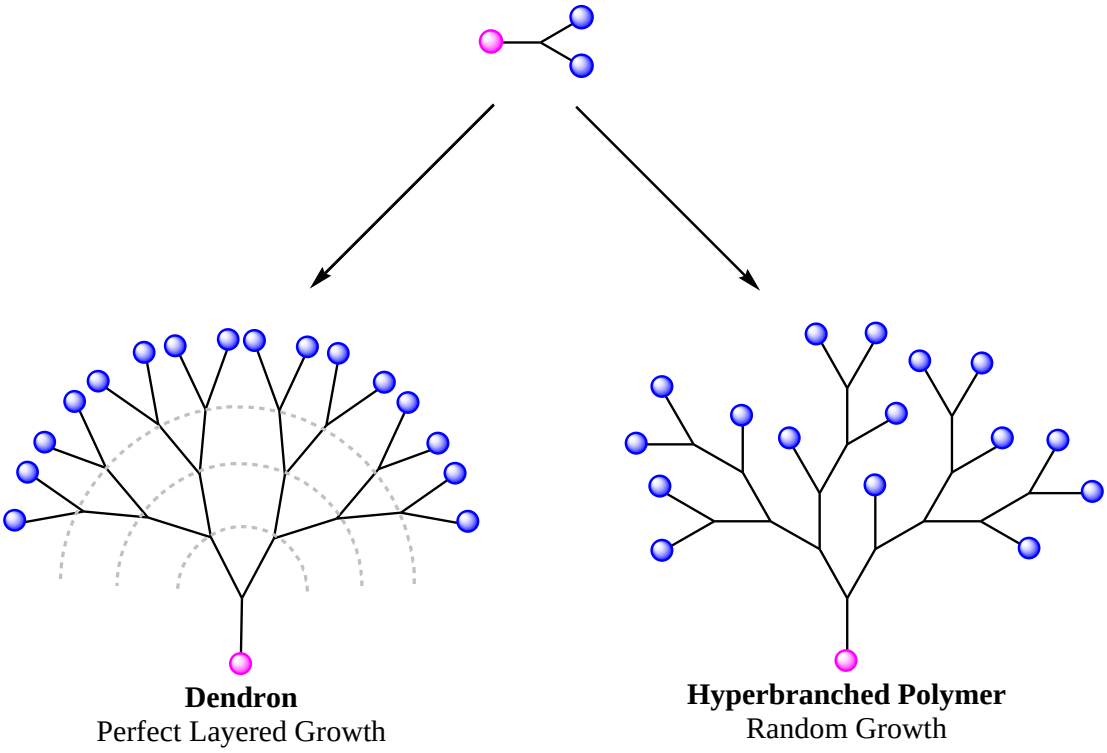

Figure 1.2- Figure representing the structures of a perfectly layered dendron and a hyperperbranched polymer.

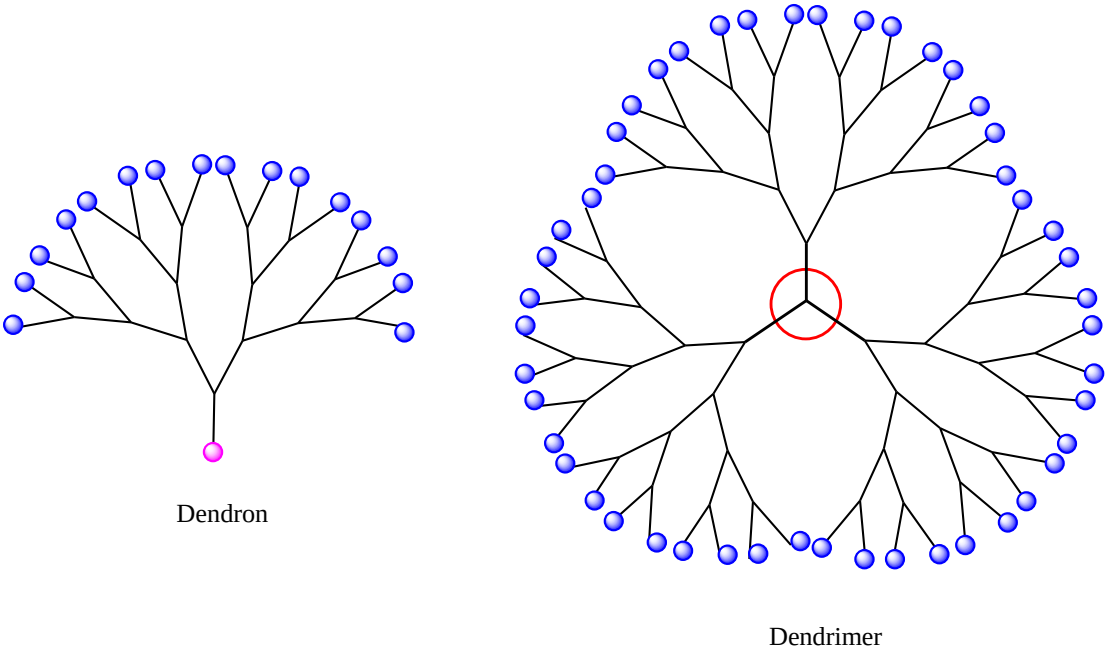

Figure 1.3- Schematic Representation of a dendron and a dendrimer.

1.1.1 Dendrimeric structure and topology

The word dendrimer came from the Greek word ***"dendron"*** which means tree or branch and ***"meros"*** means part, therefore a dendrimer contains a tree - like structure which contains lots of branches. Therefore, dendrimer is a macromolecule with branches, spherically symmetric around the core and prepared as a discrete, highly pure, monodispersed molecule. Dendrimers are also known as starburst, cascade or arborols but the word dendrimer is more prominent. The globular structure of dendrimer is shown in **Figure 1.4** where G1, G2…… are representing generation numbers. Dendrimers comprise of a series of regular branching monomer throughout their structure, surrounding an inner core. The size, shape and morphology of a dendrimer are determined by the branching, surface functional groups i.e. terminal units and also by the number of layers surrounding the core. Dendrimers are composed of ABn monomer units, where every layer of the repeat units generated with each stepwise reaction, which gave rise to the new "generation" of branching units. These units are inter-reliant of each other providing a dendrimer with its exclusive molecular shape.[11] The value of n determines the amount of terminal groups on the periphery of the molecule; if n=2 the number of terminal groups will double with each increasing generation and if n=3 then the number of the peripheral groups will triple.[12] As a general rule, low generation dendrimers form more open structures and a higher molecular weight i.e. a bigger generation dendrimer leads to globular and denser architecture. Bigger dendrimers form more closed structure with the increased branching due to the crowding.[13] Dendrimeric growth is mathematically restricted; therefore, at a specific generation there is a steric limit to growth which is known as De Gennes Packing.[14] Dendrimers also contain some special properties which differentiate them from normal polymers such as low viscosities and high solubility at high molecular weight. The above properties are responsible for diverse applications of dendrimer in the different areas such as in light harvesting,[15] biomimetics,[16-18] mechanical property modifiers,[19,20] non-linear optics,[21] nanocomposites[22,23] drug and gene delivery[24] etc.

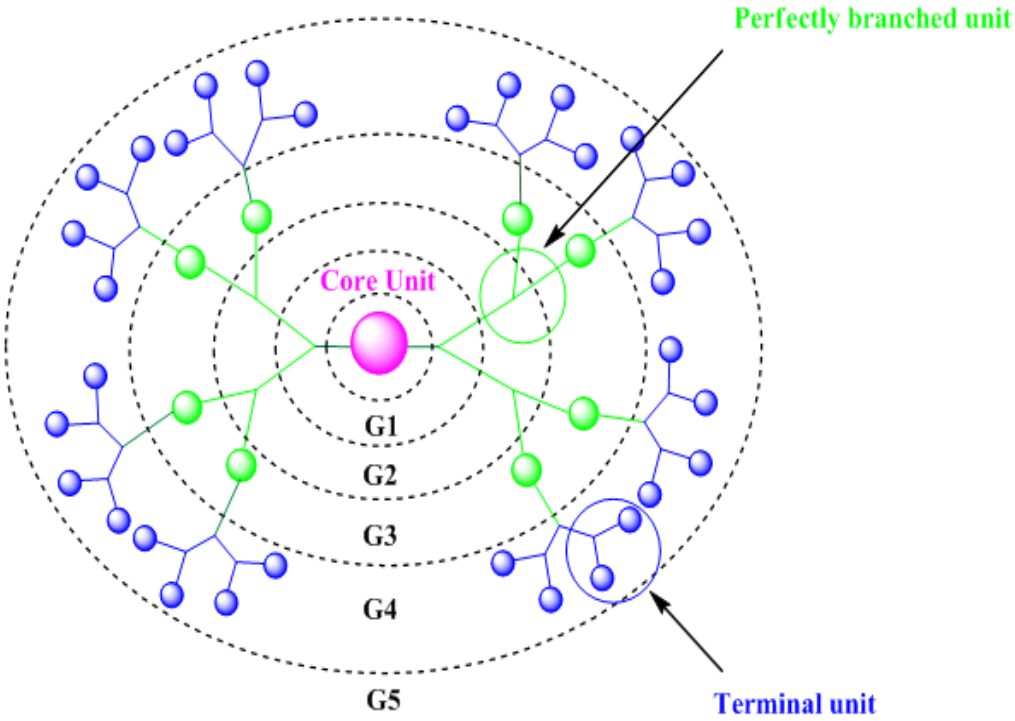

Figure 1.4 - Figure representing the structural components of a dendrimer.

1.1.2 Dendrimeric polymer properties

Dendrimers are monodisperse macromolecules unlike linear polymers. The size, shape and molecular mass of dendrimers can be controlled during their synthesis, which distinguishes them from an analogous linear polymer, which has also led to the various noted differences in their physical and chemical properties.[25] These highly branched macromolecules exhibit contrasting behaviour to the linear polymers in solution.[26] In solution, linear chains exist as flexible coils; where as the dendrimer form a tightly packed ball. This has a great impact on their rheological properties. In linear polymers viscosity of linear polymers increases as the molecular weight increases, this is due to the increase in chain entanglement. On the other side, dendritic polymers show lower viscosity, when the molecular weight of the dendrimer increases their intrinsic viscosity goes through a maximum at the fourth generation and then begins to decline. This is likely to be because of the way in which dendrimer shape changes with generation i.e. the lower generations adopt a more open planar–elliptical shape with transition to a more compact spherical shape for higher generations.[27] The relationship between the molecular weight and intrinsic viscosity can be illustrated by the Mark-Houwink-Sakurada equation:

$$\eta = kM^{\alpha} \qquad \text{---------- (1)}$$

Where η represents intrinsic viscosity, M is the molecular weight and k and α are constants, which are particular for the polymer-solvent system in question. In general, values of α fall within the range of 0.5 and 1.0 for linear polymers. The dendritic polymers have been reported to have values of α lower than the 0.5, providing evidence for the globular morphology they adopt in the solution.[28]

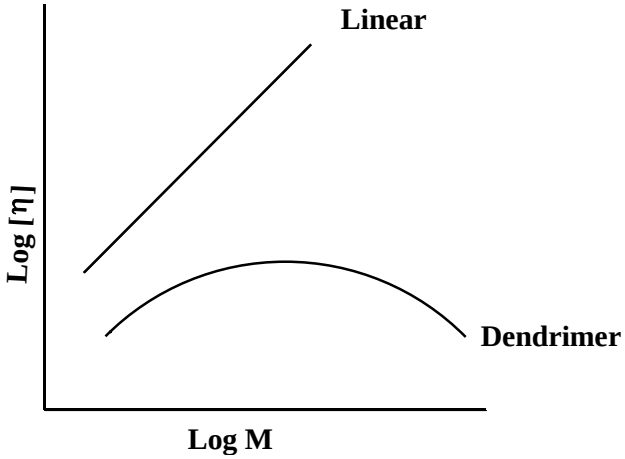

Figure 1.5 - Graphical representation of log[η] (intrinsic viscosity) against logM (molecular weight) of the polymer.

Compared to the linear polymer, dendritic macromolecules possess smaller hydrodynamic volume. The dendrimeric polymers also showed high solubility and reactivity due to the presence of many chain end groups.[29]

Dendrimeric solubility is strongly influenced by the nature of the surface groups. Dendrimers with hydrophilic end groups are soluble in the polar solvents and hydrophobic end groups soluble in the non-polar solvents. The globular shape and the presence of internal cavities, which can encapsulate guest molecules, make them distinctive from linear polymers. Dendrimer architecture produces a molecule with the large surface groups having very large surface area in relation to the volume (up to 1000 m^2/g).[27] The presence of large surface groups and intrinsic cavities in the

dendrimer make them highly soluble, reactive and gives higher binding trends with other molecules.

1.1.3 Synthesis of Dendrimers

Dendrimers are synthesised by fully controlled step-by-step methods. There are two main methods to synthesise dendrimers:- ***convergent and divergent method***.[30]

(1) Divergent Method

In divergent method, the dendrimer are built outwards from the multifunctional core by forming layers. These layers are known as generations. The core reacts with the monomer molecules containing one reactive site. For the formation of second generation dendrimer, the periphery functional groups of the molecule are activated for the reaction with another monomer as illustrated in **(Figure 1.6)**.

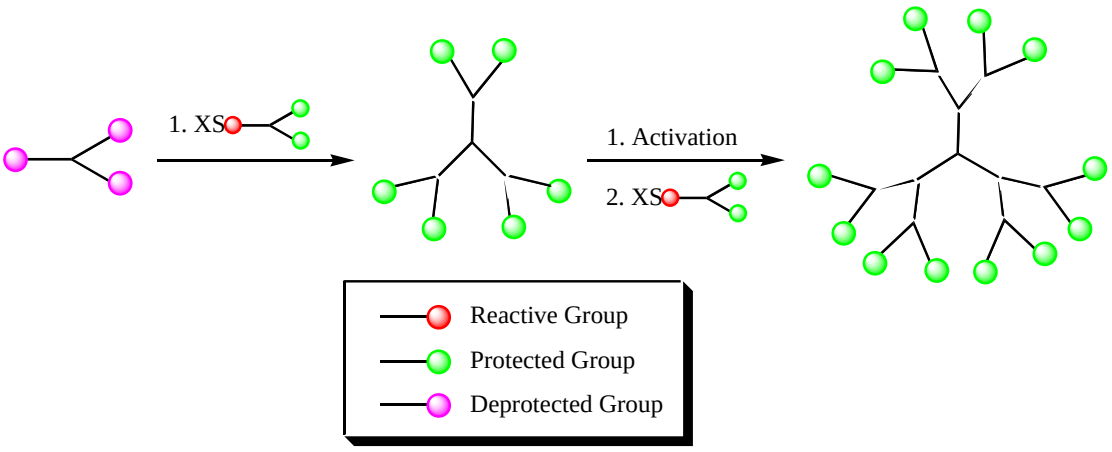

Figure 1.6 - Divergent method for the dendrimer synthesis**.**

Vogtle and his co-workers used this method for the synthesis of the first dendrimer. The divergent method is a very simple and successful method for the production of large quantities of dendrimers, however, this method also has some drawbacks which are related to the higher generation dendrimers. When the dendrimer size increases, the number of periphery functional groups also increases, which lead to a considerable number of side reactions with by-products containing size, mass and

properties very close to the desired dendrimer. These side reactions sometimes give the structural defect which causes the difficulties in the purification of the dendrimers as well. Hence to get the desired dendrimer result the appropriate reagents are required in large quantities.

(2) Convergent Method

This method was reported by Frechet and Hawker in 1990.[31] This method uses the symmetrical nature of these molecules in an advantageous way. In this method dendrimers are built inwards starting from the end groups in a stepwise manner to the focal point and gradually working inwards results in the formation of a reactive dendron. In order to create a globular dendritic architecture, several dendrons are further reacted with a polyfunctional core molecule.[18] A schematic representation of convergent method is illustrated in **(Figure 1.7)**. Therefore the convergent method deviates from the divergent approach, as the core is incorporated to the macromolecule in the ultimate reaction step.[75]

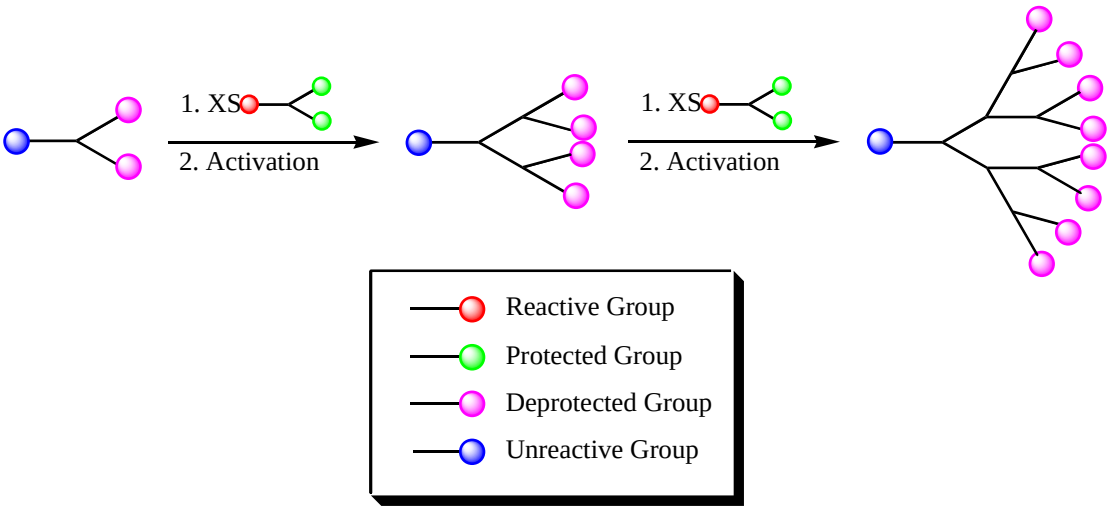

Figure 1.7 - Convergent method for the synthesis of dendrimer**.**

The advantage of the convergent method over the divergent method is that this method involves two reactions simultaneously therefore the chances of formation of by-products are reduced and also the mass difference between any by-product and desired product is quite large, which makes the separation easy. However, this method has certain drawbacks such as the formation of higher generation dendrimers.

The functional groups at the focal point becomes masked by growing the dendrimer, thus this steric crowding can decrease its reactivity. The convergent method also suffers from low yields in the synthesis of higher dendrimers.

1.2 APPLICATIONS OF DENDRIMERS

Dendrimer chemistry is an expanding area of modern science. In recent years dendrimers have been used in the areas of science; materials, supramolecular chemistry and in surface sciences. The use of dendrimers in different fields of science is due to the defined molecular structure of the dendrimer, which contains very high numbers of the functional groups on the surface, their ability to bind guest molecules within the branches and the special encapsulating microenvironment at the dendrimer core as shown in **(Figure 1.8)**.[30]

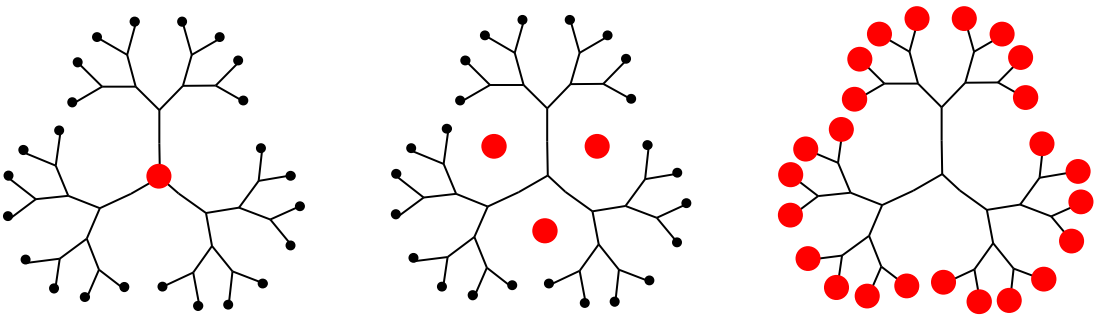

Figure 1.8 - Different binding sites of dendrimer structures.

1. Dendritic sensors

Dendritic sensors have been designed to detect organic and inorganic species. Balzani et al. examined the fourth generation poly(propylene amine) dendritic sensor with 30 aliphatic amine units in the interior and 32 densyl groups on the surface. This dendrimer showed strong fluorescence when Co^{2+} ion was incorporated into dendrimer.[32] Similarly, Sanki and co-workers synthesised a dendritic sensor to detect organic molecules, which contains eight boronic groups and anthracene groups as periphery.[33]

2. Medical Applications

Dendrimers are widely used in the medical field as vehicles for drug delivery inside the body and also in Magnetic Resonance Imaging (MRI). Fernandez and co-workers formed a targeted drug delivery system by attaching a dendrimer with saccaride groups on the surface to the rim of β-cyclodextrin. The modified cyclodextrin show high binding ability in Conacanavalin A lectin.[30,34] MRI is a very powerful method in medical diagnostics for creating an image of "soft" tissue in the blood vessels, by using contrast agents of Gd^{3+} ions. The complexes of Gd^{3+} ion such as $[Gd(DTPA)]^{2-}$, $[Gd(DOTA)]^{-}$, [Gd(HP-do3a)] are usually used as contrast agents in the clinical use.[30,34] The main limitations of low molecular weight Gd^{3+} chelates is that they diffuse very fast in the extracellular matrix and they rapidly eliminate from blood vessels. The dendritic complexes of Gd^{3+} with high molecular weight containing high numbers of Gd^{3+} ions at the surfaces sites, has been found more useful than low molecular weight chelates, which showed longer lifetime in blood vessels after injection and also showed the high quality tissue imaging by accelerating the proton relaxation. [34]

Dendrimers have also been used as non-viral gene transfer agents for targeting genes to selected parts of the body.[30] Dendrimers such as polyamidoamine (PAMAM) and poly(propyleneimine) (PPI) containing amine groups on the surfaces, are protonated under physiological conditions. These polycations attracted polyanionic DNA by using electrostatic interactions, which showed dendrimer potential as non-viral gene transferring agents.[34] The higher generation dendrimers were found more useful as the gene transfer agents from different studies. Dendrimers have also been used in Boron neutron capture therapy (BNCT), which is used for treatment of cancer. BNCT theory is based on the $^{10}B(n,\alpha)^{7}Li^{3+}$ reaction. In this therapy the dendrimer complexes with boron atoms is delivered to tumour tissue, then highly energetic α and $^{7}Li^{3+}$ ions are produced by neutrons which help to damage the tumour cells.[34] Dendrimers have also got some antimicrobial properties such as quaternary ammonium compound (QACs) used as disinfectants.

3. Dendritic Catalysts

Dendrimers with high solubility and high numbers of surface functional groups make them useful as catalytic supporters. There are two ways to introduce catalysts, first by attaching catalytic groups on dendrimer surfaces and secondly, catalysts can be introduced to the central core of the dendrimer. These catalysts can easily be recycled and separated from the reaction product. The Van Koten group established the first catalytic dendrimer and these dendrimers can be used in addition reactions of polyhaloalkanes.[35] The dendritic catalyst showed advantageous characteristics of homogenous catalysts, as well as benefits inherent of heterogeneous catalysts. Hoveyde and co-workers reported recyclable dendrimeric ruthenium-based catalytic complex.[36]

4. Energy Transfer Funnels

In dendrimers, dendrimer branches act as energy transfer funnels by absorbing and transferring energy to the dendrimeric core, which showed dendrimer ability as light harvesting systems as shown in **(Figure 1.9)**. Moore and co-workers synthesised a perylene terminated dendrimer, which was found to transfer energy through branches to the core.[37] The energy transfer was analysed by using steady-state and time resolution fluorescence spectroscopy. The light harvesting in dendrimers increases with the generations by growing the number of energy collecting sites.[30] Similarly Frechet et al. reported a family of poly(aryl ether) dendrimers which was found to absorb and transfer energy very quickly.[38]

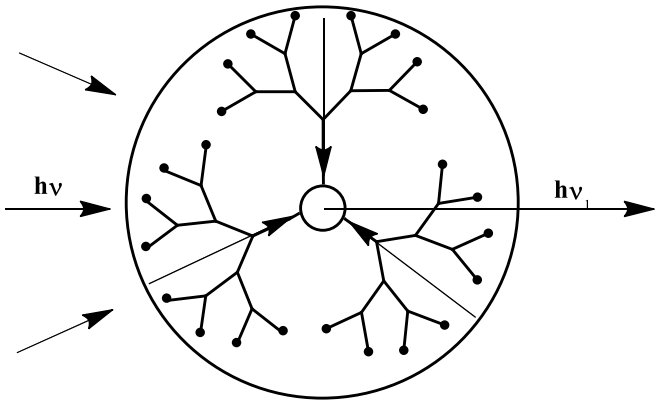

Figure 1.9 - Represents dendrimeric light-harvesting system.

5. Other Applications

Dendrimer films are used as anticorrosive coating agents on metal surfaces.[39] Dendrimers also contain the potential to form monolayers at the aqueous organic phase interface or gas liquid interface. Amphiphilic dendrimers form liquid membrane between water and in organic solvents.[40] Hydrophilic dendrimers with hydrophobic functional groups on the periphery form micelles in organic solvents. Dendrimer films are also used as purifiers.

1.3 Light harvesting dendrimeric models

To fulfil our daily energy needs, modern civilisation uses non-renewable energy resources such as fossil fuels. The consumption of fossil fuels is 500,000 times faster than its production. For future energy needs it is very necessary to invest in the renewable energy sources. For our planet the sun is the most abundant renewable energy resource. Each day the sun covers the earth with roughly 10^{22} J of solar radiation, providing society's yearly energy in just an hour.[68] Research into capturing and making use of solar energy has focused on studying natural photosynthesis. Photosynthesis "A natural light-harvesting system" is the most important chemical process on this planet. Through the harvesting of solar energy, organisms such as plants, algae and cyanobacteria provide all the biological energy for life on earth. This harvesting of energy happens under special arrangement of molecules that efficiently collect sunlight and transfers this energy. Understanding the way that these natural light-harvesting systems work is of profound interest to chemists. The challenge of understanding and replicating the light-harvesting systems of these natural organisms has led to the development of a wide range of artificial light-harvesting systems.

1.3.1 Natural light-harvesting systems

In natural light harvesting systems (photosynthesis) the Purple bacteria is the most studied group of bacteria. According to studies [41-45], in purple bacteria, photosynthesis occurs in the photosynthetic unit (PSU). In 1995, the first X-ray crystallography was performed in order to understand a bacterophotosynthetic system. Studies showed, this photosynthetic unit contains two pigment-protein complexes, the first one is the reaction centre (RC) and the second one is light-harvesting complex (LH). A schematic representation of the light-harvesting system in purple bacteria is shown in **(Figure 1.10)**. The centre of light-harvesting complex is a pair of chlorophyll molecules called reaction centre (RC), which play an important role in the process of photosynthesis. Immediately surrounding the RC is the LH1 complex, which is a ring shaped assembly of chlorophyll molecules and further away from RC is LH2, which has the same composition as LH1. The role of these LH complexes is to absorb and transfer the light-energy efficiently to the reaction centre, where light energy changes into chemical energy.

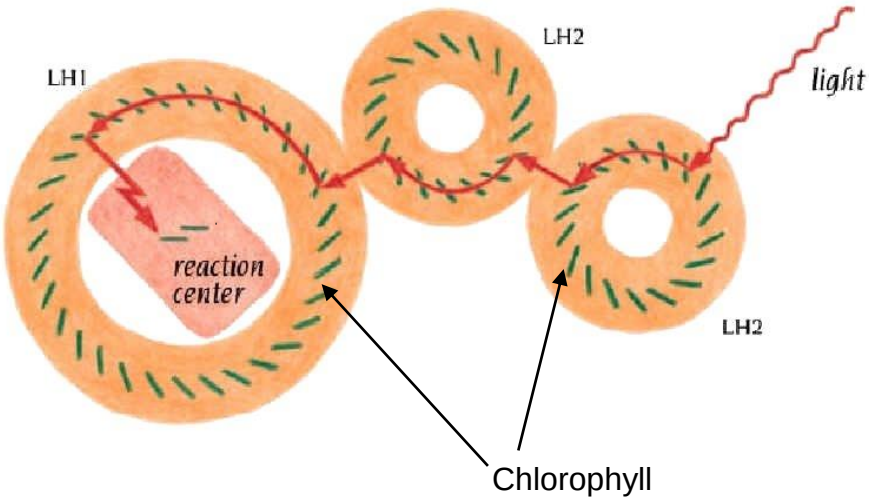

Figure 1.10 - Schematic representation of natural light-harvesting system (Branden & Tooze, *Introduction to Protein Structure*, 2nd ed, Garland publishing, 1999)

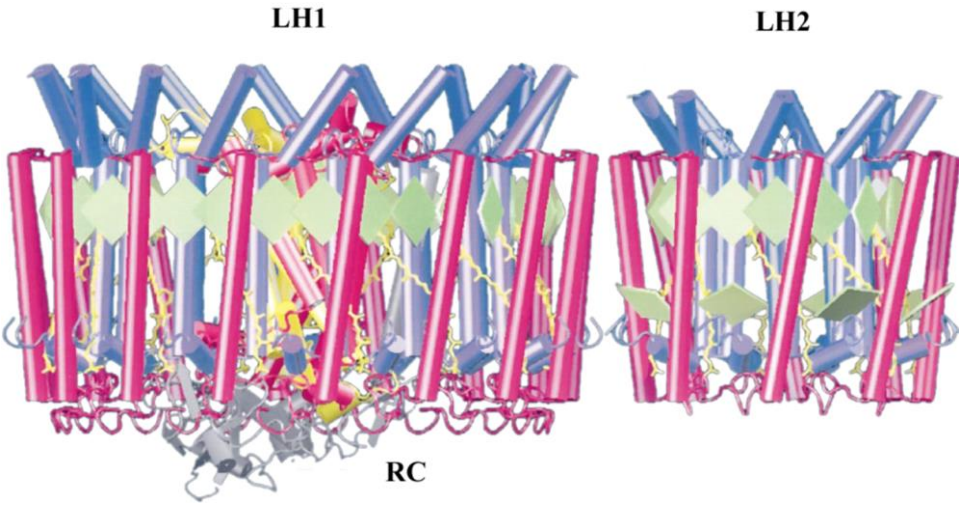

Figure 1.11 - Molecular models for the LH1-RC and LH2 light-harvesting complexes. Chlorophylls are shown as green squares.[46]

The size of the PSU is variable in many species, depending on the light intensity at which the the cells were grown. In purple bacteria, the light-harvesting complex LH2 complex is composed of B800 and B850. B800 contains nine bacterochlorophyll arranged in circular plannar form, whereas B850 has 18 bacterochlorophylls arranged in a barrel form perpendicular to B800. In LH1, 30 bacterochlorophylls are arranged similar to B850. The light-harvesting system of purple bacteria has regular arrangements of bacteriochlorophyll. The highly ordered arrangements of bacteriochlorophyll in these photosynthetic organisms is not, however, essential to

succesful light-harvesting. The photosynthetic system of cyanobacteria, as well as those found in higher plants, exhibit an apparently random arrangement of bacteriochlorophylls surrounding the reaction centre.[69-73] A variety of artificial light-harvesting antenna systems have been synthesised that mimic the energy transfer in purple bacteria using covalent and non-covalent approach.

1.3.2 Artificial dendrimeric light-harvesting systems

As explained above, natural light-harvesting systems have a large array of chlorophyll molecules surrounding a single reaction centre and channel the absorbed solar energy to the reaction centre. In artificial light-harvesting systems, dendrimers are the attractive candidates, having numerous chain ends all emanating from a single core. It is possible to synthesise the dendrimers containing a variety of chromophoric groups organised in the dimensions of time, energy and space so as to obtain the efficient light-harvesting device that can be useful for solar energy conversion.[47] Recently, studies of energy transfer in the dendrimers have been widely carried out by numerous groups.[47,48] The chromophores can be accurately located at the core, focal point, periphery or even at each branching point of the dendrimeric structure. In the dendrimeric light-harvesting system, the energy transfer process starts with the absorption and the transfer of the photon from light by chromophores which act as donor and acceptor. The observed non-radiative energy transfer proceeds by one of the following type of mechanism[49]:-

(1) Foster mechanism
(2) Dexter mechanism

(1) In Foster resonance, energy transfer proceeds by Columbic interactions. The Foster mechanism relatively show long-range dipole-dipole coupling and the overlapping between the donor and acceptor is not necessary. Thus the distance between the acceptor and donor could be in the range of 10-100 Å. Thus the foster mechanism is a long range mechanism. The rate of energy transfer depends on the square of interaction energy (U) of the two dipoles with a R^{-6} dependence.

$$K_{ET} = \frac{9000(\ln 10)k^2 \phi_D J}{128\pi^5 n 4 N \tau_D R^6 DA} \qquad \text{----------(2)}$$

Where R is the separation distance between the acceptor and donor, κ^2 is the orientation factor related to the orientation of donor and acceptor transition dipole moments, Φ_D is the donor quantum yield in the absence of acceptor, *J* is the overlap integral, n is the index of refraction of solvent, N is Avogadro's number, τ_D is the donor lifetime in the absence of acceptor.

(2) In the Dexter mechanism, energy transfer occurs by electron exchange interaction. Dexter mechanism is a short range distance which requires the overlapping between the wavelengths of acceptor and donor. According to Dexter, the rate of energy transfer by electron exchange exponentially depends upon the separation distance between the donor and the acceptor. For the Dexter mechanism, the distance between donor and acceptor should be less than 10 A°, therefore for energy transfer the orbital overlap is needed.

$$k_{ET} = Kj\exp(-2R_{DA}/L) \qquad \text{----------(3)}$$

Where K is related to specific orbital interactions, j is the normalised spectral overlap integral, R_{DA} is the donor acceptor separation relative to their Van der waal radii or Bohr radius, L depending on the system under consideration.

The structural properties of dendrimers can be easily controlled and vary greatly, which helps in the energy and electron transfer within the dendrimer. The properties of the dendrimer such as rigidity, conjugation, size and polarity all depend upon the branching units that are utilised in the energy transfer mechanisms and the electron transfer process. In dendrimers, peripheral groups could act as chromophores by absorbing light. The relatively short through space distance from the periphery to the core, due to back folding, make the high efficiency energy transfer possible.[50] Various research groups worked on artificial light-harvesting systems in which they used dendrimers as scaffolds, as chromophores etc. In the following section some examples of light-harvesting dendrimeric systems will be discussed.

In early 1990s Balzani and co-workers reported the first class of light-harvesting dendrimers.[51] These dendrimers have been synthesised up to third generation and

were based upon Ru^{II} and Os^{II} polypyridine complexes. Due to their ideal absorption, luminescence and redox properties, these kinds of metal-ligand dendrimers can absorb visible light and undergo energy transfer process within the dendritic backbones dominated by Dexter electron exchange mechanism. However, from these aforementioned dendrimers, a unidirectional energy gradient from the periphery to the centre, could not be obtained, this did not make them ideal natural light-harvesting complexes. After that organic chromophores such as pyrene and naphthalene were introduced to the periphery of polynuclear metallic dendrimers to establish a unidirectional energy funnel.[50,52]

1.3.2.1 Dendrimers as scaffold in light-harvesting systems

Non conjugated poly(aryl ester) dendrons function just as a scaffold, which holds acceptor at the core and donor chromophores at the periphery, together in a dendrimeric light-harvesting system. In this type of system where the dendrimer did not play an antenna role in the energy transfer process i.e. photochemically silent, energy transfer takes place by a through-space mechanism, in which orbital overlapping is not necessary.[50] This type of dendrimeric system was reported by the Frechet group, using a pair of laser dyes, coumarin 2 and coumarin 343. These dyes worked as donor/acceptor pair shown in **(Figure 1.12)**.[53,54] The reason for choosing these coumarin dyes, was their strong spectral overlap between the emission spectrum of donor and the absorption spectrum of acceptor, this is a crucial requirement for energy transfer. The dendrimeric backbone poly(benzyl ether) were constructed convergently. In this system the emission spectrum of donor overlaps with the absorption spectrum of donor and the absorption spectrum of dendrimer also matched the sum of absorption spectrum of model donor and acceptor which implies that the dendron just acts as a scaffold to hold donor and acceptor. Steady-state and time-resolved studies showed that the efficiency of energy transfer was quantitative for up to three generations, with only a slight drop for the fourth generation. The reason of decreases in the energy transfer for higher generation dendrimers could be the increasing distance between donor and acceptor.[49]

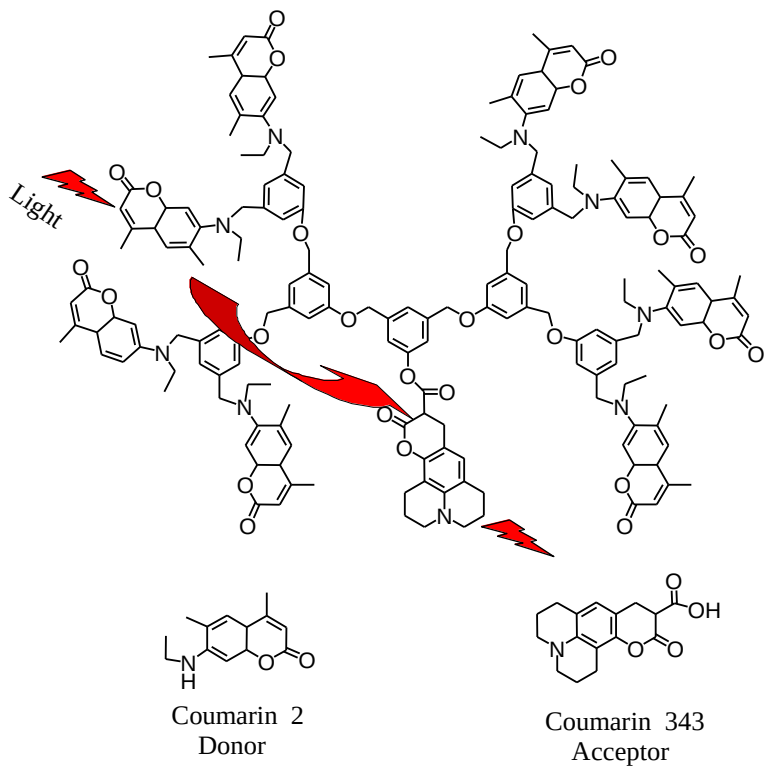

Figure 1.12 - Schematic representation of energy transfer between coumarin behaving as donor and acceptor units.

Several works have been carried out by replacing the energy acceptor by other chromophores.[55] Using this methodology, in which the dendrimer act as a scaffold, various light-harvesting systems were constructed using different dendrimers and donor/acceptor groups.[49]

1.3.2.2 Dendrimer as chromophore in light-harvesting system

In the light-harvesting system the dendrimer backbone can also act as a donor chromophore by facilitating the energy transfer. In 1994 Xu and Moore reported a dendrimeric system in which phenylacetylene chains were selected for this system.[56-58] They synthesised a phenylacetylene dendrimer up to generation six with perylene as a core, where peripheral phenylacetylene units acted as donor units and the perylene core as an acceptor unit as shown in **(Figure 1.13)**. The fluorescence quenching and emission spectrum was observed by UV light and results indicated that all the absorbed energy was channelled to the core. Moore and co-workers also reported a phenylacetylene dendrimer by arranging the dendrimeric branches with

decreasing energy gaps from periphery to centre by increasing the conjugation length as shown in **(Figure 1.14)**.[50,59] Peng and co-workers reported other types of unsymmetrical branched phenylacetylene dendrimers, which can harvest the energy from periphery to core acceptor with efficiency.[60] In this system the energy transfer efficiencies did not decrease with increasing generations, due to the π conjugation along the para-substituted phenylacetylene branch.

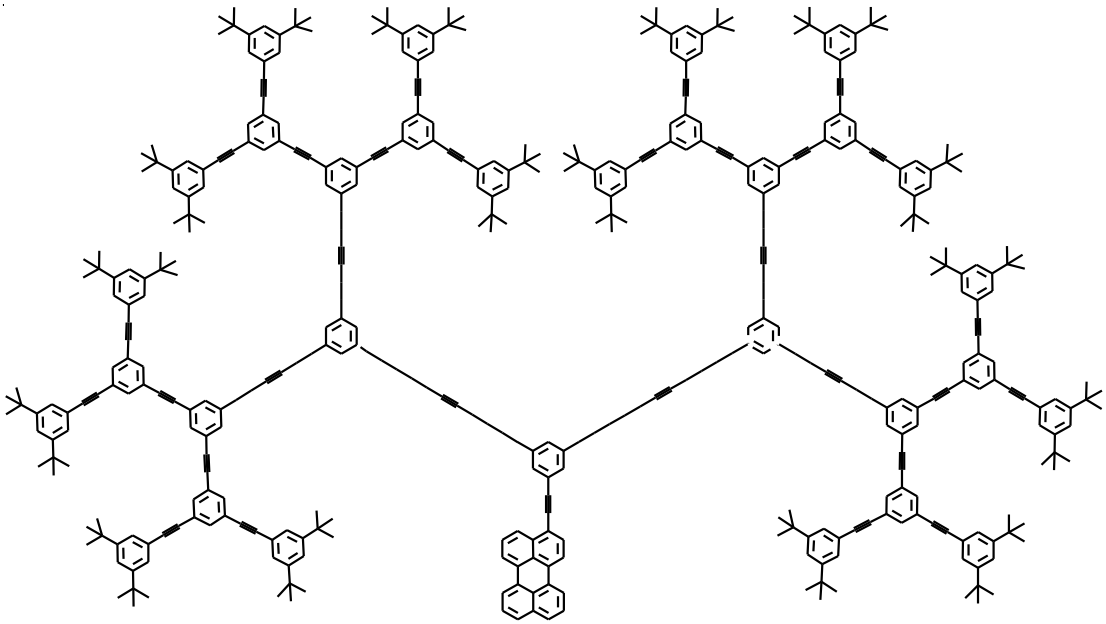

Figure 1.13 - Schematic representation of perylene-core phenylacetylene dendrimers.

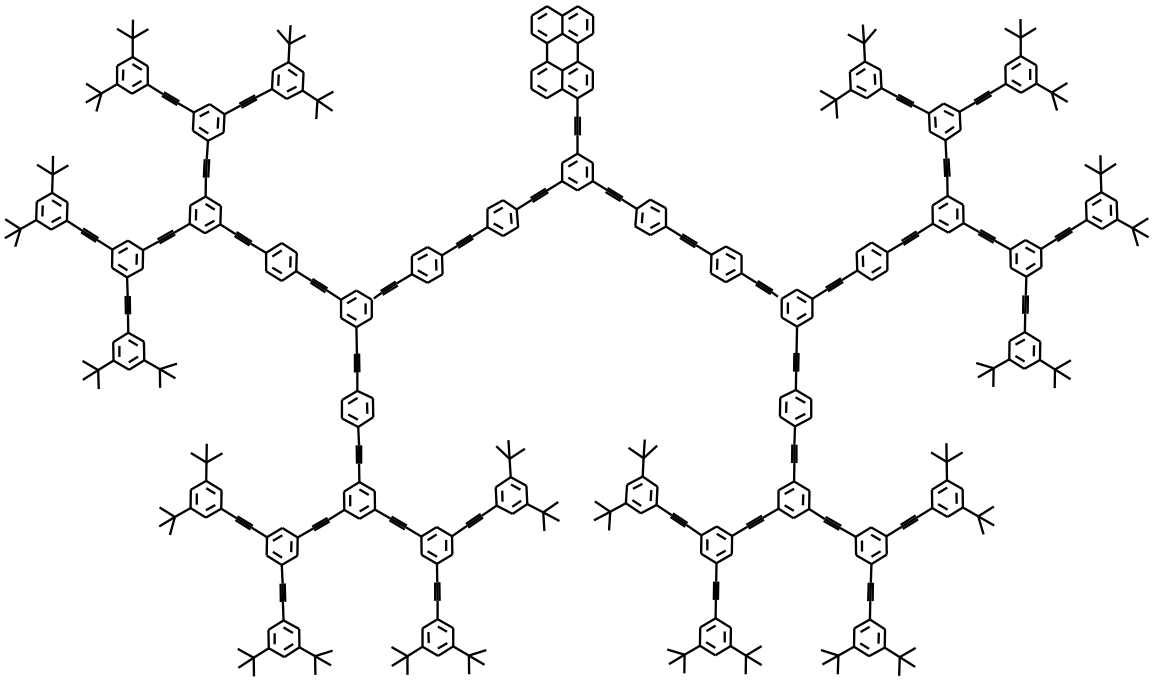

Figure 1.14 - Structure of perylene-core phenylacetylene dendrimers with an energy gradient.

Frechet and Kawa reported an organometallic self–assembled dendrimeric light-harvesting system, based upon ionic interactions between a cationic lanthanide core and anionic carboxylate groups present at the focal point of the convergent polyether dendron as shown in **(Figure 1.15)**.[61] In this type of self-assembled dendrimer lanthanides ions were shielded from each other by dendrons, applicable in fibre optical amplification. In this type of dendrimer antenna, a transfer of energy through dendrons to lanthanide core occurred by the Foster-type mechanism.

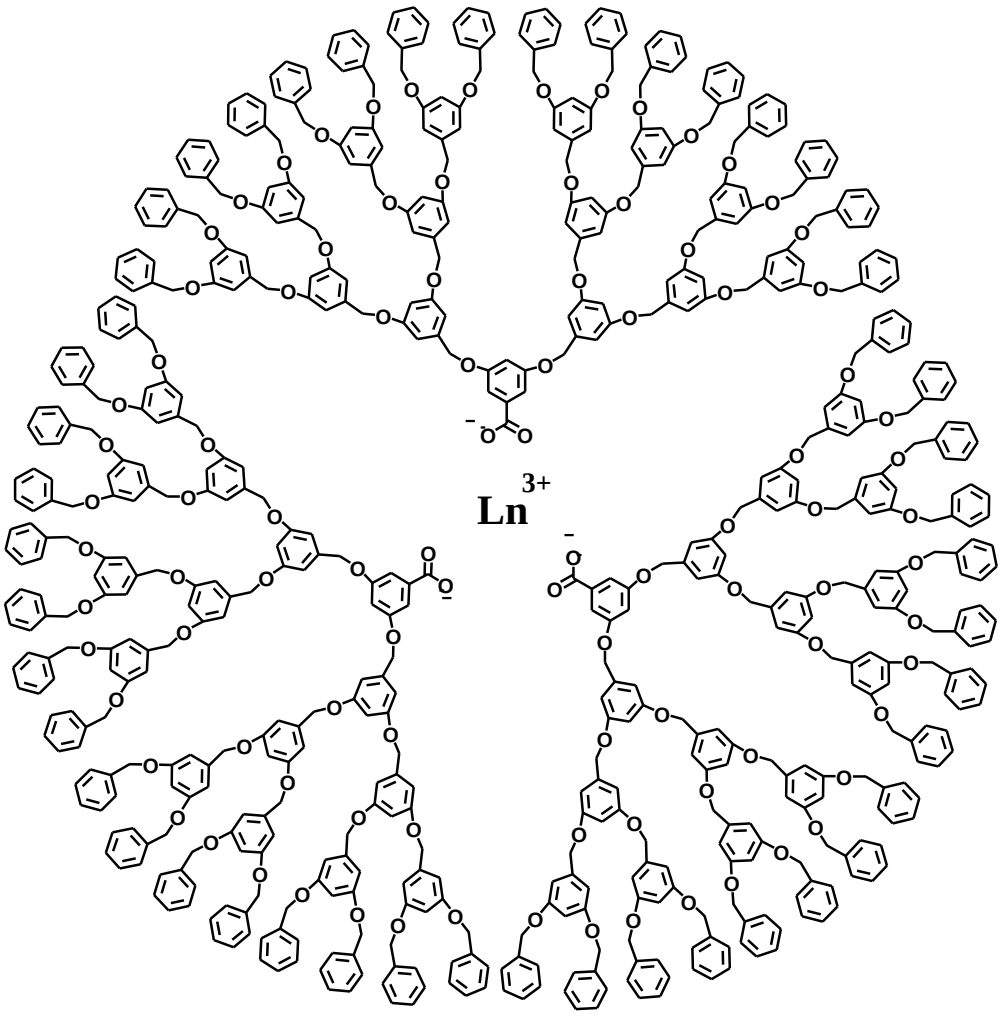

Figure 1.15 - Schematic representation of poly(benzyl ether) dendrimer with lanthanide core.

A porphyrin-core dendrimeric light-harvesting system was reported by Jiang and Aida using a Frechet-type dendron substituted at the meso position of the porphyrin core as shown in **(Figure 1.16)**.[62] In their system the emission band of the dendron partially overlaps with the Soret band of the porphyrin, which favours the energy transfer to the porphyrin core. It was also found that the tetrasubstituted porphyrin dendrimer, exhibit higher energy transfer efficiency than the partially substituted analogues. The crowded dendrimer array facilitates higher energy transfer than for conformational dendrimer freedom, as found by temperature dependency of energy transfer efficiency and fluorescence depolarisation experiments.

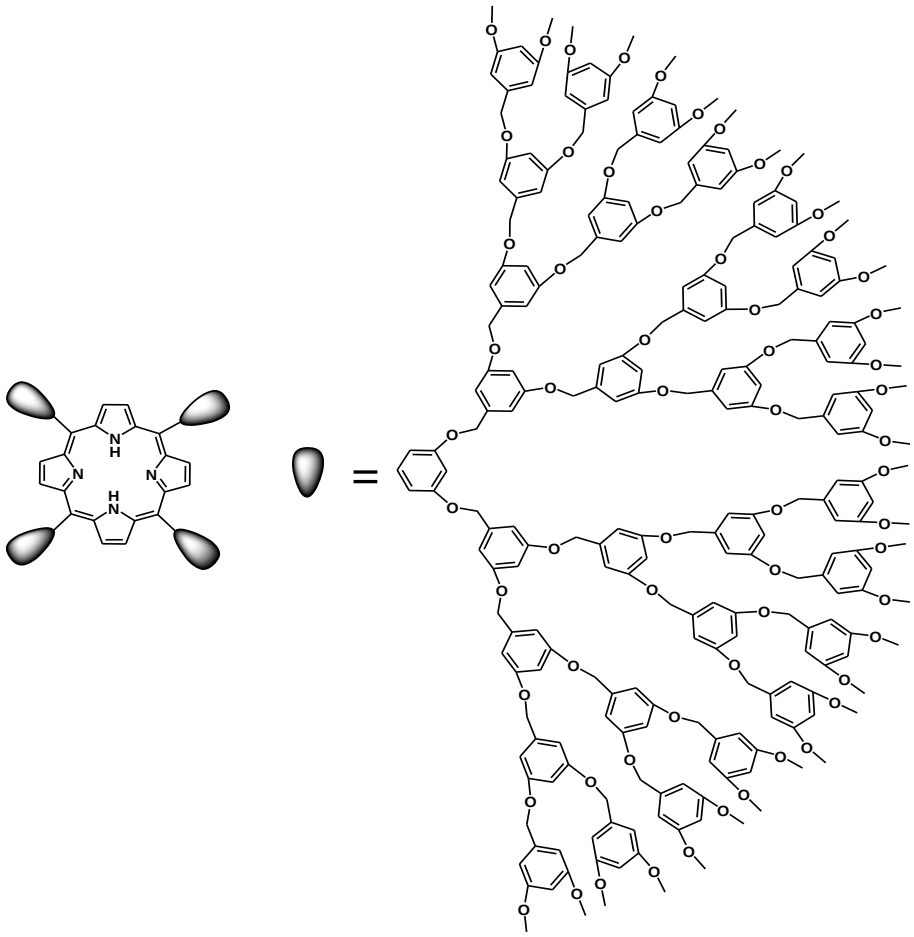

Figure 1.16 - A poly(benzyl ether) dendrimer with a porphyrin core, reported by Jiang and Aida.

1.3.2.3 Electron transfer in dendrimeric light-harvesting system

In natural photosynthesis electron transfer is the key reaction, which happens between electron-donor and electron-acceptor pairs. The efficiency of electron transfer in these systems depends on the distance between acceptor and donor. Mullen and co-workers reported a dendrimeric system in which intermolecular electron transfer took place in functionalised polyphenylene dendrimers containing perylenediimide core and triphenylamine end groups as shown in **(Figure 1.17)**. High efficiency electron transfer took place from periphery to core in polar solvents.[63] The results from steady-state and transient spectroscopy showed that the decreasing dendrimer generation gave more significant energy and electron transfer, which is due to the shorter distance from the amine donor to the perylenediimine acceptor. De Schryver et al. also studied the dynamics of photoinduced electron transfer and the influence of oxygen on the electron transfer in these dendrimers by single-molecule

spectroscopy.[64] In order to mimic complete photosynthetic occurrence, Thomas et al. designed a dendrimeric system containing both energy and electron transfer properties. In this system benzthiadiazole derivatives acts as energy and electron transfer acceptor core and diarylaminopyrene units as energy and electron donor unit at the periphery as shown in **(Figure 1.18)**.[65] Energy transfer took place by Foster mechanism with efficiency. This energy transfer is high in higher generations. In addition, from the cyclic voltammogram the oxidation potential of benzthiadiazole units was obtained at 595 mV and 444 mV for diarylaminopyrene units, thus this electrochemical data suggested that it is possible for the excited state of the chromophore at the core to be reduced by peripheral chromophores. The charge transfer in these dendrimers was calculated to be as high as 70% in the high polar solvent DHF and the overall efficiency of the photon to charge-separated state was calculated at approximately 50%.

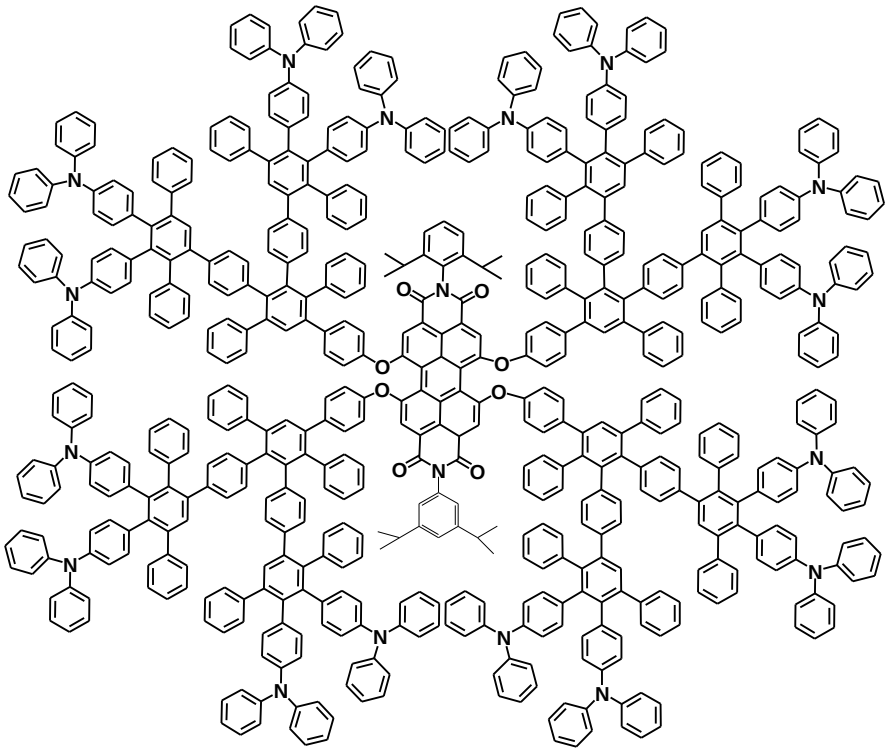

Figure 1.17 - Polyphenylene dendrimer consisting of triphenylamine units periphery and a perylenediimide core.

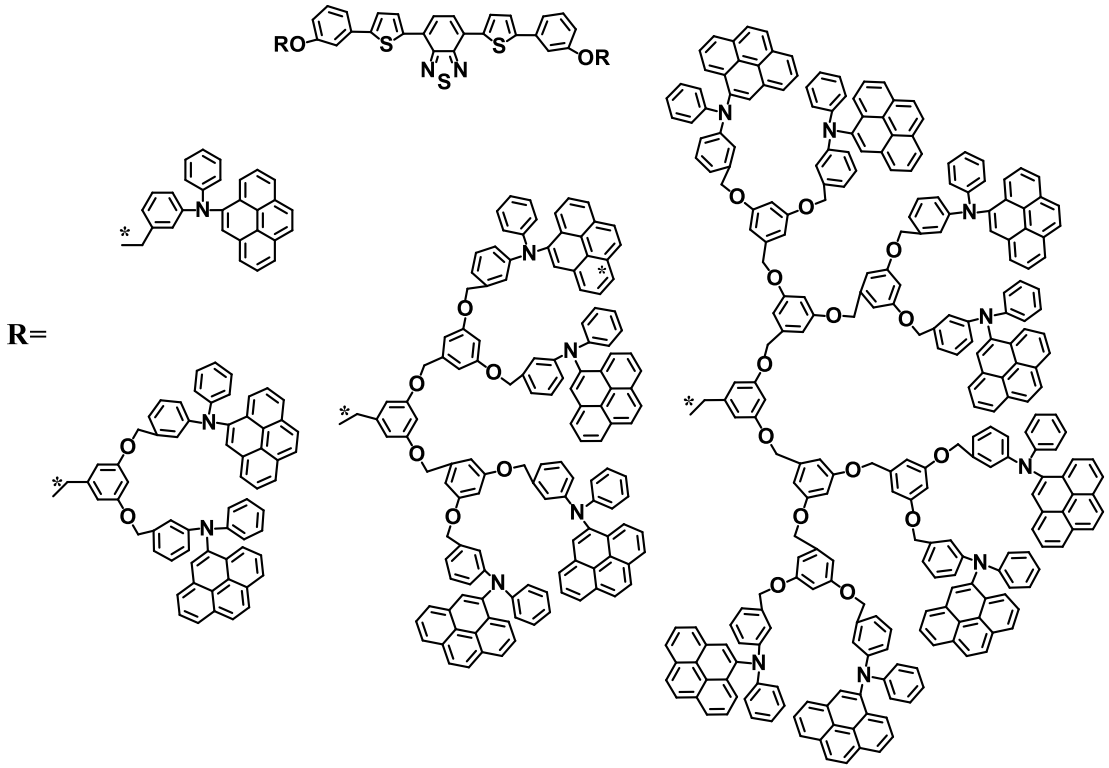

Figure 1.18 - Light-harvesting dendrimers containing benzthiadiazole derivatives at the core and diarylaminopyrene at the periphery.

1.3.2.4 Energy transfer in the self-assembled host-guest light-harvesting system

In self-assembled light-harvesting systems energy transfer can take place between dendrimers with the donor and the acceptor groups connected by non-covalent bonds instead of covalent bonds. In designing artificial systems these types of light-harvesting supramolecular dendrimers are very significant. These types of systems can easily be modified due to presence of weak bonds.

Meijer and co-workers reported a self-assembled dendrimeric system, in which they modified the surface group of poly(propylene imine) dendrimers with oligophenylenevinylene (OPV) units affording amphiphilic structures that function as host, which is capable of extracting a water-soluble guest (sulforhodamine B) into the organic phase as shown in **(Figure 1.19)**.[66] When periphery OPV units were excited, the OPV units showed quenching and the emission of sulforhodamine B arose, which indicated the energy transfer from periphery to core with efficiency of 40% at maximal loading. This efficiency is obviously lower than the dendrimer system in which donor and the acceptor units are attached to each other with covalent bonds.

This could be due to poor overlapping between donor emission and acceptor absorption spectram.[48]

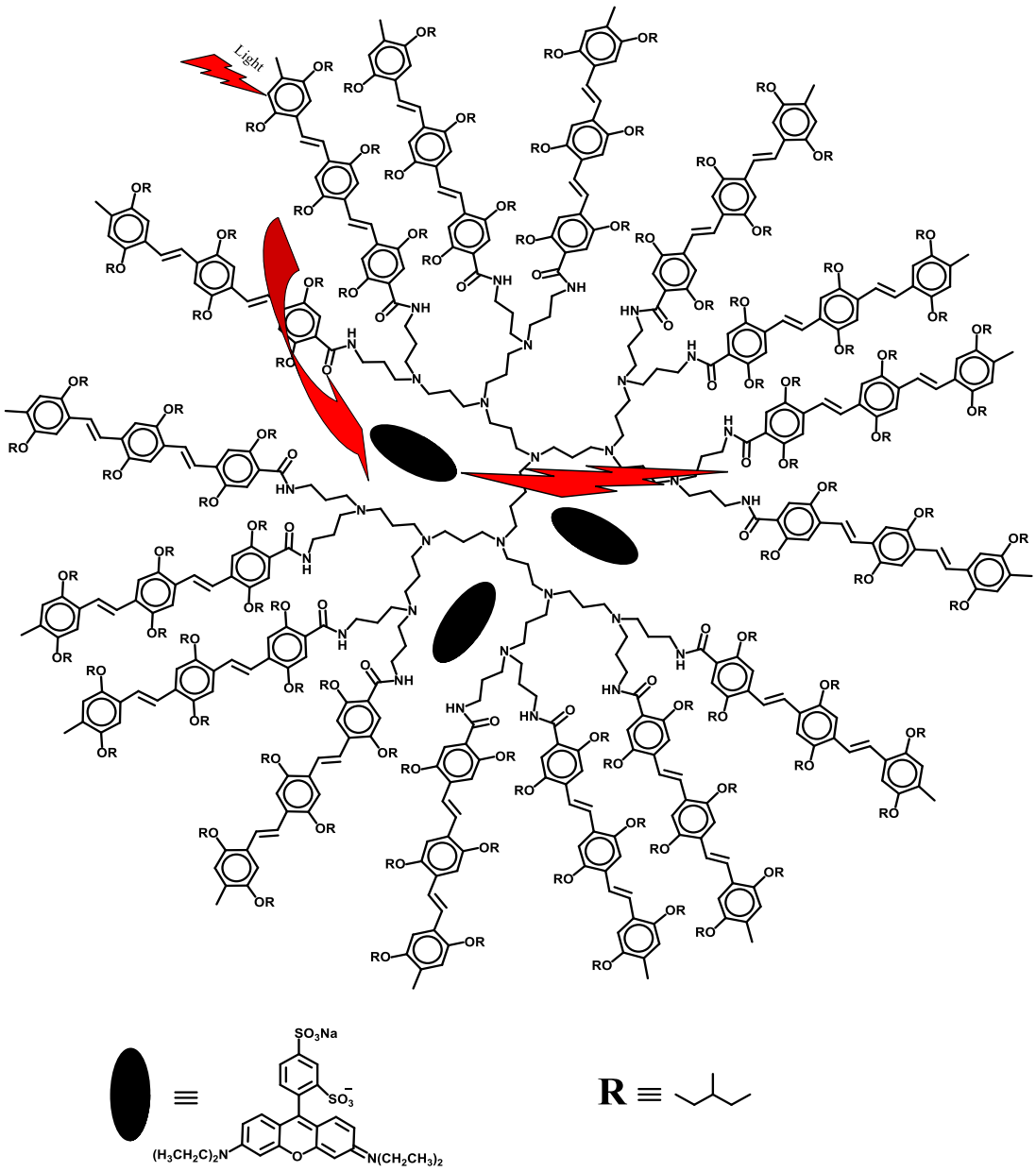

Figure 1.19 - Energy transfer from OPV-terminal dendrimer to the encapsulated dyes.

Similarly Balzani and co-workers have investigated a series of light-harvesting systems in which host and guest are attached with non-covalent bonds.[67,68] The energy transfer in these self-assembled host-guest dendrimers was achieved via Foster mechanism owing to the effective spectral overlap between acceptor and donor units.

Chapter 2
Aims

The purpose of our research is to synthesise a light-harvesting system by mimicking photosynthesis. The Natural photosynthetic system is a vast array of light-harvesting chromophores i.e. chlorophyll molecules that channel the absorbed energy to a single reaction centre. By mimicking natural light-harvesting systems, our research aim is to try and develop a system that can efficiently transfer light energy from each of its surface donor molecules to a single acceptor unit at a core, which will act as a reaction centre as shown in **(Figure 2.1)**. In our system the acceptor molecule must efficiently emit light energy in specific and useable form. The polymer will simply act as a scaffold to hold acceptor and donor unit at a specific distance from one another so that efficient energy transfer can take place.

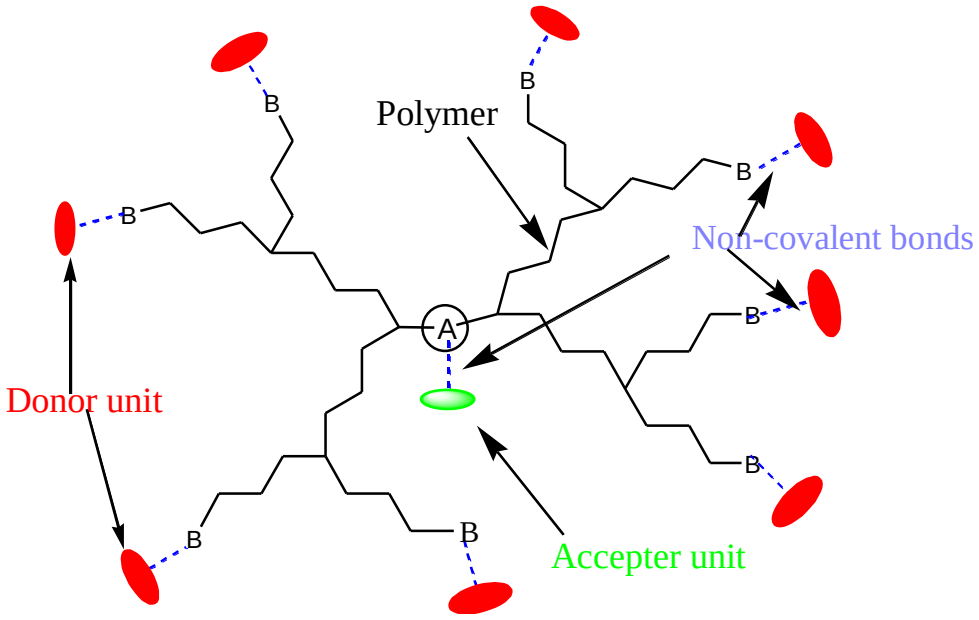

Figure 2.1 - Representation of the targeted artificial light-harvesting system.

As in natural light-harvesting systems, molecules are held in place by non-covalent interactions. Therefore, by adopting Nature's approach we will assemble donors and the acceptor within and around a polymer scaffold using non-covalent interactions. However, by using covalent chemistry we can get a very robust structure from a synthetic and evolutionary point of view, however, it is impossible to make modifications to the final structure. In case unpredicted error occurs while designing our system, and if these errors cannot be corrected, then we have to redesign our system from the beginning. Also if we have to investigate how minor changes to the

acceptor or donor will affect the efficiency of the light-harvesting system, a whole series of discrete but similar macromolecules must be constructed. Thus a complete non-covalent approach will allow us to study a variety of acceptor/donor combination without the need to start from the beginning. Therefore, we can use the same polymer scaffold which can hold a variety of acceptor/donor molecules. Hence, non-covalent chemistry will give us many advantages with respect to synthetic versatility, diversity and will simplify the future investigations.

2.1 Selection of polymer scaffold

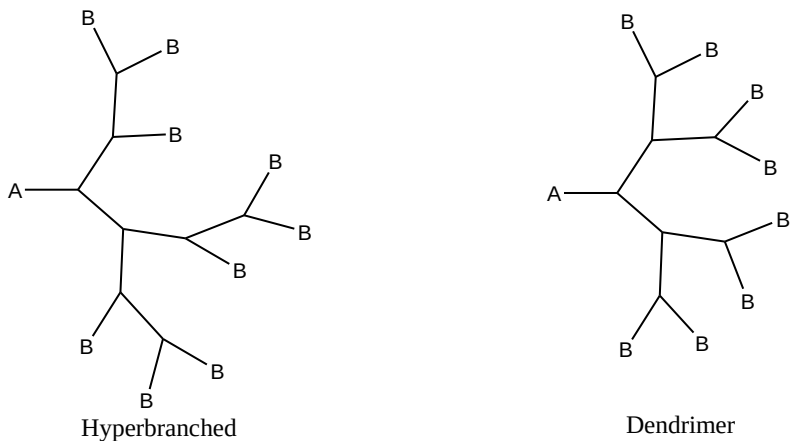

Figure 2.2 - Diagrames of different polymers.

Dendrimers were preferable candidates over hyperbranched polymers for mimicking natural light-harvesting systems. As shown in **Figure 2.2**, hyperbranched polymers and dendrimers are both globular, but dendrimers contains uniform branches emerging from the core. These branches can hold surface molecules at a uniform distance from each branching point, which is not possible in hyperbranched polymers. In order to mimic natural light-harvesting systems, a great number of chromophores need to be incorporated in the system in such a way that they facilitate efficient energy transfer. Thus, dendrimers acquire all the desired requirements in order to mimic the natural light-harvesting system. In addition, during synthesis we can easily control the size, shape and molar mass of dendrimer but in hyperbranched polymer synthesis this is not possible. With this advantage, we can easily position our surface groups at a required distance from the core, according to our system requirement. Now this raises the question of which dendrimer is more suitable for our system? As

mentioned earlier, dendrimers are acting as a scaffold to hold the acceptor and the donor units. Therefore, a dendron with one focal point to facilitate the non-covalent bonding with a single acceptor unit, with various terminal groups to hold the donor molecules is needed. Thus, an acid core dendron with amine or ester terminal groups would be a suitable candidate for our system.

2.2 Selection of chromophores as donor and acceptor

In natural light-harvesting systems, incoming light is captured efficiently by one of the chromophores and distributed widely in the surrounding space then transferred to the reaction centre. Nature employs chlorophyll-a and -b or corresponding bacterio-chlorophyll as chromophores. These chlorophyll molecules have an extinction coefficient as large as 10^5-10^6 $cm^{-1}M^{-1}$ near the regions at 400 nm and 600 nm. Thus, in order to mimic natural light-harvesting systems, it is very important to choose chromophores that could effectively absorb, transfer and emit energy. Porphyrin and phthalocyanine are the closely related chromophores to the natural chromophores. Thus we will be using these molecules as chromophores in our light-harvesting system.

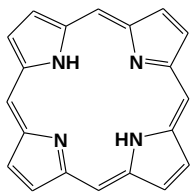

Porphine

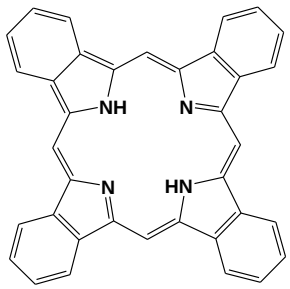

Phthalocyanine

2.3 Self-assembly of dendron and chromophores

In order to mimic natural photosynthesis self-assembly is an important term. Self-assembly is one of the important categories of supramolecular chemistry.[73] Self-assembly involves the union of two components via non-covalent interactions (hydrogen bonding, hydrophobic or van der Waal's interactions, metal coordination and π-π interactions or electrostatic interactions). In other words, self-assembly is a spontaneous and reversible association of two or more components to form a larger

non-covalently bound component or aggregate.[74] Nature uses self-assembly processes ubiquitously. An important example of natural self-assembly is DNA's double-helix structure, where two opposite strands join each other via hydrogen bonding and π-π stacking. In addition, protein folding and virus assemblies are important examples of the self-assembly. In this work, for self-assembly between dendron and chromophores, metal-coordination self-assembly was used. Metal coordination provides a strong inter-molecular force among other supramolecular assemblies such as hydrogen bonding, ionic interactions and π-π stacking interactions. For metal coordination, the nature of metal ions has a great effect. It was decided to use tin porphyrin as an acceptor molecule and zinc porphyrin as a donor molecule. The reason for using tin porphyrin was due to the fact that tin(IV) metal cation can be easily inserted in the porphyrin. Furthermore, a tin(IV) centre is six-coordinate with two diaxial ligands and these ligands can be easily manipulated by significant changes in the chemical shifts using NMR spectroscopy and the Soret band shifts in the UV/Vis spectroscopy. However, most importantly, the oxophilicity of the tin(IV) centre makes it preferable by showing significant coordination with carboxylates. The oxophilic nature of tin(IV) will facilitate bonding between the acid functionalised dendron core and porphyrin, as shown in **(Figure 2.3)**.

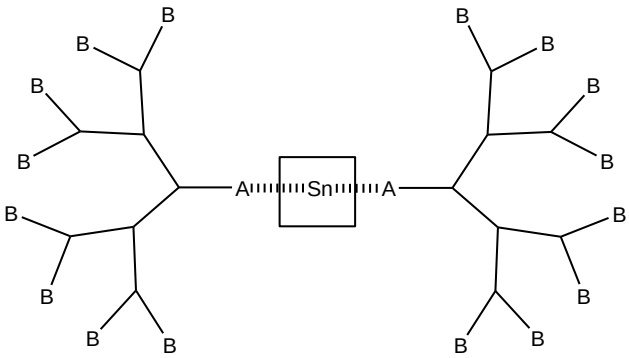

Figure 2.3 - Representation of self-assembly between tin porphyrin and acid functionalised dendron core.

The Zn(II) metal was chosen for the donor porphyrin. This is because complexes of Zn(II) are practically stable toward heat, acidic conditions and oxidation. In addition, Zn(II) is penta-coordinate by accepting only one axial ligand and it affords strong

stability with nitrogen ligands. All these properties make the Zn(II) metal ion suitable in our system. Therefore, after the insertion of zinc(II) into the porphyrin, zinc porphyrin can facilitate self-assembly with the amine functionalised terminal dendrons as shown in **(Figure 2.4)**.

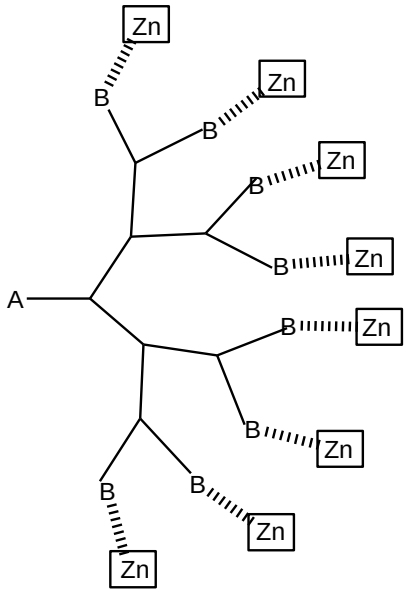

Figure 2.4 - Representation of self-assembly between dendron terminal amine group and zinc porphyrin.

The final step towards completing our light-harvesting model system will be the observation of energy transfer between chromophores. In order to get energy transfer from the donor units to a central acceptor unit, these chromophores should be suitable for the Foster energy transfer i.e. the emission spectrum of the donor units should overlap with the absorption spectrum of the acceptor unit as shown in **(Figure 2.5)**. For this energy transfer testing, we will be using fluorescence and UV/Vis spectrometer to obtain the emission spectrum of the donor and the absorption spectrum of the acceptor unit respectively.

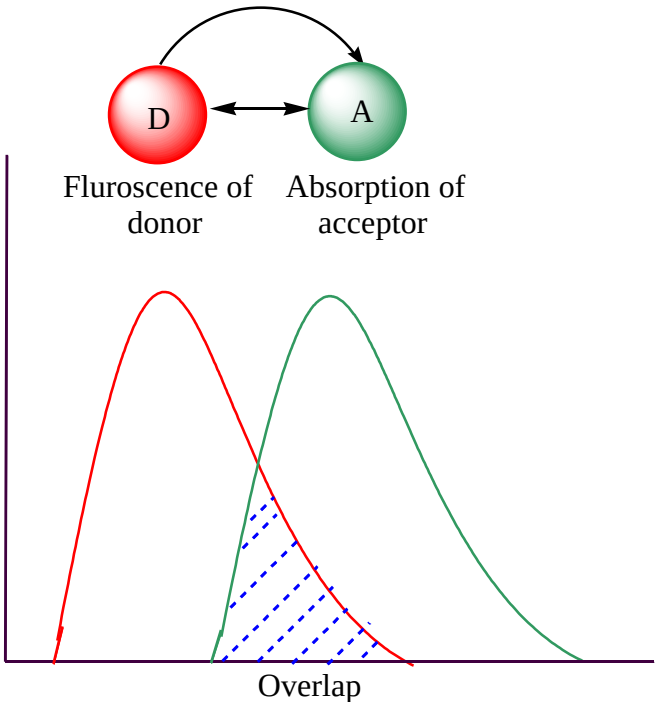

Figure 2.5 - Overlap of emission spectrum of donor and absorption spectrum of acceptor units.

After obtaining the overlap, there will be a light-harvesting test in which, with the excitation of the donor unit, there should be an emission from a single acceptor unit and the intensity of the core emission should increase with the increase in the number of the donor unit i.e. with the increasing generations of dendrons.

Chapter 3

Result and Discussion

3.1 Dendritic macromolecule as scaffold

As described beforehand, the main aim of this research is to produce a self-assembled light-harvesting system by mimicking Nature's approach. In order to achieve these aims, the first step was to synthesise a range of different generations of PAMAM dendrons. These dendrons could then be applied as a scaffold to hold different chromophores. The unique physical and chemical properties of PAMAM dendrons made them preferable for our light-harvesting system. The different generations of PAMAM dendron were successfully synthesized by using a divergent method, which involves two iterative steps; 1,4 Michael addition, using methyl acrylate and amidation, using ethylenediamine. Michael addition resulted in the half generation dendrons possessing ester terminal groups and the amidation step gave rise to the whole generation dendron with amine terminal groups. **Figure 3.1** represents a series of synthesised half and whole generation PAMAM dendrons.

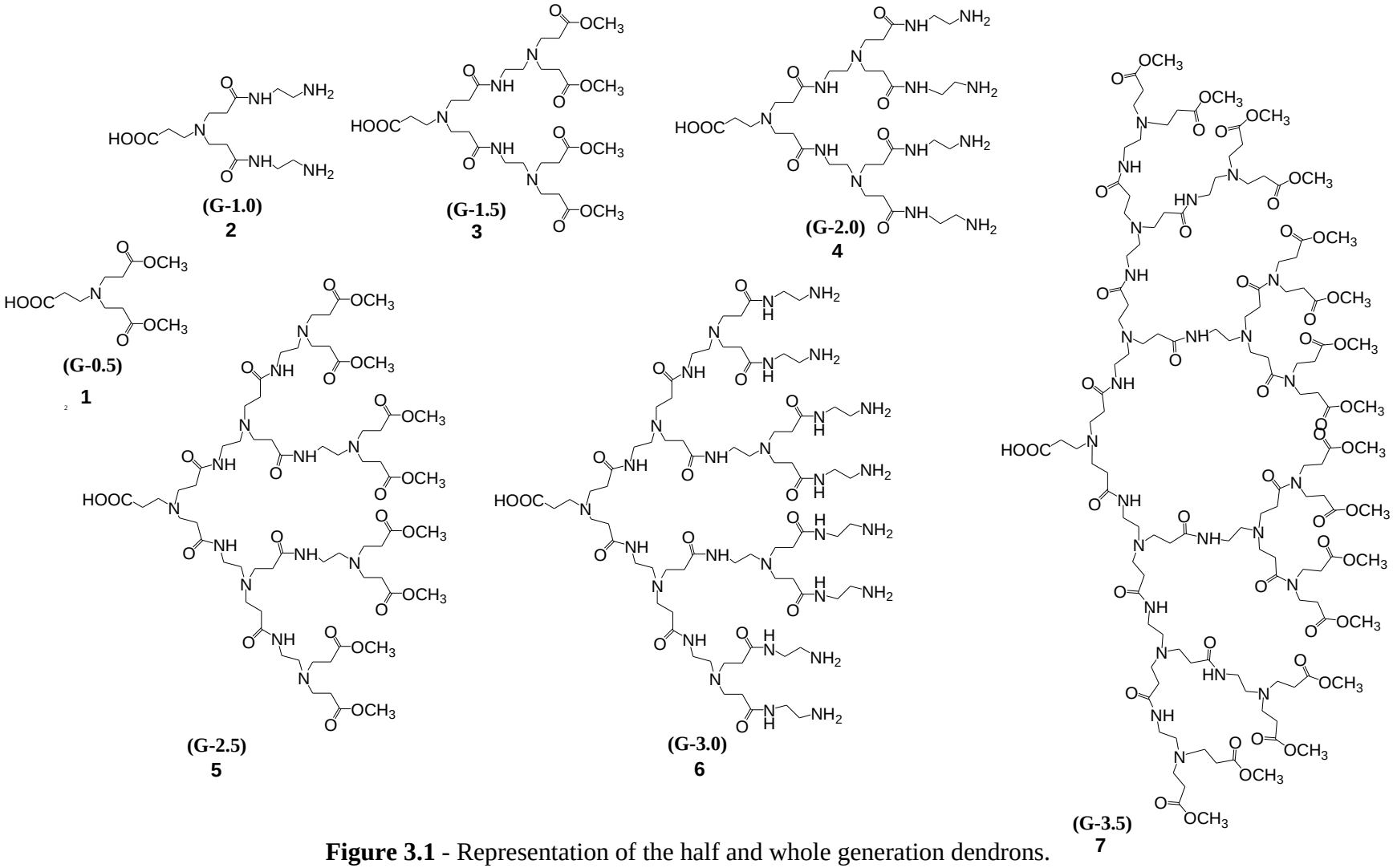

Figure 3.1 - Representation of the half and whole generation dendrons.

In general, Michael addition is a conjugate nucleophilic addition reaction which involves the α,β-unsaturated carbonyl compounds. The carbonyl substituent has an electron withdrawing effect, generating a delta positive charge on the alpha carbon atom. Due to resonance stabilisation, the beta carbon is thereby rendered electropositive and is therefore disposed to nucleophilic attack. In dendron synthesis, the alpha beta carbonyl system is methyl acrylate and the nucleophile is an amine, **(Scheme 3.1)**.

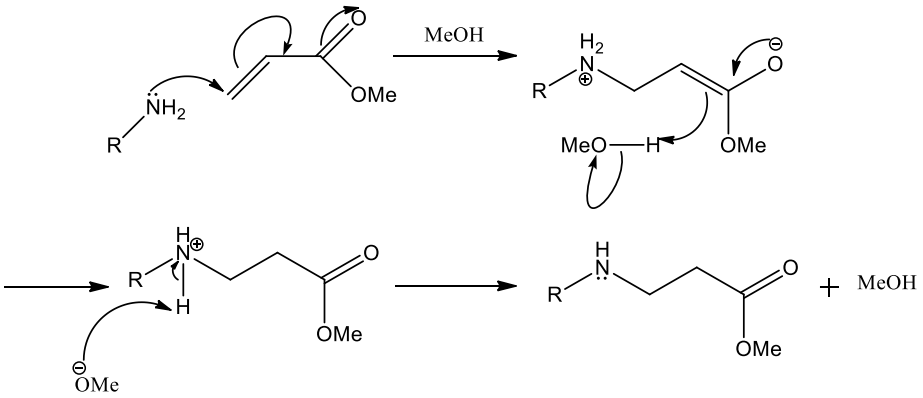

Scheme 3.1 - The reaction mechanism for 1,4 Michael addition.

In the amidation step, the nucleophilic nitrogen from ethylenediamine attacks the carbonyl of the terminal carbomethoxy group ($COCH_3$). A schematic representation is shown in **(Scheme 3.2)**.

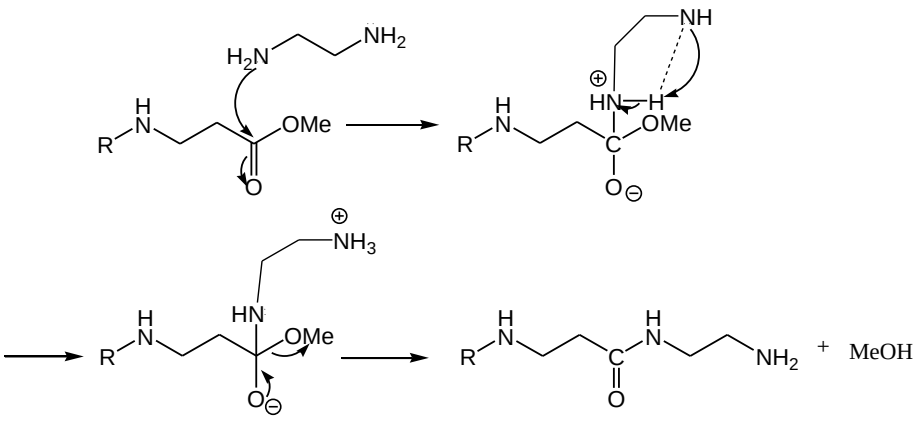

Scheme 3.2 - Reaction mechanism for amidation.

3.1.1 Synthesis of ester terminal dendrons

The ester terminal dendrons were synthesised by using β-alanine. The acid group of β-alanine is designed to form the dendron core, which will ultimately bond to an acceptor group. In the first step of this synthesis, β-alanine was dissolved in methanol. β-alanine can easily form a zwitterion and this zwitterion is unreactive towards methyl acrylate. Therefore, to proceed with this reaction, Et_3N was added as a base to generate ionised β-alanine, which can then react with methyl acrylate. The scheme is shown in **(Scheme 3.3)**.

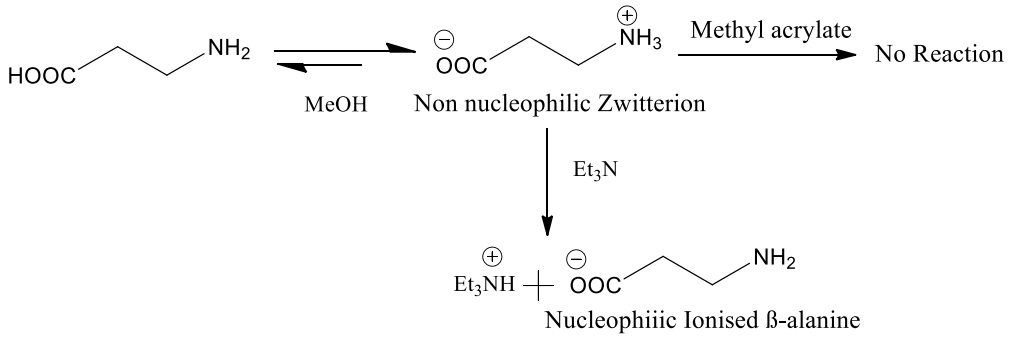

Scheme 3.3 -The Reaction of Et_3N with β-alanine.

Following this, an excess of methyl acrylate was added drop wise to the solution at 0℃ and left to react at room temperature. After 24 hours, unreacted methyl acrylate and methanol were removed by using a rotary evaporator. For the completion of reaction, the product was monitored by ^1H NMR. The product formed was a viscous honey yellow oil.

3.1.1.1 Characterisation and purification of half generation dendrons

For the purification of half generation dendrons, the solvent and unreacted methyl acrylate was easily removed by a rotary evaporator, due to their high volatility. Characterisation of half generation dendrons is achieved by using ^1H NMR, ^{13}C NMR spectroscopy, mass spectroscopy and IR spectroscopy. For half generation dendrons the methoxy peak is the most important signal for characterisation. **Figure 3.2** represents the ^1H NMR of G-0.5 dendron with a strong methoxy peak signal (e) at 3.66 ppm. The methylene protons next to acid core of the dendron gave rise to a

triplet signal (a). In addition, one multiplet and one triplets attributed as (b) (c) and (d) arise due to the presence of different proton environments.

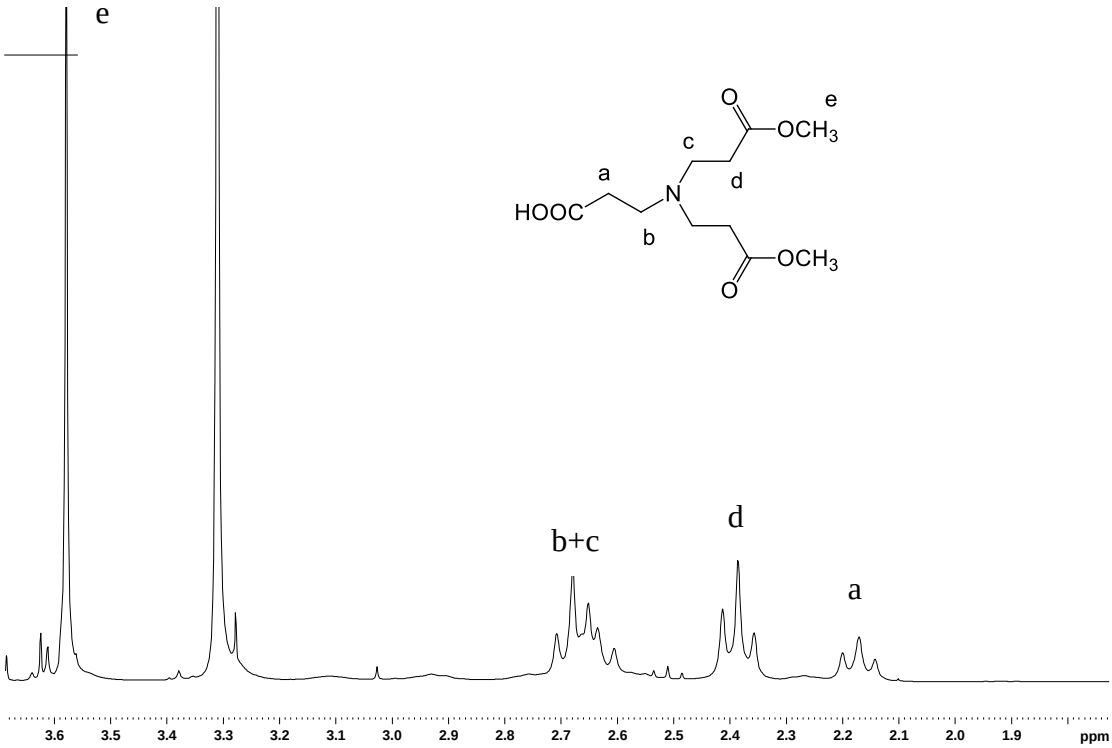

Figure 3.2 - ^{1}H NMR of G-0.5 dendron

The spectram for higher generation dendrons were significantly more difficult to interpret. This was due to the presence of the increasing number of protons. As a result, there were large regions of overlap and broadened peaks. Although the spectra for higher generations were not straight forward as for smaller generations, the classification was still achieved with a sufficient level of accuracy using chemical shift and integration. Another valuable tool for the characterisation of the product is ^{13}C NMR. **Figure 3.3** shows the ^{13}C NMR of G-0.5 dendron. The acid carbon showed a peak at 178.9 ppm and carbonyl of methoxy group showed a peak at 175.3 ppm. Similar to ^{1}H NMR, ^{13}C NMR becomes complicated due to increasing numbers of carbon atoms with growing generations.

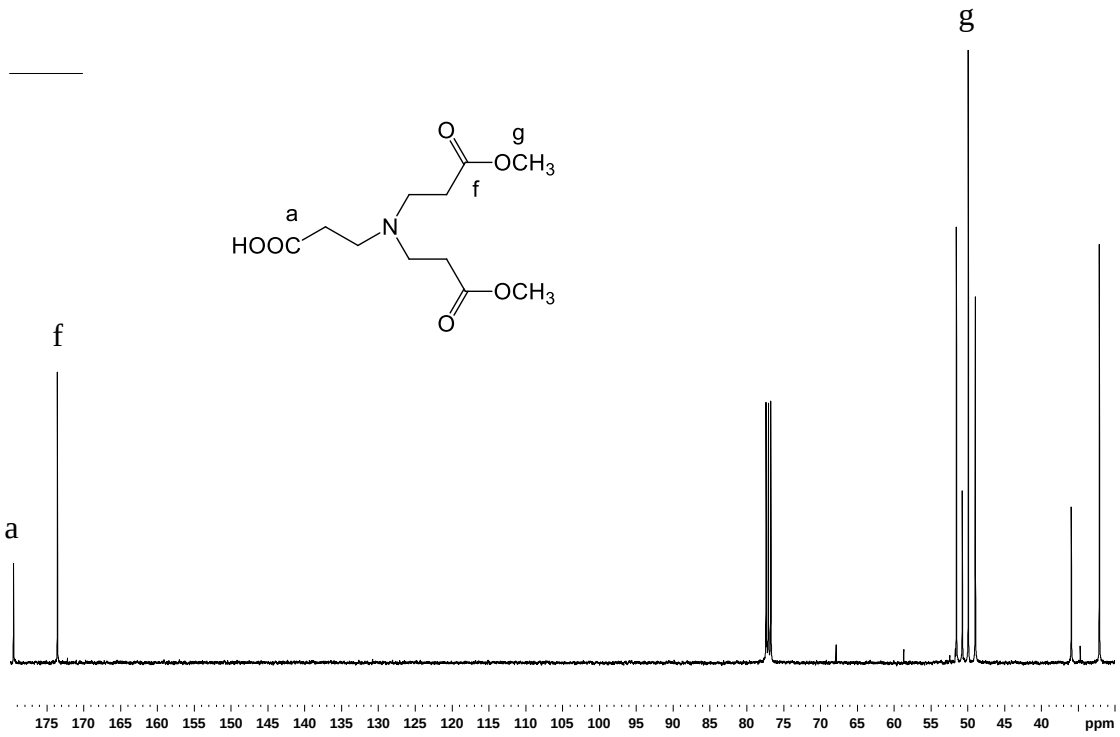

Figure 3.3 - ^{13}C NMR of G-0.5 dendron.

Mass spectroscopy is also an important tool in dendrimer characterisation, due to their molecular uniformity and monodispersity. The results showed the molecular ion peaks corresponded to the exact molecular ion peaks for the half generation dendrons. IR also provided the useful information about functional groups. The ester terminated dendrons showed carbonyl peak at 1730 cm^{-1}.

3.1.2 Synthesis of amine terminated dendrons

The amine terminated dendrons were formed by the amidation step as shown in **(Scheme 3.2)**. In this reaction, the nucleophilic nitrogen from ethylenediamine (EDA), attacks the positive carbonyl carbon of methoxy group. In order to get the desired product, an excess of ethylenediamine was added to ensure the completion of the reaction. Where as, an insufficient amount of ethylenediamine could result in the loss of uniformity and monodispersity to the product, forming defects in the structure. For amine terminal dendron synthesis, G-0.5 dendron was dissolved in methanol and EDA was added dropwise at 0˚C for half an hour and the reaction left stirring for 2 days. After the removal of solvents and purification, a honey yellow oily product was formed.

3.1.2.1 Characterisation and purification of amine terminated dendrons

Characterisations of amine terminated dendrons were achieved by using ^{1}H NMR, ^{13}C NMR spectroscopy, mass spectroscopy and with the help of IR spectroscopy. The amine terminal dendrons showed amide N-H peak at 3200 cm^{-1} and amine $-NH_2$ peak came at 1640 cm^{-1}.

In the amidation step, purification of the product was crucial to remove the unreacted EDA. If the purification of the product is not thorough, the outcome will be unwanted by-products and defects within the dendron structure. Therefore, full removal of EDA is compulsory. If not fully removed, unreacted EDA can behave as a new initiator centre resulting in smaller G-0.5 dendrons as shown in **(Scheme 3.4)**.

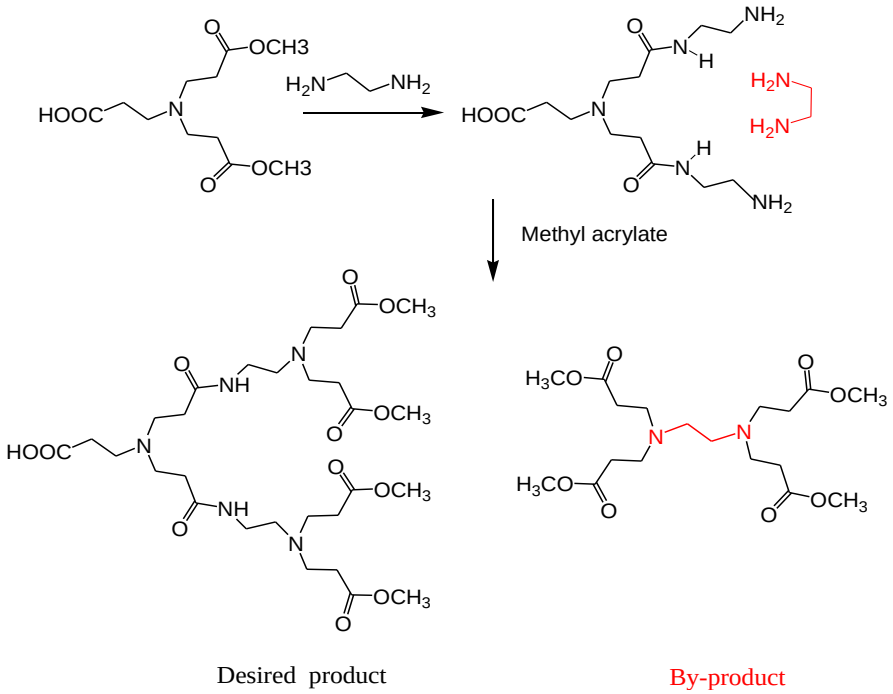

Scheme 3.4 The schematic representations of production of by-product with unreacted EDA.

In the Michael addition step, methyl acrylate was easily removed by rotary evaporation, due to high volatility of the solvent. However, the removal of EDA was slightly more difficult because of the formation of strong hydrogen bonds between

internal amide and terminal amine groups of the dendron and EDA. Therefore, to overcome this hydrogen bonding, purification was carried out by using an azeotropic mixture of toluene and methanol in 9:1 ratio, followed by the methanol wash. Methanol was used as a strong competitor for the hydrogen bonding sites in EDA. However, methanol has a lower boiling point than EDA and can easily be removed before the full removal of EDA. Thus, in order to increase the boiling point the azeotropic mixture of toluene and methanol was used, which facilitated the removal of EDA. The product was washed with the azotropic mixture and subsequently placed upon the rotary evaporator to remove all traces of the solvents and ^{1}H NMR was used to ensure EDA was completely removed, so as to prevent unwanted side reactions. With the increase in dendrons generation, the chance of side reactions also increases. As explained earlier, the full removal of EDA is necessary and as this removal was examined by ^{1}H NMR. However, for large generation dendrons ^{1}H NMR contains broad signals and overlap. Therefore, mass spectroscopy is required. Thus, for bigger generation dendrons the cautious examination is needed.

Dendrons up to generation 2.0 were synthesised successfully. However, some impurities were reported for G-2.5 dendron by mass spectroscopy. For the purification of dendron G-2.5, size exclusion chromatography was used using a bio bead column. For the preparation of column, the bio bead slurry was made in THF, which was left overnight to swell. The pre-swollen bio bead slurry was transferred into a glass column and THF was eluted to the bed level under gravity. Then THF was then removed with three bed volumes of DCM. After preparing the column, G-2.5 dendron was dissolved in minimum quantity of DCM and carefully added. The column was eluted with DCM under gravity. The eluted product with DCM collected in 5 fractions. DCM was removed and fractions were analysed using ^{1}H NMR, mass spectroscopy and analytical GPC. Fractions containing desired product were combined and used for further dendron synthesis for higher generations. As a result, the dendrons up to G-3.5 was synthesised successfully. After the successful synthesis of the dendrons, the second step towards our aim was the synthesis of chromophores.

3.2 Chromophores (acceptor and donor unit)

In order to design a self-assembled light-harvesting system, the second step was the selection and synthesis of appropriate chromophores. Porphyrin was selected for the light-harvesting system because of its structural similarity to chlorophyll. The word porphyrin is a Greek word which means purple and all porphyrins are intensively coloured. Porphyrin molecules are heterocyclic compounds which contain 4 pyrrole rings linked with each other at the α carbon atom via a methine (=CH-) bridge, as shown in **(Figure 3.4)**. The porphyrin ring system is very stable and ring exhibits aromatic character by obeying Huckel rule (4n+2π) electrons. Porphyrin has an ability to bind a variety of metal ions by deprotonating nitrogen atoms. Porphyrin without metal ion bound is called a free base porphyrin. Porphyrin with iron(II) metal bound is called heme (which transfers oxygen in the living tissues), myoglobin (works as oxygen storage component) and porphyrin with magnesium metal in core forms chlorophyll molecules and is the most vital part of photosynthesis. Hence, porphyrins are one of the vital chemical units essential for several life processes on the earth. Schematic representation of porphine, heme and chlorophyll is shown in **(Figure 3.4)**.

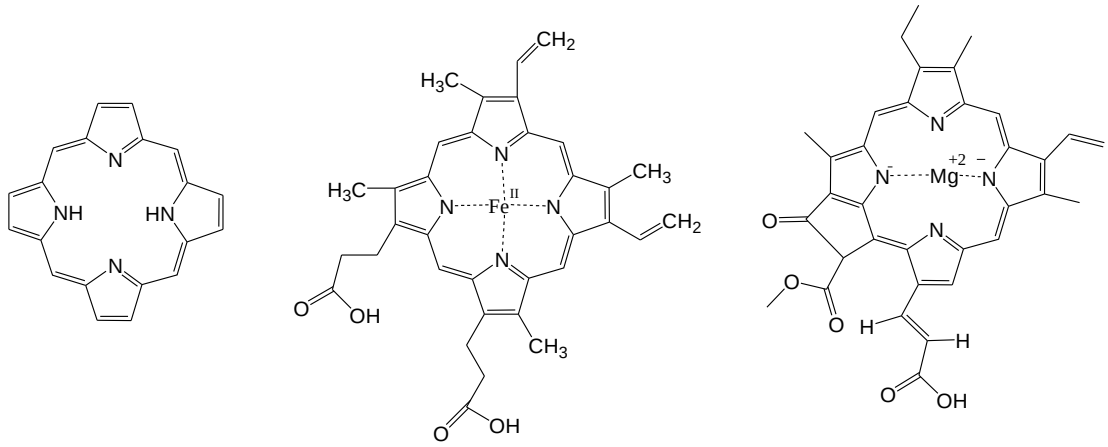

Porhyrin Heme B Chlorophyll

Figure 3.4 - Structural representations of porphine, Heme B and chlorophyll.

As shown in **(Figure 3.4)**, porphine has a central cavity which can accommodate a variety of metal ions. Due to this potential and the presence of porphyrin molecules in Nature, it was decided that this type of molecule i.e. tetraphenylporphyrin with different metals at the core, would be used as chromophores in our light-harvesting

system. Tin(IV) metal porphyrin would be used for the acceptor molecule and zinc for the donor molecules. The decision to use the tin porphyrin was due to the fact that tin metal can be easily inserted in the porphyrin. In addition, tin(IV) centre is six-coordinate with two axial ligands and these ligands can be easily manipulated by NMR and Uv/Vis spectroscopy. Most importantly, the oxophilicity of the tin(IV) centre makes it preferable, showing significant coordination with carboxylates. The oxophilic nature of tin(IV) facilitates bonding between the carboxylic acid dendron core and the porphyrin in our system as shown in **(Figure 3.5)**.

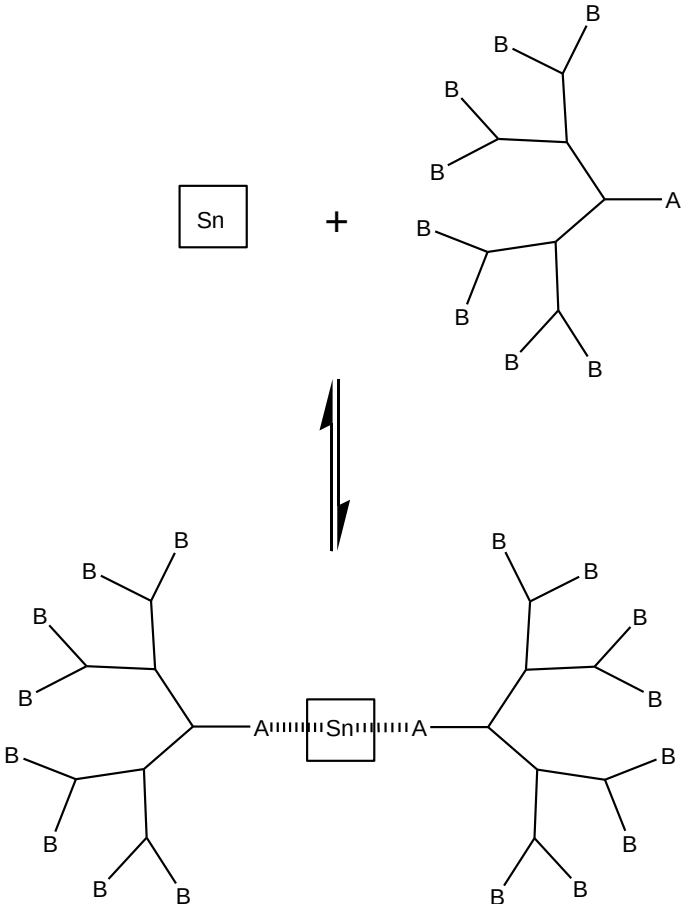

Figure 3.5 - Representation of self-assembly between tin porphyrin and dendron core.

Zn(II) metal was selected for the donor porphyrin. This was because complexes of Zn(II) are particularly stable toward heat, acidic conditions and oxidation. Additionally, Zn(II) is penta-coordinate by accepting only one axial ligand and it

affords strong stability with nitrogen ligands. All these properties, makes Zn(II) metal ion favourable in our light-harvesting system. After the insertion of the Zinc into porphyrin, it can easily make metal coordination with amine terminal groups of the dendrons as shown in **(Figure 3.6)**.

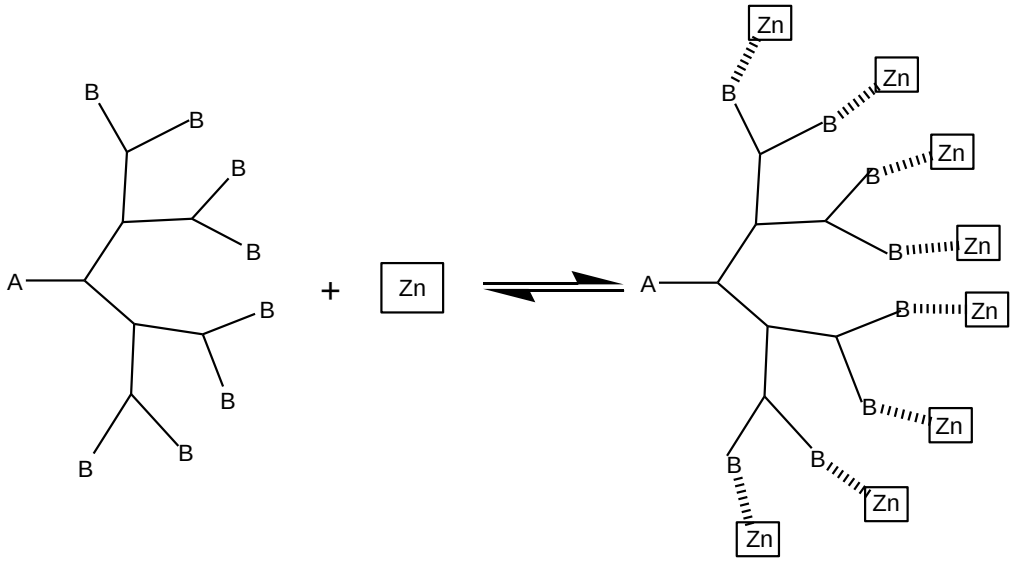

Figure 3.6 - Representation of self-assembly between dendron terminal amine group and zinc porphyrin.

In order to synthesise the acceptor and donor chromophores, the first step was the synthesis of tetraphenylporphyrin and the second step involves the insertion of tin and zinc metal in TPP as described below.

3.2.1 Synthesis of tetraphenylporphyrin (TPP)

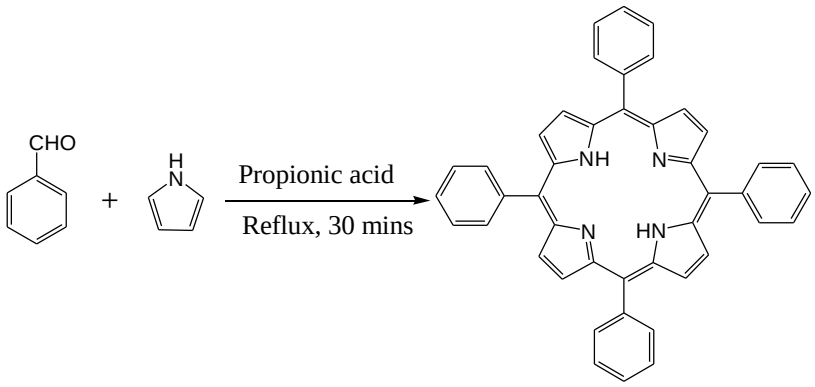

8

Scheme 3.5 Synthesis of tetraphenyl porphyrin (TPP) **8**

TPP was synthesised by the reaction of benzaldehyde and pyrrole, refluxing in propionic acid as shown in **(Scheme 3.5)**. The reaction mixture was cooled, filtered and washed with hot methanol followed by hot water to remove unwanted impurities. This reaction involved a series of electrophilic substitution reactions between benzaldehyde and pyrrole followed by the oxidation. The reaction mechanism is shown in **(Scheme 3.6)**. The product was purified by column chromatography using silica as stationary phase and chloroform as mobile phase. The purple product was characterised by using UV/Vis spectroscopy, which gave a soret band at 419 nm and four Q bands at 516, 549, 590 and 647 nm. Also, the ^{1}H NMR showed a sharp peak at 8.91 ppm, which was attributed to 8 protons directly attached to pyrrole. The two deshielded doublet peaks at 8.25 and 7.81 ppm which were referred to the phenyl group protons were also observed. Also, NH protons gave a highly shielded peak at -2.69 ppm. This showed good agreement with literature reports. Molecular ion peak at 614 also confirmed the synthesis was successful.

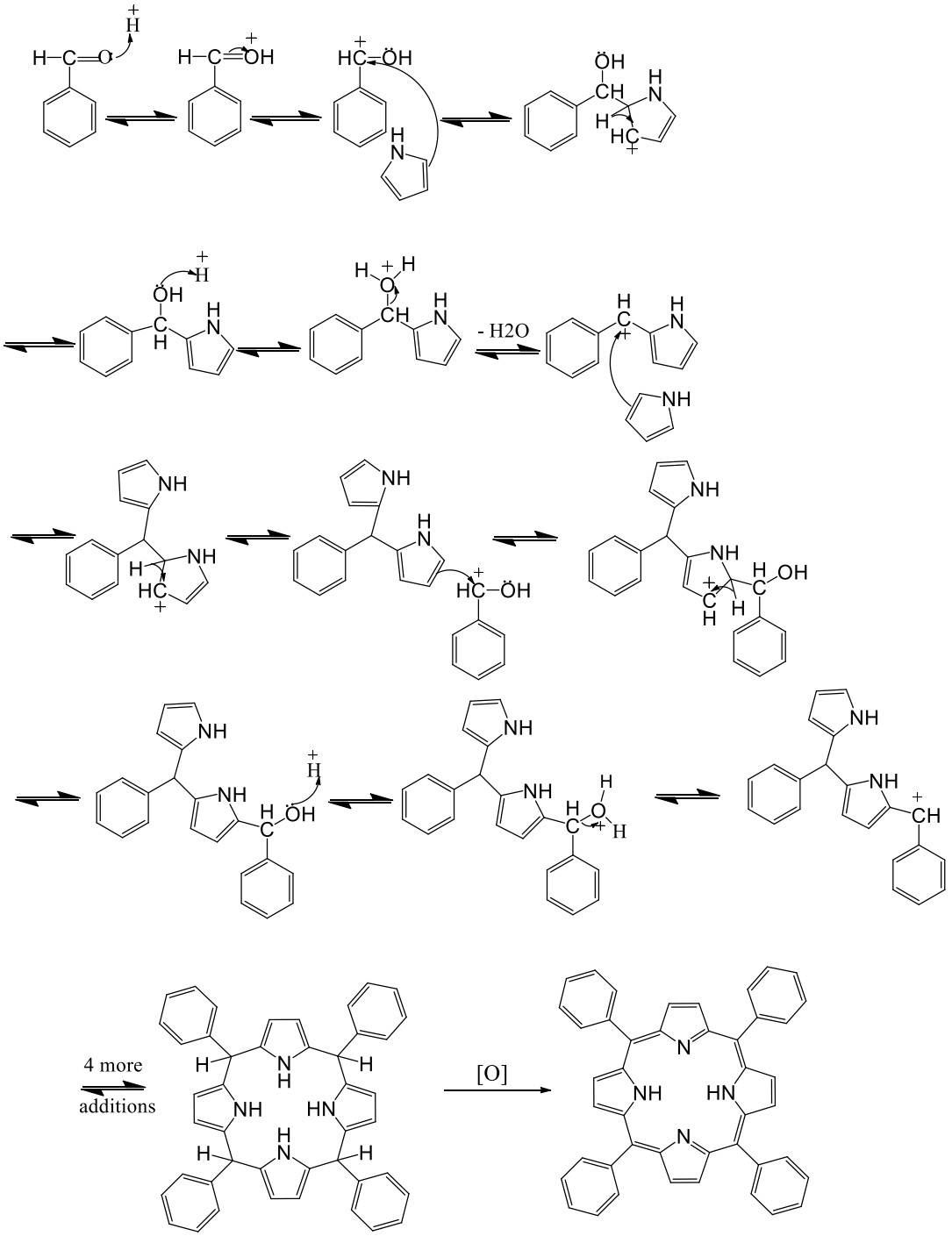

Scheme 3.6 - The mechanism of tetraphenylporphyrin synthesis under acidic conditions. (F. Algarra, M. A. Esteves, V. Fornes, H. Garcia, J. Primo, ***New. J. Chem.***, 1998, 22, 333).

3.2.2 Synthesis of tin(IV) (5,10,15,20-tetraphenylporphyrin) dihydroxy ($SnTPP(OH)_2$)

$SnTPP(OH)_2$ was synthesised by using the Wohrle method.[76] TPP and tin(II) chloride dihydrate were stirred and refluxed in pyridine for one hour **(Scheme 3.7)**.

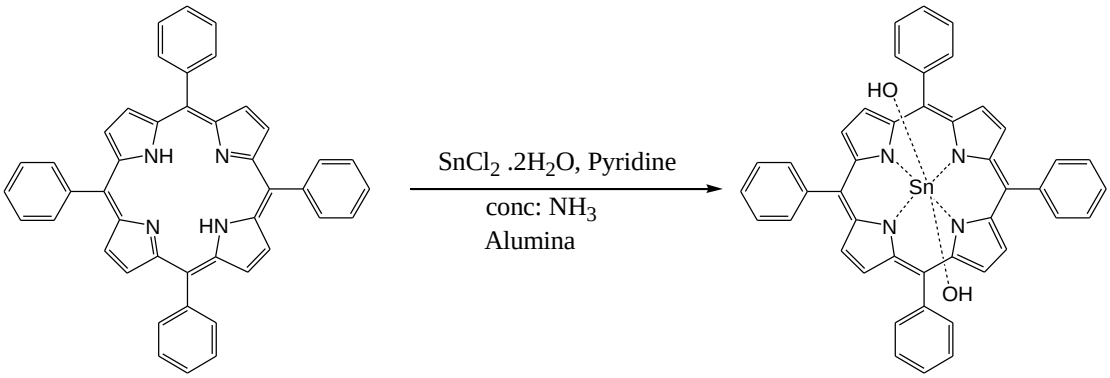

9

Scheme 3.7 The synthesis of tin (IV) (5,10,15,20-tetraphenylporphyrin) dihydroxy **9**.

After cooling to 50˚C concentrated ammonia was added carefully and left stirring for an hour. Precipitation was carried out by adding water to the slurry. Precipitates were collected by filtration and washed with water. Then the solid was digested with chloroform, which dissolved the tin porphyrin complex. After filtration the filtrate was dried over anhydrous sodium sulphate to remove water. For purification the filtrate was concentrated and passed through a short neutral alumina column with activity V. The purple band of crude product was eluted with chloroform. For further purification, recrystallisation was carried out, using chloroform and hexane. The confirmation of the product was provided by IR spectroscopy, in which the appearance of two peaks at 3646 cm^{-1} and 3109 cm^{-1} confirmed the presence of the –OH ligands. Also ^1H NMR showed a high field broad peak at -6.79 ppm corresponds to the –OH ligands bound to the tin (IV), along with 2 multiplets and singlet corresponds to the pyrrole and phenyl protons. Further successful functionalisation was provided by UV/Vis spectroscopy, in which soret band of the starting material was shifted to 427 nm from 419 nm as shown in **(Figure 3.7)**. The mass spectroscopy also agreed the insertion of tin metal with axial ligands was a success and showed a molecular ion peak at 749, which corresponds to $[M\text{-}OH]^+$.

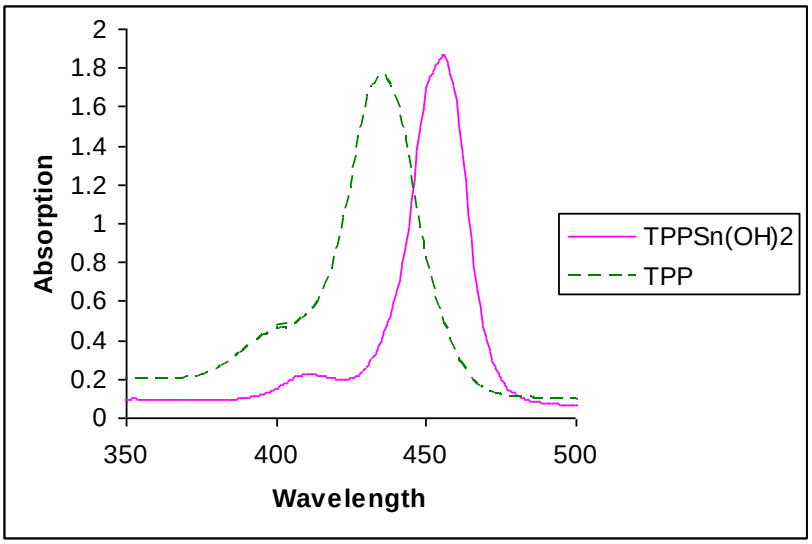

Figure 3.7 - UV/Vis spectrum of TPP and $SnTPP(OH)_2$.

It has been shown that in tin(IV) porphyrin complexes, hard metal centres endow strong oxophilic character. Therefore, carboxylate complexes of acids can be effectively and rapidly synthesised by mixing a large excess of free carboxylic acids with dihydroxy complexes of tin(IV) porphyrins.[78] Therefore, for the structural confirmation of dihydroxy tin(IV) porphyrin complex, we treated our product with an excess of carboxylic acids. The proposed mechanism for the formation of tin-carboxylate complexes is shown in **(Scheme 3.8)**.

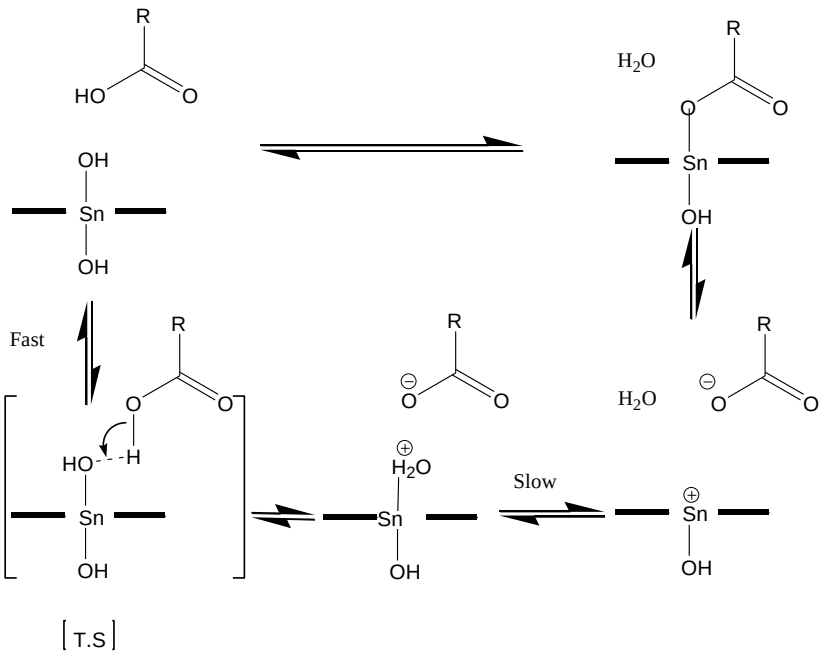

Scheme 3.8 - Proposed mechanism for tin(IV) carboxylate complexes of porphyrin.

3.2.3 Synthesis of tin(IV) (5,10,15,20-tetraphenylporphyrin) diacetoxy ($SnTPP(OCOCH_3)_2$)

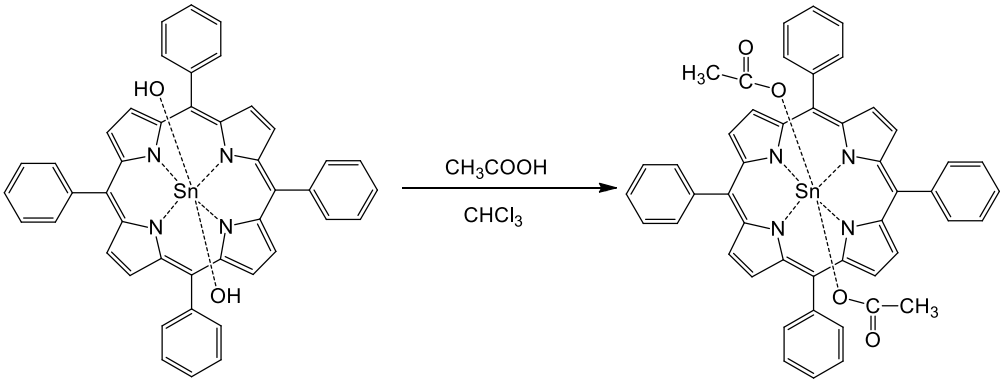

10

Scheme 3.9 - Synthesis of tin(IV) (5,10,15,20-tetraphenylporphyrin) diacetoxy **10**.

The compound **10** was chosen as a model compound, the main factor which determined our selection, was the ease with which replacement of hydroxy ligand can be easily observed from the carbon and proton NMR.

$SnTPP(OCOCH_3)_2$ **10** was synthesised by mixing acetic acid with a solution of $SnTPP(OH)_2$ in chloroform. This mixture was stirred 15 minutes. After 15 minutes, anhydrous Na_2SO_4 was added and stirring was continued for another 15 minutes. Then the solution was filtered. The solvent was removed using a rotary evaporator. The formed purple crystals were recrystallised with hexane. **Scheme 3.9** shows the synthetic procedure. Confirmation of the product was carried out by comparing the ^{13}C NMR spectra of the compound **10** with acetic acid. As shown in **(Figure 3.9)**, compound **10** acetoxy group carbonyl (a) showed peak shift from 178.0 ppm (C=O peak (a) for acetic acid) to 168.3 ppm, as a result of porphyrin shielding region. Thus, the appearance of peak at 168.3 ppm confirms the replacement of hydroxy ligand with acetoxy ligand. ^{1}H NMR also showed 6 protons of two methyl groups peak at -1.01 ppm and phenyl protons gave two multiplets in the range of 8.30-8.32 and 7.80-7.86 ppm, along with the pyrrole protons peak at 9.21 ppm. The integration of proton spectrum confirmed the presence of **10** i.e. tin(IV) porphyrin with the two acetoxy axial ligands. IR spectroscopy also showed results in the agreement with literature values. All above analytical techniques showed the confirmation of compound **10**

with two axial acetoxy ligands. However, mass spectroscopy showed the presence of only one acetoxy axial ligand in a molecular ion peak at 790 $[M\text{-}OCOCH_3]^+$. Then, the decision was made as to perform the X-ray crystallography of the compound **10** to confirm the presence of two acetoxy axial ligands. The obtained X-ray crystallography results confirmed the presence of the two axial ligands non-covalently attached to the tin porphyrin. The structural representation of $SnTPP(OCOCH_3)_2$ determined by X-ray crystallography is shown in **(Figure 3.8)**. The obtained crystal data and other information determined by X-ray crystallography are shown in the appendix at page 158. Crystals were prepared by dissolving the purple product in chloroform and left for slow evaporation in the fume hood. Thus, despite seeing only one ligand in mass spectroscopy, the ^1H NMR integration, ^{13}C NMR complete shift and X-ray crystallography results confirmed the presence of the two acetoxy axial ligands. Later, the literature was found, which proved the presence of $(M\text{-}L)^+$ is common in the tin porphyrin diaxial complexes.[77]

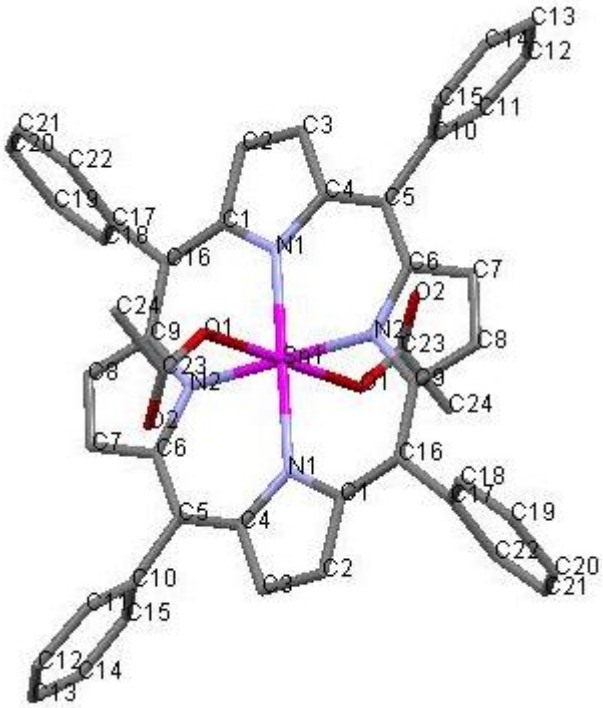

Figure 3.8 - The X-ray structure of tin(IV) (5,10,15,20-tetraphenylporphyrin) diacetoxy **10**.

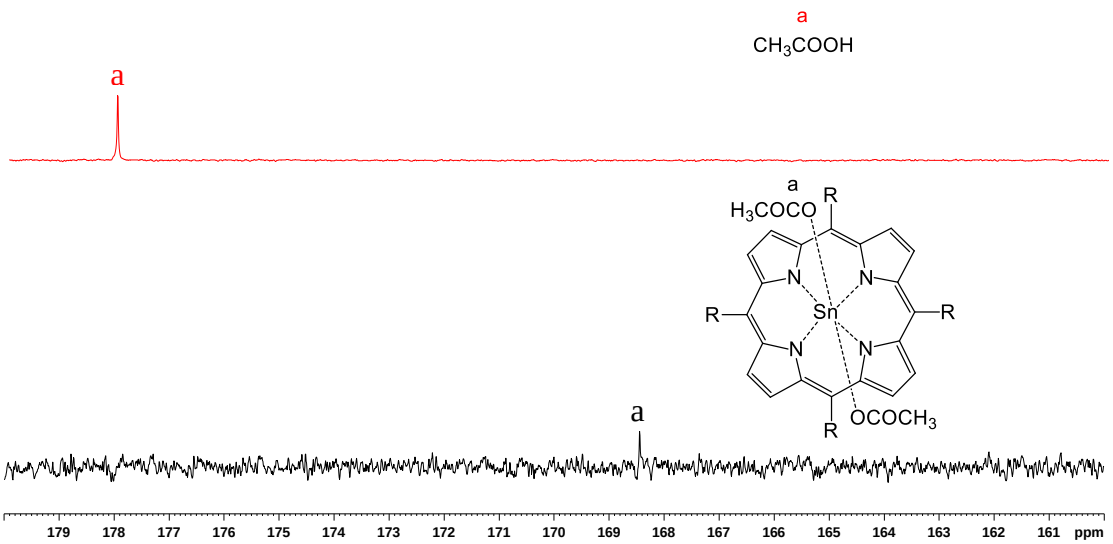

Figure 3.9 - ^{13}C NMR of acetic acid and tin(IV) (5,10,15,20-tetraphenylporphyrin) diacetoxy **10** (In figure R = $-C_6H_5$), Showing the complete shift of the C=O peak.

3.2.4 Synthesis of tin(IV) (5,10,15,20-tetraphenylporphyrin) dibenzoxy ($SnTPP(OCOC_6H_5)_2$)

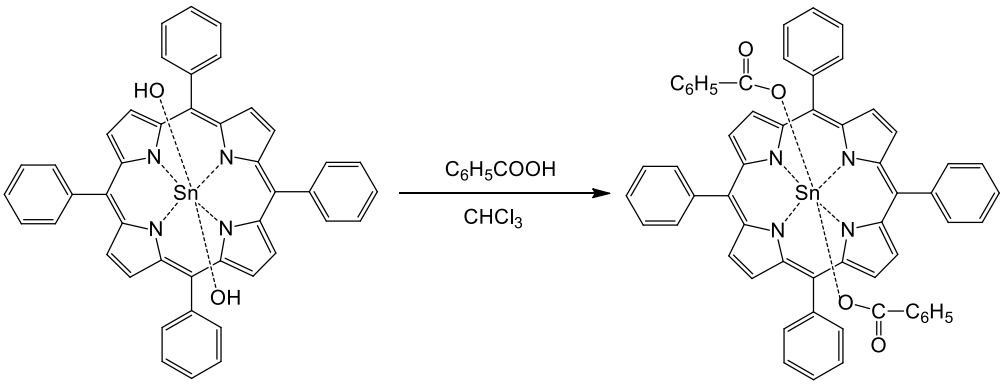

11

Scheme 3.10 - Synthesis of tin(IV) (5,10,15,20-tetraphenylporphyrin) dibenzoxy **11**.

$SnTPP(OCOC_6H_5)_2$ was also synthesised by mixing the benzoic acid in the solution of $SnTPP(OH)_2$ in chloroform. This mixture was stirred magnetically for 15 minutes. After 15 minutes, anhydrous Na_2SO_4 was added and stirring was continued for another 15 minutes. Then the solution was filtered and the solvent was removed using a rotary evaporator. Formed purple crystals were recrystallised with hexane. **Scheme 3.10** represents the synthetic procedure. Nuclear magnetic resonance for both proton

and carbon were performed, confirming the identification of the product. The ^{1}H NMR spectrum showed a multiplet at 4.87-4.93 ppm which was corresponding to the ortho protons and multiplets at 6.67-6.71 ppm, 6.32-6.38 ppm, representative of para and meta protons of axial phenyl group and integration confirmed the presence of the both ligands. Further confirmation was carried out by ^{13}C NMR, the presence of a peak at 162.8 ppm for C=O due to the tinporphyrin shielding. Mass of the product was determined by the MALDI-TOF technique which showed the expected molecular weight of the product 853$(M\text{-}OCOC_6H_5)^+$ i.e. $(M\text{-}L)^+$ similar to the compound **10**. However, for further confirmation of the presence of the both ligands, it was decided to perform X-ray crystallography. The molecular structure of the product is shown in **(Figure 3.7)**. The obtained data confirmed the presence of the two axial ligands. Crystal data and other information determined by crystallography are shown in the appendix at page 158.

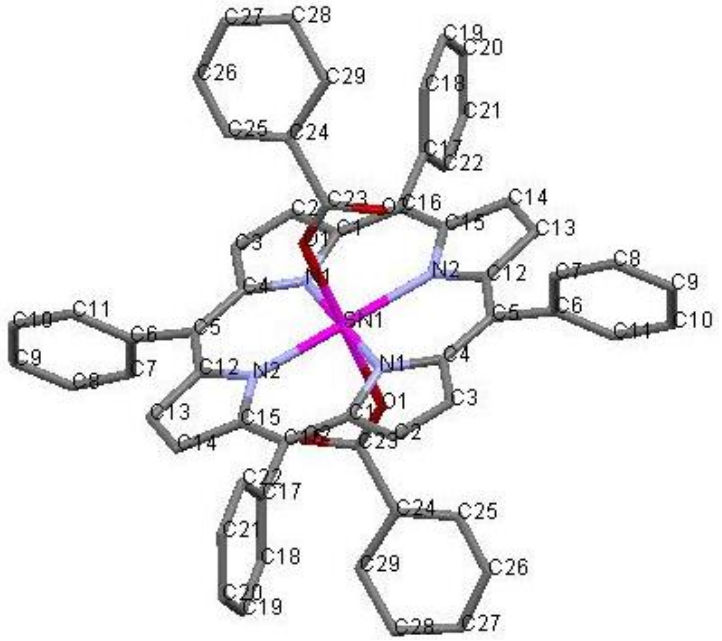

Figure 3.10 - The X-ray structure of tin(IV) (5,10,15,20-tetraphenylporphyrin) dibenzoxy **11**.

From the above model compounds results, it was concluded that the self-assembly of the C=O group to the tin porphyrin, could be simply confirmed using ^{1}H, ^{13}C NMR

and mass spectroscopy (in which the presence of $(M-L)^+$ is obvious and is consistent with the literature).[78]

3.3 Self-assembly of dendrons with acceptor unit

In order to achieve a self-assembled dendritic model system, self-assembly between the dendron and the acceptor unit (reaction centre) was the preliminary step. As mentioned beforehand, a supramolecular approach was employed for self-assembly between the dendron and acceptor unit. To obtain the strong intermolecular interaction, metal coordination self-assembly was used between dendron and the acceptor unit.

The first attempt, in order to achieve self-assembly between carboxylic acid core ligand i.e. dendron and tin(IV) (5,10,15,20-tetrapenylporphyrin) dihydroxy, was an unsuccessful attempt. After the several unsuccessful attempts, it was decided to synthesise another dendron batch using potassium carbonate instead of triethylamine as a base and after the synthesis of G-0.5 **1**, the successful self-assembly was carried out between dendron G-0.5 **1** and tin(IV) (5,10,15,20-tetraphenylporphyrin) dihydroxy **9** was a success. After this successful self-assembly, further batches of dendrons up to G-4.0 were synthesised and used for self-assembly with **9**.

Self-assembly between dendrons and the acceptor unit i.e. dihydroxo(5,10,15,20-tetraphenylpoprhyrin)tin(IV) was carried out by simply stirring the different generations of dendron, containing ester terminal groups with tin(IV) porphyrin in the chloroform solvent. The self-assembled complexes of different generation of dendrons with tin(IV) (5,10,15,20-tetraphenylporphyrin) dihydroxy **9** are shown in **(Figure 3.11)**.

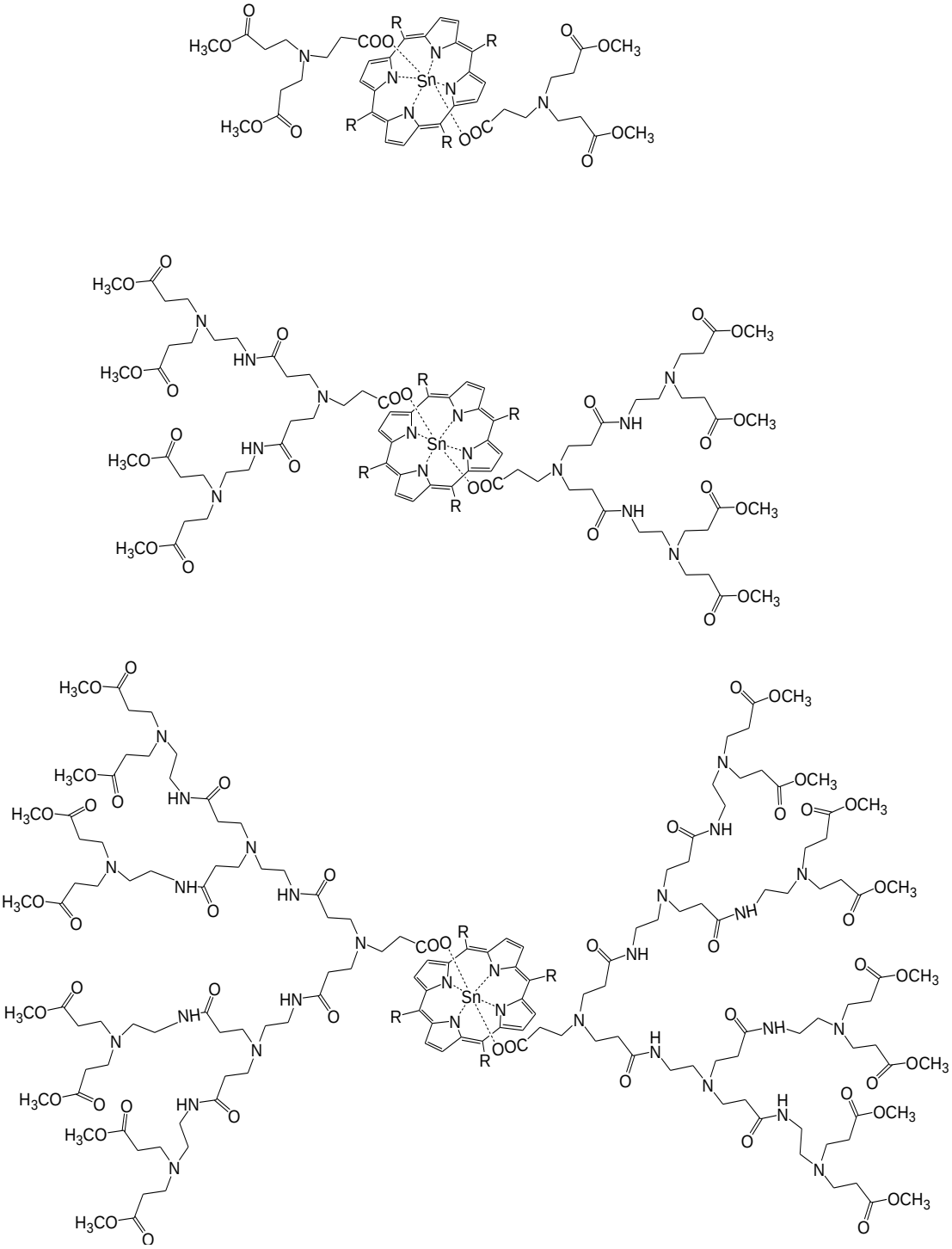

Figure 3.11 - Self-assembled complexes of G-0.5, G-1.5 and G-2.5 with tin(IV) (5,10,15,20-tetraphenylporphyrin) dihydroxy.

3.3.1 Self-assembly of dendron G-0.5 (1) with tin(IV) (5,10,15,20-tetraphenylporphyrin) dihydroxy (9)

For self-assembly $SnTPP(OH)_2$ (1 mole) and dendron G-0.5 (2 moles) were dissolved in $CHCl_3$ and stirred for an hour. After an hour, the reaction mixture was passed through a small plug of anhydrous sodium sulphate. A purple sticky product was formed after removing the solvent using a rotary evaporator. The synthetic procedure for the self-assembly is shown in **(Scheme 3.11)**.

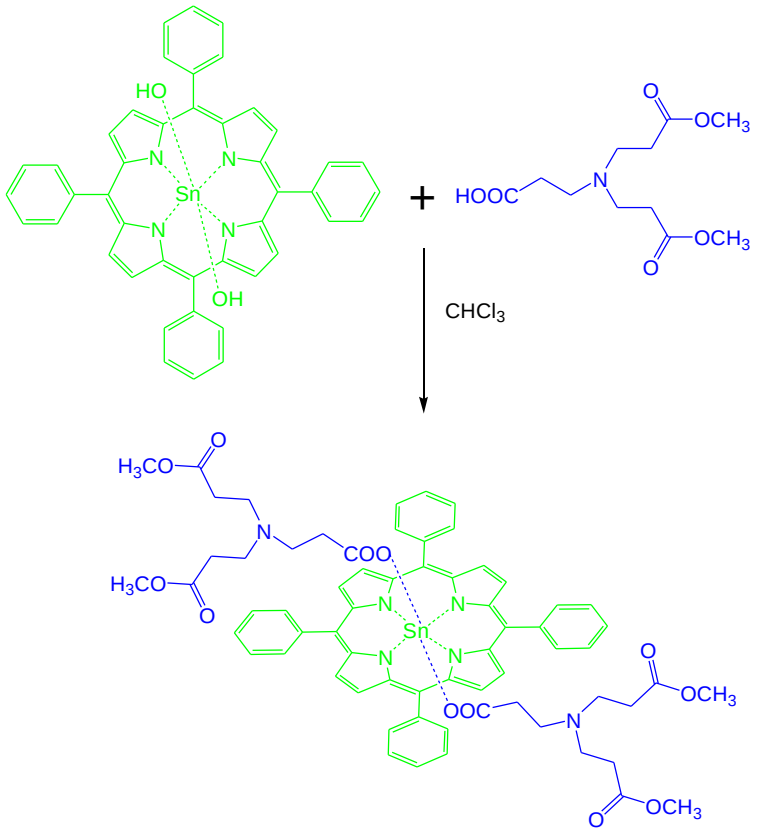

12

Scheme 3.11 - Reaction scheme for self-assembly between G-0.5 and $SnTPP(OH)_2$.

The characterisation of the self-assembled complex **12** was carried out using ^{13}C NMR, in which disappearance of core acid carbonyl peak (a) at 178.9 ppm and the appearance of peak at 168.5 ppm (a') corresponds to the non-covalently bonded carbonyl group to the tin porphyrin (similar to acetoxo (5,10,15,20-tetraphenylporphyrin)tin(IV) **10**) provided evidence for the self assembly. ^{13}C NMR also showed two peaks (f' and f'') for terminal ester group carbonyl as shown in

(Figure 3.12). These two peaks could be caused by the two different conformations of the self-assembled complex (open and closed conformations), when NMR was performed at 50° C, only one peak was visible, which confirmed the presence of dynamic conformations resulting in different C=O environments. Similarly ^{1}H NMR showed up field shift for methylene protons next to the core due to their appearance in the porphyrin shielded region. The terminal ester group also showed a signal characterisation peak at 3.66 ppm for ester terminated dendrimers and the integration confirmed the presence of the two axial dendron ligands to tin(IV) porphyrin. The mass of the product was investigated using MALDI-TOF technique, which showed molecular weight of the product 991[M-G(0.5)]$^{+}$ as expected ((M-L)$^{+}$). Unfortunately, the X-ray crystallography could not be performed due to the stickiness of the dendrons. However, as explained in the **(section 3.2.3)**, it can be concluded that despite only seeing one ligand in mass spectroscopy, the ^{1}H NMR integration and complete C=O shift from 178.9 ppm to 168.5 ppm, along with no free dendron peak (C=O peak at 178.9 ppm) in the ^{13}C NMR, confirms the presence of two dendron axial ligands. Further confirmation of product was provided by IR data, in which the binding mode of carboxylate ligands to the tin ion showed peaks at 1640-1649 cm^{-1} and 1430-1470 cm^{-1} consistent with the reported literature.[79,80] This combined with UV/Vis spectrum where a slight shift of the Soret band from 426 to 424 nm as shown in **(Figure 3.13)**, confirmed that the self-assembly was a success.

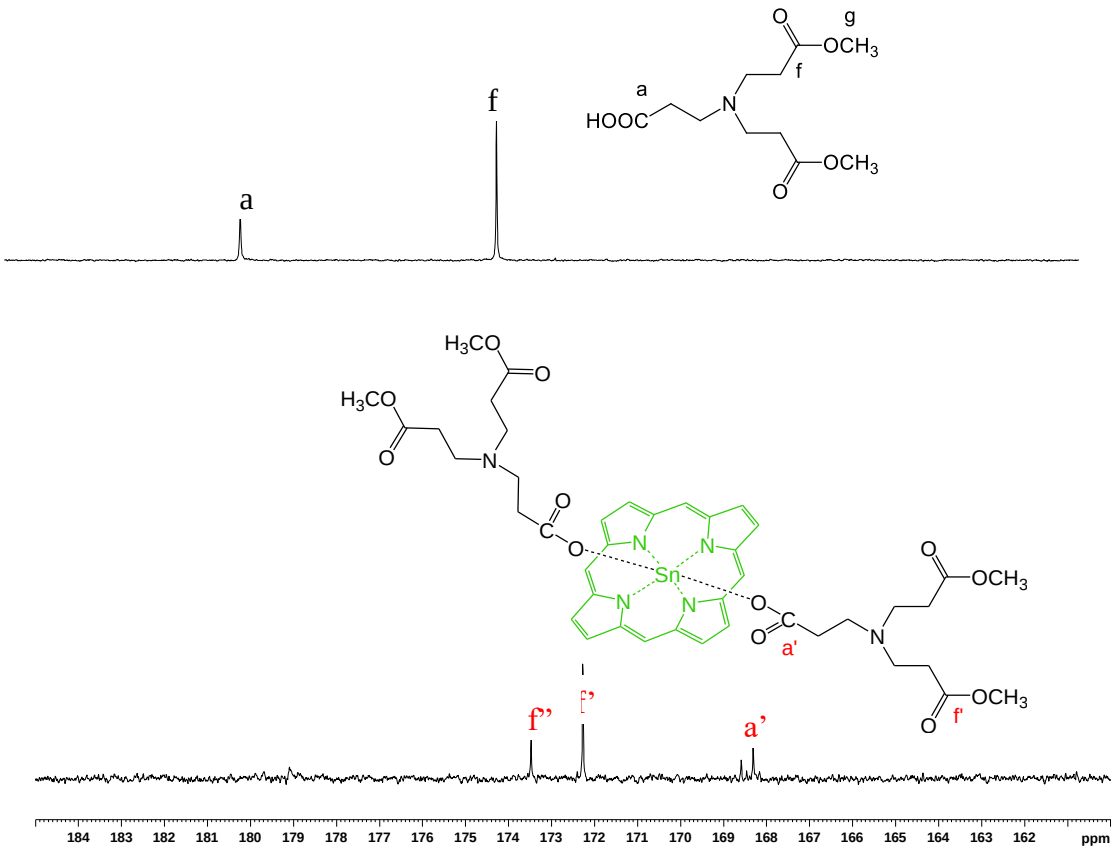

Figure 3.12 - ^{13}C NMR of dendron G-0.5 **(1)** and self-assembled complex (**12)** in range 160-185 ppm.

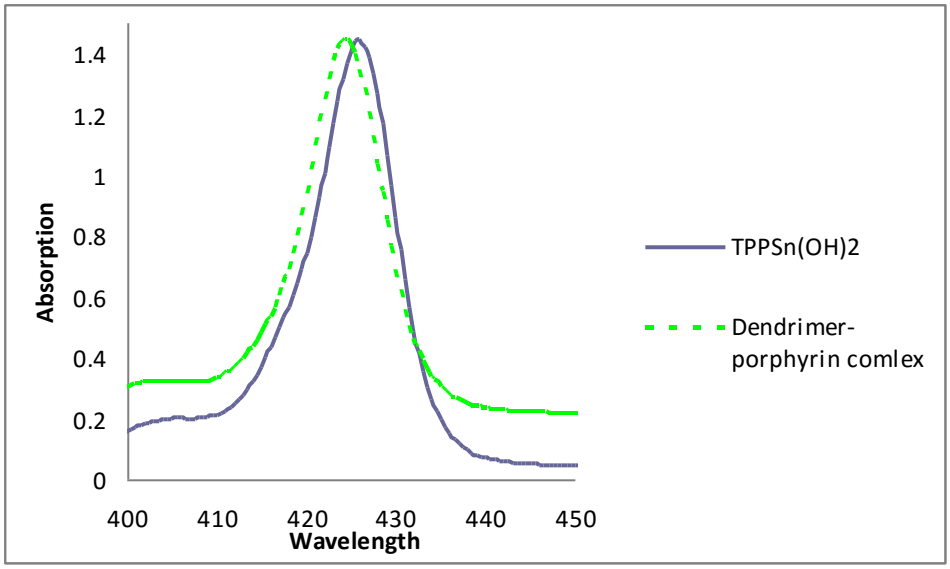

Figure 3.13 - Overlay of TPPSn(OH)$_2$ and self-assembled dendron-porphyrin complex **12** in range 400-450 nm.

Self-assembly between bigger generation dendrons and dihydroxy tin(IV) porphyrin complexes were also carried out successfully using a similar procedure. Obtained ^{13}C NMR and molecular weights for the model compound **10** and self-assembled complexes of bigger generation dendrons are shown in **(Table 3.1)**.

	C=O δ ppm	***Expected molecular weight g mol^{-1}***	***Measured molecular weight (M-L)$^{+}$* g mol^{-1}***
Dendron G-0.5	178.9	261	261
Porphyrin + OCOCH$_3$	168.5	850	790
Porphyrin + G-0.5	168.3	1252	991
Porphyrin + G-1.5	168.7	2053	1392
Porphyrin + G-2.5	168.3	3056	2194

Table 3.1- C=O chemical shift and molecular weights for compound **10** and self-assembled complexes of different generation dendrons. (^{1}H NMR confirmed the presence of two ligands. However, mass spectrum only showed (M-L)$^{+}$ as consistent with literature report for mass spectroscopy).*[77]

3.4 Self-assembly of dendron with donor unit

For the self-assembly between dendron and the donor unit, a metal-coordination approach was also applied. Metalated porphyrin was selected as a donor group because of its structural similarities with the chlorophyll molecule. Also, metalated porphyrin has an ability to bind a large number of electron donating species particularly amines. Therefore, by choosing zinc porphyrin as a metal centre, interactions with different generations of dendrons containing amine groups can be quantitatively measured, by observing changes in the UV/Vis absorption, which provide a very sufficient and precise measurement. Upon zinc insertion, the porphyrin loses its two protons and zinc metal makes a coordination complex with the four inner nitrogen atoms of porphyrin ring. The fifth coordination site of zinc will allow the binding of a single axial ligand. Hence, after the insertion of the metal into the porphyrin, the metal centre acts as a Lewis acid by accepting a lone pair of electrons from a ligand and amines can easily donate their lone pair to zinc metal by forming an axial ligand. Upon ligation, the soret band shows bathochromic shift (418 nm to 428 nm) as shown in **(Figure 3.14)**.

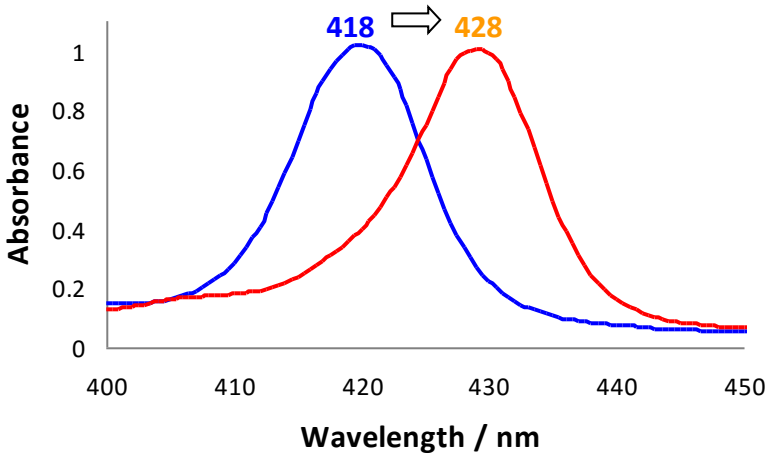

Figure 3.14 - Overlay of TPP Soret bathochromic band shift upon ligation.

Zinc can be easily inserted into the porphyrin by gently heating free porphyrin with zinc acetate for 30 minutes as shown in **(Scheme 3.12)**.

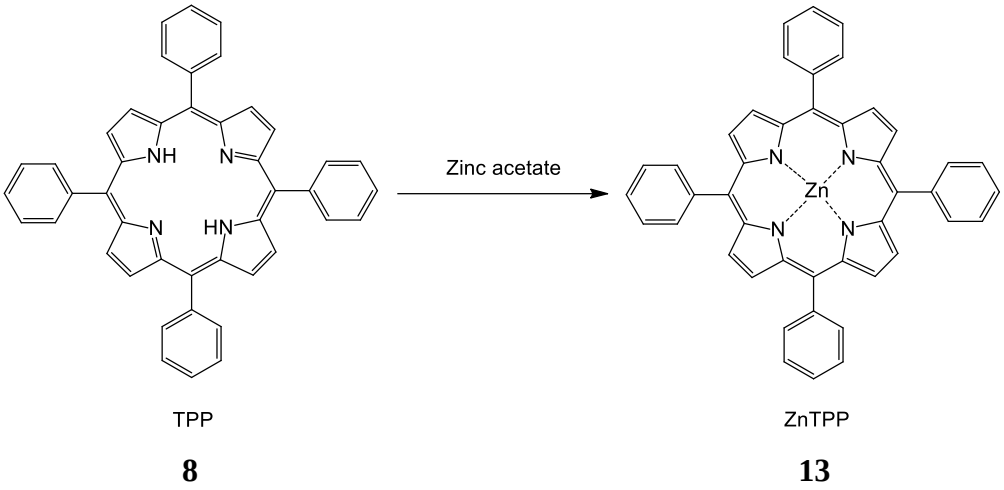

Scheme 3.12 Zinc ion insertion into tetraphenylporphyrin.

Our aim in this section is to calculate the binding interactions for later concentration dependent light-harvesting (LH) experiments particularly at the low concentrations. These binding interactions were measured via self-assembly between a dendron and the donor unit which is a zinc tetraphenylporphyrin as shown in **(Figure 3.15)**.

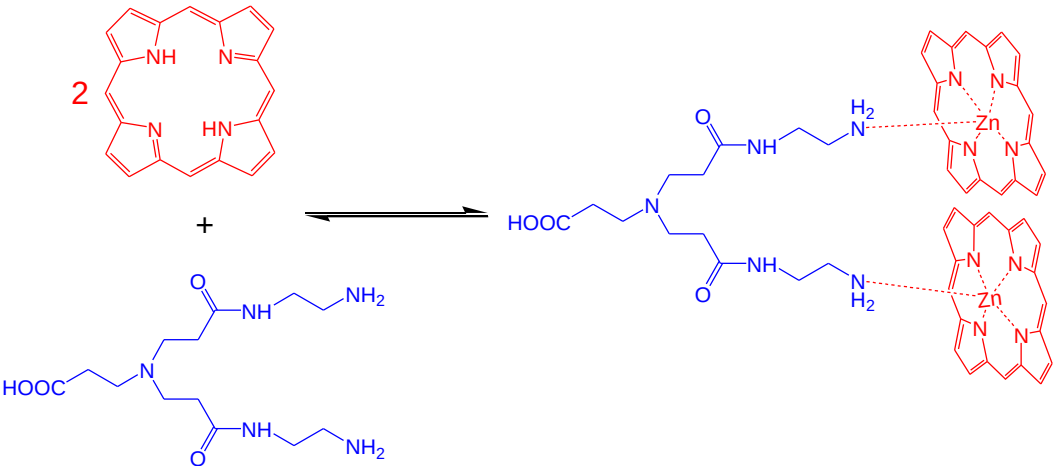

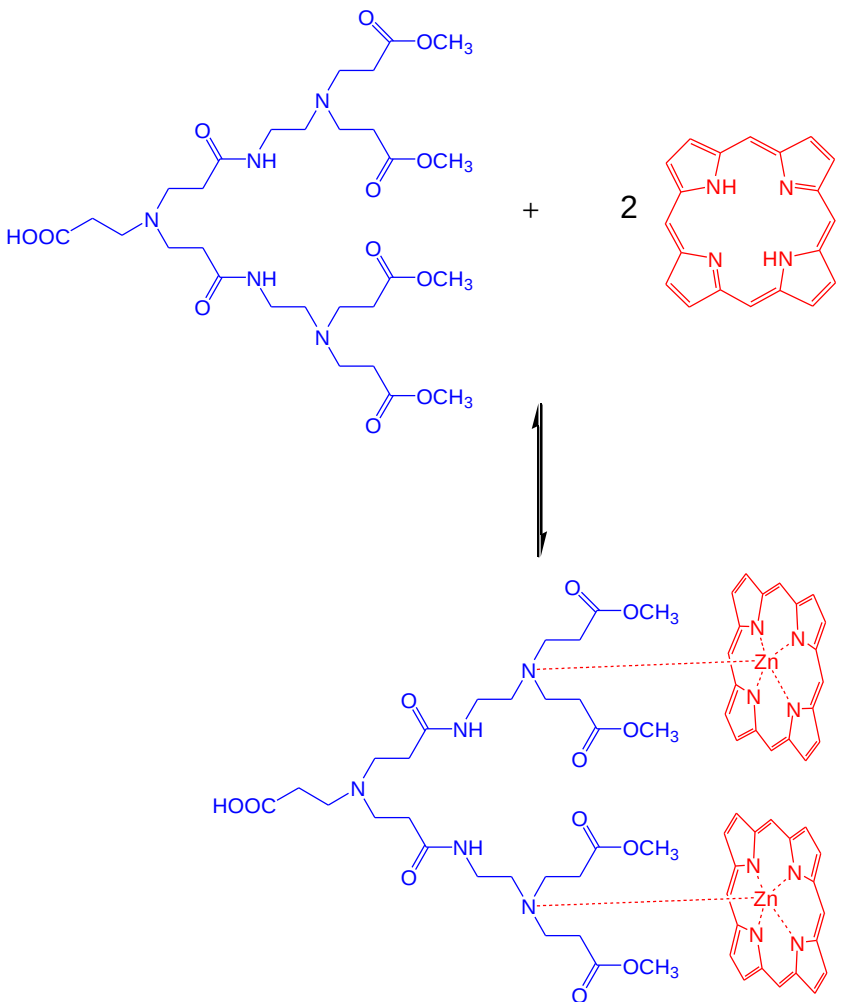

Figure 3.15 - Proposed self-assembly between dendron with terminal ester or amine groups and ZnTPP using metal coordination.

3.4.1 Synthesis of zinc tetraphenylporphyrin (ZnTPP)

Insertion of zinc into TPP was carried out by simply heating TPP with an excess of zinc acetate in chloroform for half an hour as shown in **(Scheme 3.12)**. After half an hour the unreacted zinc acetate was removed by filtration through filter paper and the purple product was obtained after the removal of the solvent.

Confirmation of the product was carried out using ^{1}H NMR, which showed the disappearance of high the shielded peak at -2.07 ppm corresponding to the inner protons of the porphyrin ring. Further confirmation of the product was provided by UV/Vis spectroscopy as shown in **Figure 3.16** where four Q bands of starting material were replaced by two Q bands. The molecular peak at 677 in the mass spectrum also confirmed the insertion of the zinc metal in the porphyrin ring.

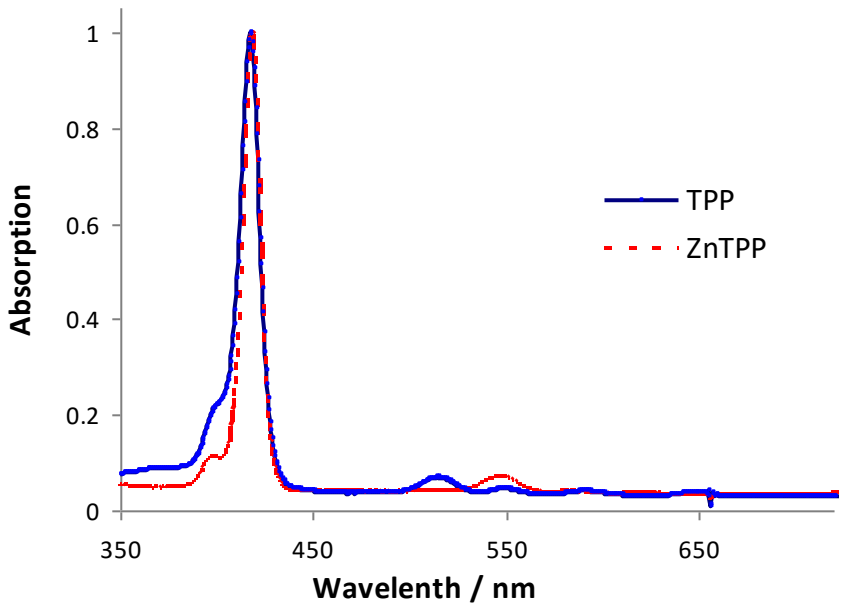

Figure 3.16 - Overlays of TPP and ZnTPP in the UV/Vis spectrum in range 350-650 nm.

After the insertion of the zinc inside the porphyrin, the next consideration was the calculation of the binding interactions between the different generations of dendrons with the zinc porphyrins. Calculation of the binding interaction is an important step in the self-assembled light-harvesting systems. To observe the light-harvesting between self-assembled complexes the K_a (association constant) should be in the range of 10^4 – 10^5 M^{-1} at low concentrations i.e. 10^{-5} - 10^{-6}M. These calculations of binding interactions were carried out using UV titrations. In order to determine binding interactions by UV/Vis spectroscopy, concentration plays an important role. Therefore, concentration must allow binding to take place in the UV/Vis absorption range. Zinc porphyrin concentration was chosen by using Beer Lambert plot. From this plot, 10^{-6}M zinc porphyrin concentration was chosen, which showed absorption at 1.0. This concentration was a good fit within the range of UV/Vis spectrometer. After a certain number of attempts, 10^{-2}M and 10^{-3}M concentrations were found appropriate for dendrons. For whole generation dendrons a few drops of methanol were added to resolve the solubility problems.

3.4.2 Binding interactions between primary and tertiary amines with ZnTPP using UV/Vis spectrometer

The dendrons contain two types of ligands, primary and tertiary amines. Thus, before carrying out the binding interactions between dendron and zinc porphyrin, it was decided to use simple primary and tertiary amines as model compounds. For the calculations of the model compounds binding interactions, firstly, a 10^{-6}M stock solution of the zinc porphyrin was made for titrations, using dichloromethane previously stirred with potassium carbonate to remove any traces of acid. Then, to find the binding constant between the zinc porphyrin and ethylenediamine (EDA) or Triethylamine, this stock solution was used to prepare titre solutions, to ensure the binding experiment was run at a constant concentration of zinc porphyrin.

The titrations were monitored by using a UV/Vis spectrophotometer, in which 2 mL stock solution was titrated against 5-20 microlitre of ligands. Upon titre addition, the zinc porphyrin Soret band showed a shift from 418 nm to 428 nm, as shown in **(Figure 3.17)**. By plotting this change in absorption λ_{max} (y) against the moles of ligand added (x), the association constant can be calculated using a curve fitting program (sigma plot).

$$y = \frac{B_{\max} x}{K_a^{-1} + x} \qquad \text{----------(4)}$$

Where K_a is the association or binding constant, and B_{max} is the maximum bound. Using sigma curve fitting software, the dissociation constant (K_d), which is reciprocal of association constant, was calculated. Each titration was repeated several times due to sensitivity of the equilibrium process and an average K_a value was calculated.

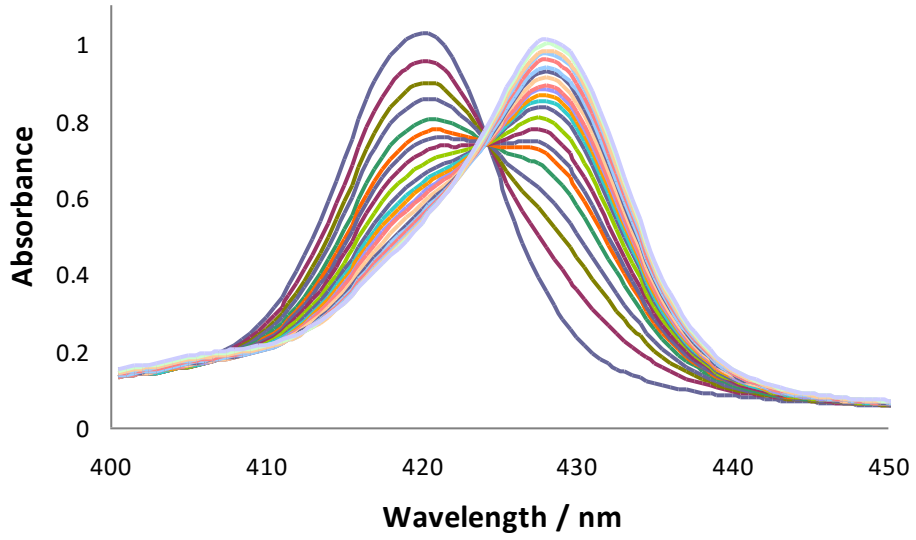

Figure 3.17 - Shifting of the Soret band from 418 nm to 428 nm.

EDA was chosen as a model compound for the terminal primary amines and Triethylamine was also studied as a model for the interior tertiary amines dendrons. The binding constant for triethylamine should be stronger than EDA because it is more basic. A binding constant (K_a) $2.4x10^4$ M^{-1} was calculated for zinc porphyrin/ EDA interactions as shown in **(Figure 3.18)**.

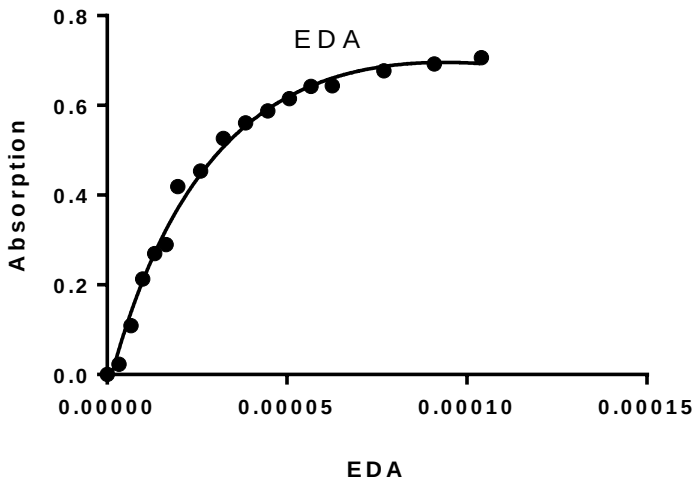

Figure 3.18 - Absorption vs. [EDA] for zinc porphyrin.

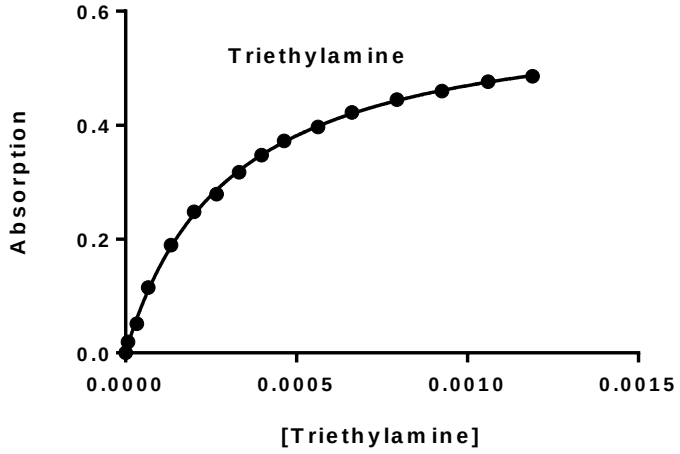

Figure 3.19 - Absorption vs. [Triethylamine] for zinc porphyrin.

EDA has 2 primary amine groups therefore each amine group has binding constant $1.2x10^4$ M^{-1}. A similar titration for Et_3N was used to obtain K_a of 3000 M^{-1}. This K_a value was much lower than expected, particularly considering Et_3N's extra basicity. The reduced binding could be due to the steric factors. Steric factors play an important role in terms of binding interactions. Strong binding occurs when the nitrogen lone pair is perpendicular to the plane of the porphyrin ring, as this maximises the overlap between nitrogen lone pair and empty orbital of zinc. Therefore, if this overlap is disturbed by steric factors, the binding constant would be affected.

Steric effect caused by ethyl groups in triethylamine limits overlap, which means weaker binding. From the above calculated binding constant results, it was expected that dendrons with primary amine terminal groups i.e whole generation dendrons would show better binding interactions with zinc porphyrins than half generation (tertiary amine terminated) dendrons. Before calculating the binding constant using dendrons, the decision to calculate the binding interactions between compounds with structural similarities to dendrons was made, as shown in **(Figure 3.21)**. The compound A (N-Acetylethylenediamine) mimics the terminal amine groups in dendrons, was ordered from Sigma Aldrich. Compound B mimics the internal tertiary amines and was formed by adding compound A to methyl acrylate, which was left for 12 hours at room temperature in methanol. The reaction scheme for synthesis of compound B is shown in **(Scheme 3.14)**.

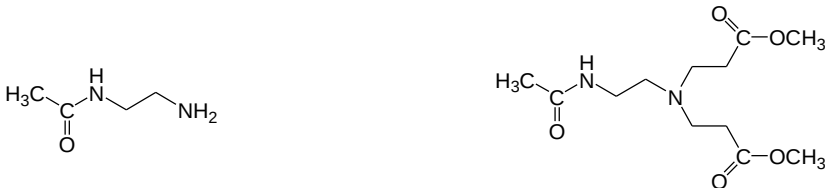

A (Mimics terminal amine groups) B (Mimics internal tertiary amines)

Figure 3.21 - Structural representation of N-Acetylethylenediamine A and B.

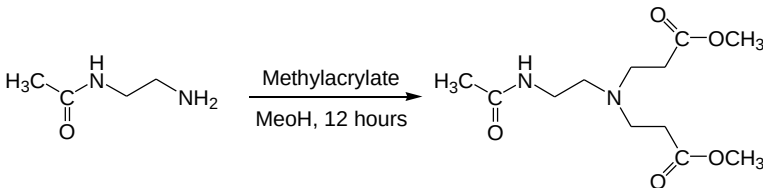

B

Scheme 3.14 - Synthesis of compound B.

Confirmation of the identity of compound B was carried out using ^{1}H NMR, in which the methoxy group showed a signal at 3.66 ppm, along with the singlet at 2.01 ppm and quartet at 3.31 ppm for methyl and methylene groups next to the amide group. Further confirmation was provided by ^{13}C NMR, in which the presence of 2 signals at 173.1 ppm and 170.0 ppm confirmed the synthesis of B. The molecular peak at 275 (MH^{+}) in the mass spectrum also confirmed the synthesis was a success.

After the successful synthesis of the compound B (containing similar structure to ester terminated half generation dendron) and compound A (similar structure to amine terminated dendrons), these compounds were titrated against ZnTPP for the calculation of the binding constant. It was expected that compound B would show better binding than compound A, on the basis of electronic effect. However, it is more sterically hindered than compound A. Therefore, at this point it is very difficult to know what effect it would have.

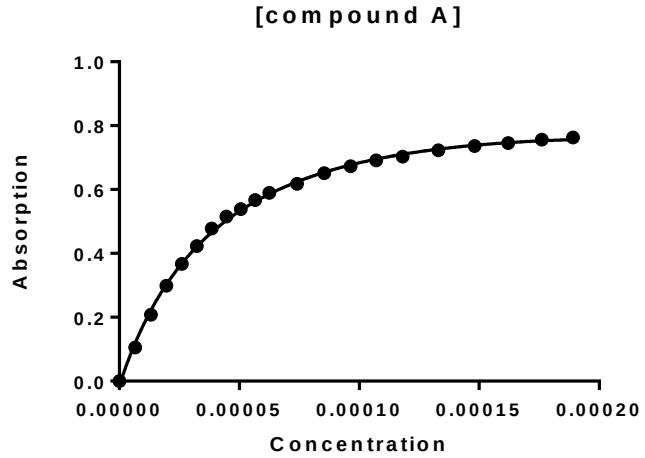

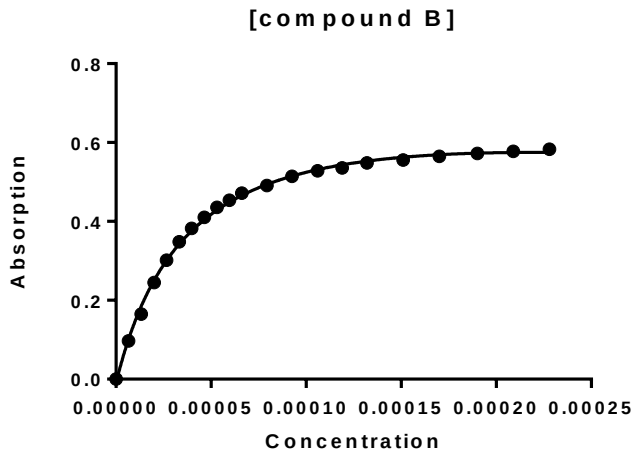

Figure 3.21 - Absorption Vs [compound A and B].

For the compound A, K_a~ $2.0x10^4$ $M^{-1}$was calculated from the binding curve and Ka~ $2.4x10^4$ M^{-1} calculated for the compound B. The calculated binding constants for both compounds were roughly same, which means steric factors are playing a less significant role towards binding. Thus, this behaviour of compound B is ascribed due to the electronic environment around the nitrogen atoms.

1 electron releasing group 3 electron releasing group

Figure 3.22 - Representing the difference between primary and tertiary amine.

In a tertiary amine, the electron density around the nitrogen atom increases due to the electron releasing property of the alkyl groups attached to the nitrogen atom as show in **(Figure 3.22)**. Therefore, in compound B the nitrogen atom binds strongly, by following the trend of highest electron density on the donating nitrogen atom. Thus, it would be expected that the ester terminated dendrons would possess slightly higher binding constants than amine terminated dendrons assuming no steric effects. However, steric effects could affect the binding in the bigger generation dendrimers.

3.4.3 UV titrations for half and whole generation dendrons

For the ester and amine terminated dendrons, 10^{-3} M and 10^{-2} M concentrations were found appropriate for the measurement of binding interactions. Solubility of the whole generation (amine terminated) dendrons was improved by adding 0.5 mL of methanol to the 99.5 mL solution of DCM. Methanol is used as a coordinating solvent. Before calculating the interactions between amine terminal dendrons and zinc porphyrin, titrations using dilute methanol (same concentration as above) were carried out to observe the effect of methanol towards binding. Titrations between methanol and zinc porphyrin, resulted in the binding constant $k_a \sim 3x10^3$ M^{-1}. This binding constant value i.e 10^3 M^{-1} is 10 times lower than the calculated binding constant value for compound A (10^3 M^{-1}), which means amine binding is 10 times stronger than methanol. In addition, the concentration of used methanol is 10 times less than for RNH_2 used, which means methanol should not play any role towards binding interactions at the used concentration. The same concentration of methanol was used for all whole generation dendrons.

When G-0.5 dendron was titrated against zinc porphyrin, no bathochromic shift was observed for zinc porphyrin. This could be due to the formation of zwitterion as shown in **(Figure 3.23)**. The higher generation dendrons showed a significant bathochromic shift with the presence of an isosbestic point. The calculated values of the binding constants for dendron generations from 1.5 to G-4.0 are summarised in **Table 3.2** and **(Table 3.3)**.

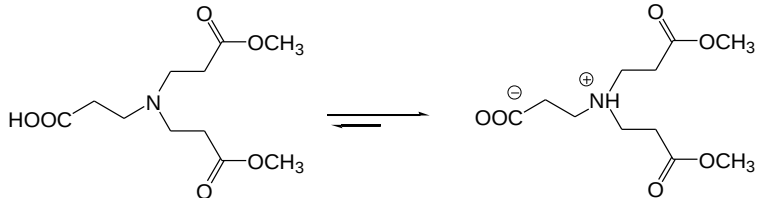

Figure 3.23 - Formation of a zwitterion for G-0.5 dendron.

Half generation Dendron	***K_a***	***K_a per terminal amine group***
G-0.5	-------	-------
G-1.5	20,898	$10*10^3$
G-2.5	34,153	$8*10^3$
G-3.5	33,156	$4*10^3$

Table 3.3 - Calculated values of binding constants for half generation dendrons.

Whole generation Dendron	***K_a***	***K_a per terminal amine group***
G-1.0	10,000	$5*10^3$
G-2.0	20,076	$5*10^3$
G-3.0	39,001	$5*10^3$
G-4.0	77,279	$4*10^3$

Table 3.3 - Calculated values of binding constants for whole generation dendrons.

Table 3.2 and **Table 3.3** - shows the following trends for comparing dendrons containing the same number of terminal primary or tertiary amines.

(1) The isosbestic point shows the presence of one binding environment.

(2) For whole generation dendrons the binding to amine is relatively constant with increasing generations.

(3) Whole generation dendrons have lower binding constants than half generation dendrons.

(4) In half generation dendrons the binding constant of per amine group decreases with increasing generations.

As shown in **(Table 3.3)**, the binding constant for whole generation dendrons are relatively constant and these K_a values are roughly similar for methanol. Thus, this binding constant is due to the methanol interaction with zinc porphyrin, which means amine terminal dendrons showed no interaction with zinc porphyrin. The K_a value for G-1.5 dendron is ~ $10x10^3M^{-1}$ per amine group, which is higher than the related binding constant for G-2.5 i.e. ~ $5x10^3M^{-1}$. This binding constant trend could be ascribed due to steric effects. As the dendron generation increases the dendron structure is more spherical, which makes the zinc and nitrogen interaction harder. This resulted in the lower binding constant for the higher generation dendrons. From the above results, the decision to use the ester terminated dendrons as a scaffold to hold the donor i.e. zinc porphyrin unit was made.

3.5 Self-assembly between acceptor, dendron and donor unit.

After the observation of the self-assembly between acceptor unit-dendron and dendron-donor unit, the decision was made to attain a self-assembled complex with acceptor, donor and the dendron as shown in **(Figure 3.24)**.

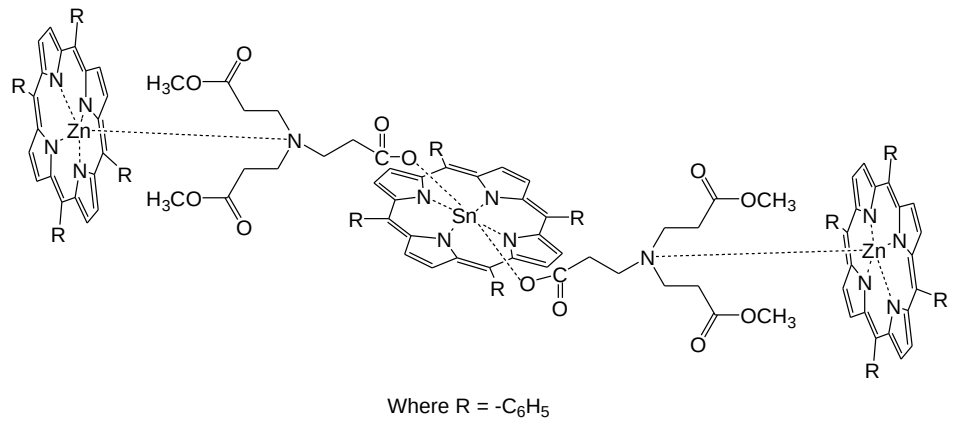

Figure 3.24 - Illustration of the self-assembled complex of the acceptor unit, dendron and the donor unit.

An experiment in a NMR tube was used to perform this self-assembly experiment. Firstly, $1x10^{-3}$M solution of acceptor unit ($SnTPP(OH)_2$) and $2x10^{-3}$ M of dendron G-0.5 were dissolved in deuterated chloroform, then the ^{1}H and ^{13}C NMR spectrum were was obtained. After this, $2x10^{-3}$ M of the donor unit (ZnTPP) was added in the same NMR tube containing acceptor and dendron solution. Then, again ^{1}H and ^{13}C NMR spectra were obtained.

For the confirmation of the self-assembly, the obtained ^{1}H and ^{13}C NMR spectra were compared for acceptor-dendron and acceptor-dendron-donor complex. The ^{1}H NMR comparison is shown in **(Figure 3.25)**. The acceptor-dendron self-assembly was confirmed by observing the upfield shift for methylene protons (a) next to the core. Thus, with the addition of the donor unit to the acceptor-dendron complex, the donor unit zinc atom makes non-covalent bonding with the dendron tertiary amine nitrogen atom. With this non-covalent bonding dendron protons (b+c) and (e) as shown in **Figure 3.25** below should show significant changes in the ^{1}H NMR by coming in the porphyrin shielded region. Therefore, after observing two broad peaks at 2.59 ppm and 2.25 ppm corresponding to (b'+c') and a multiplet at 3.59 ppm (e') for dendron protons as shown in **(Figure 3.25)**, it was concluded that this self-assembly experiment was a success.

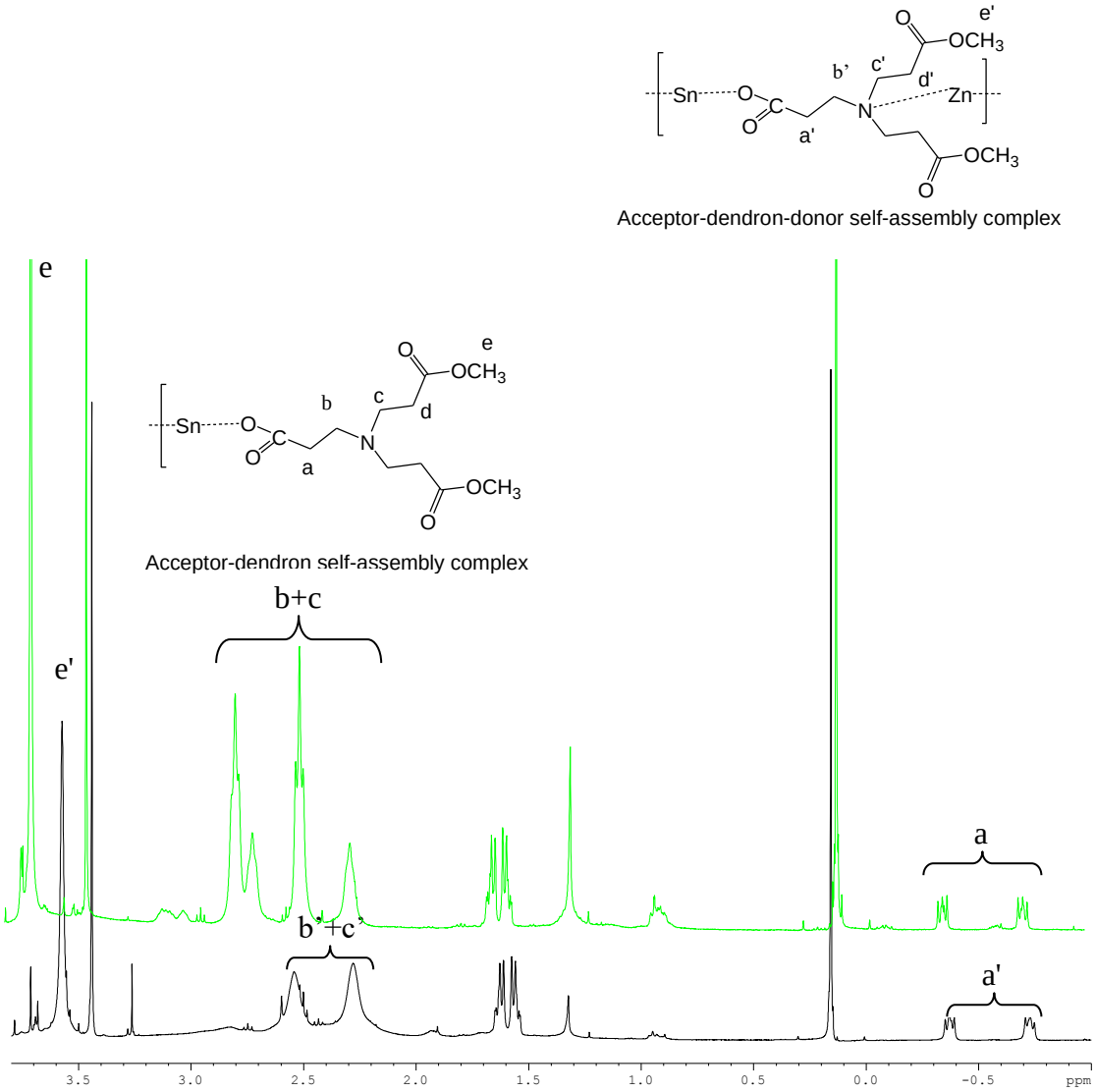

Figure 3.25 - ^{1}H NMR spectrum of acceptor- dendron complex **12** (top) and acceptor-dendron-donor unit (bottom).

Similar steps were followed to achieve self-assembly for higher generation dendrons as well. This self-assembly between the dendron scaffold, acceptor and the donor was

a success particularly for ester terminated dendrons. However, the binding interactions between the donor unit and the dendrons are not strong enough for fluorescence analysis i.e (10^{-5}- 10^{-6} M), which means higher binding constants were needed. Thus, in order to achieve higher binding, it was decided to use a cooperative effect using a porphyrin dimer as explained below.

3.6 Synthesis of zinc porphyrin dimer

In order to achieve higher binding constants at lower concentrations between the dendron scaffold and donor molecules, the porphyrin dimer was synthesised. It was expected that the porphyrin dimer would increase the binding constant via a cooperative effect. In the cooperative effect, two or more binding sites produce a combined interaction which is much stronger than the sum of interaction produced by two single sites as shown in **(Figure 3.26)**.[81] One example of a cooperative effect is haemoglobin. It was expected that the zinc porphyrin dimer would show a similar effect, by increasing the binding interactions. Synthesis of the zinc porphyrin dimer involves five reaction steps:-

1. Synthesis of TPP
2. Nitration of TPP
3. Reduction of nitroTPP to amineTPP
4. Synthesis of porphyrin dimer
5. Insertion of zinc in porphyrin dimer

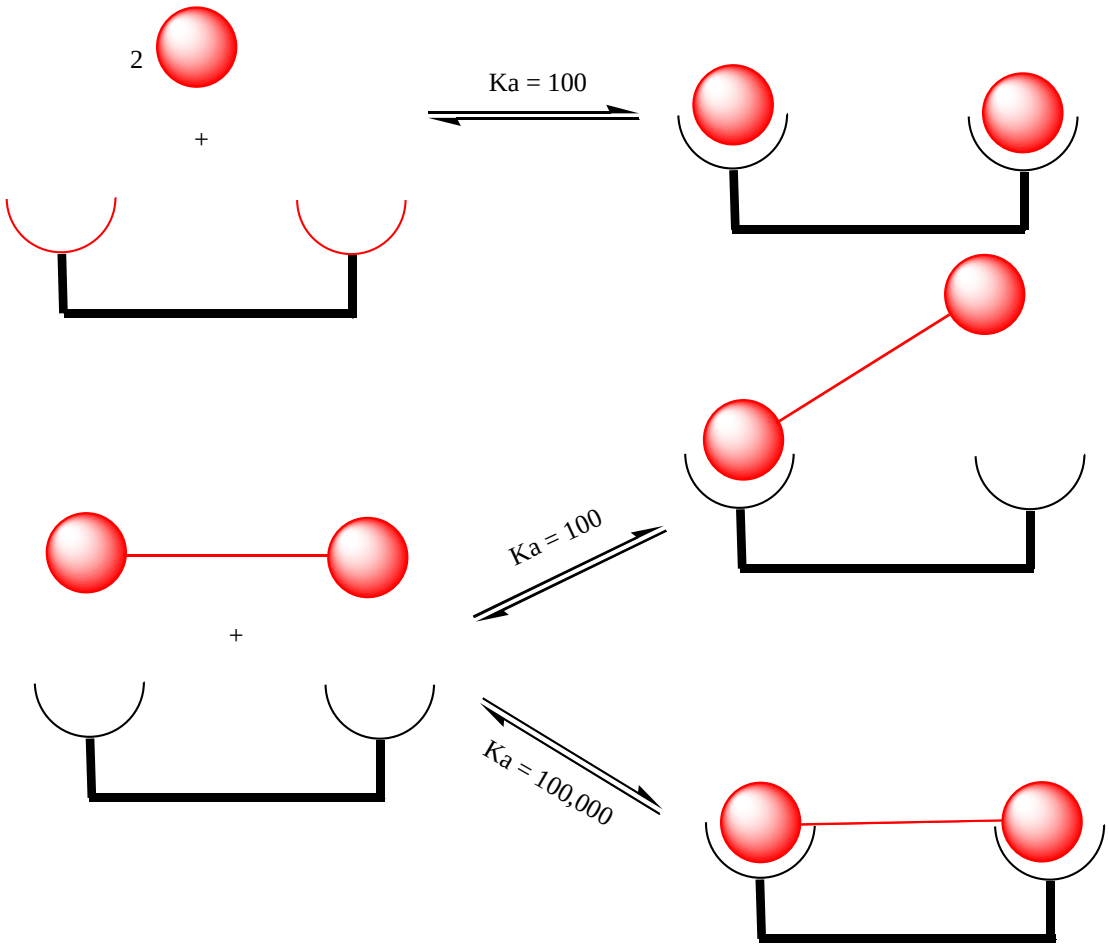

Figure 3.26 - Illustration of the cooperative effect.

The porphyrin dimer was synthesised by coupling pyromellitic anhydride and aminoTPP, under anhydrous conditions in the presence of DMF, as shown in **(Scheme 3.15)**.

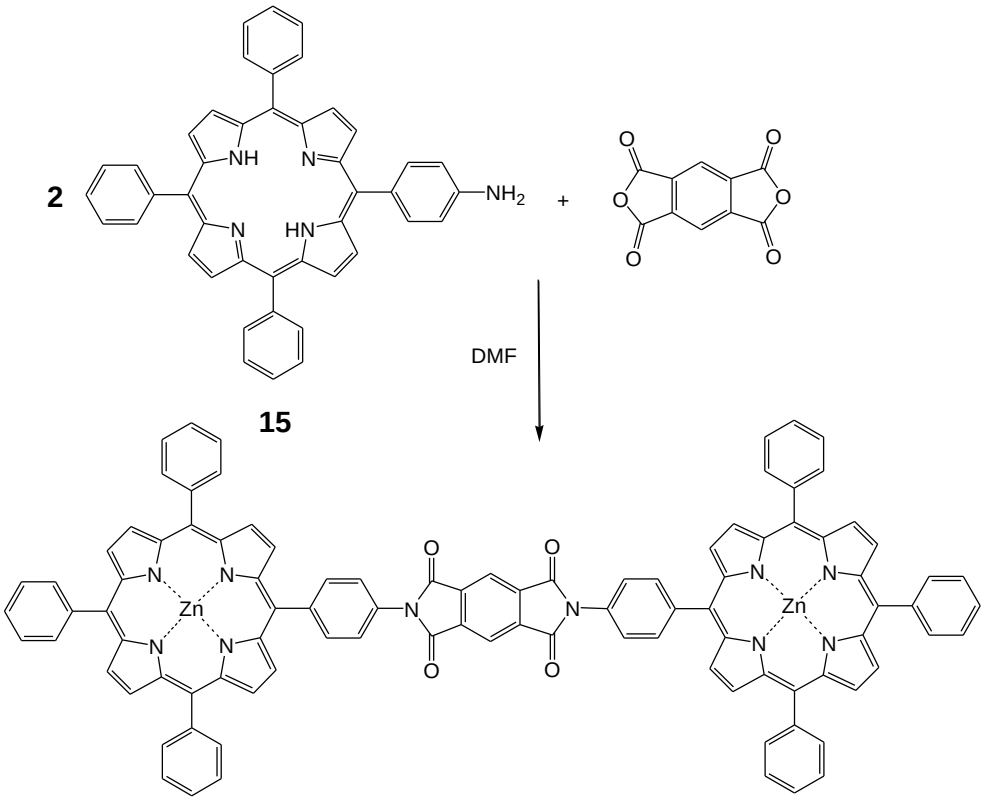

16

Scheme 3.15 Synthesis of porphyrin dimer

3.6.1 Synthesis of NitroTPP 13

The nitroporphyrin **14** was synthesised by reacting TPP with sodium nitrite in trifluoroacetic acid (TFA).[87] In the synthesis reaction, sodium nitrite first reacts with TFA, this leads to the synthesis of a reactive intermediate, which then undergoes electrophilic substitution with one of the phenyl group forming the product as shown in **(Scheme 3.16)**. The reaction mixture was then quenched with water after 2 minutes 45 seconds. This short and precise time is required in order to prevent over nitration of the porphyrin. Dichloromethane was added and the organic layer was washed with water and dried. After the filtration, the crude was purified using column chromatography. The product was eluted with 1:1 dichloromethane and petroleum ether solvent system.

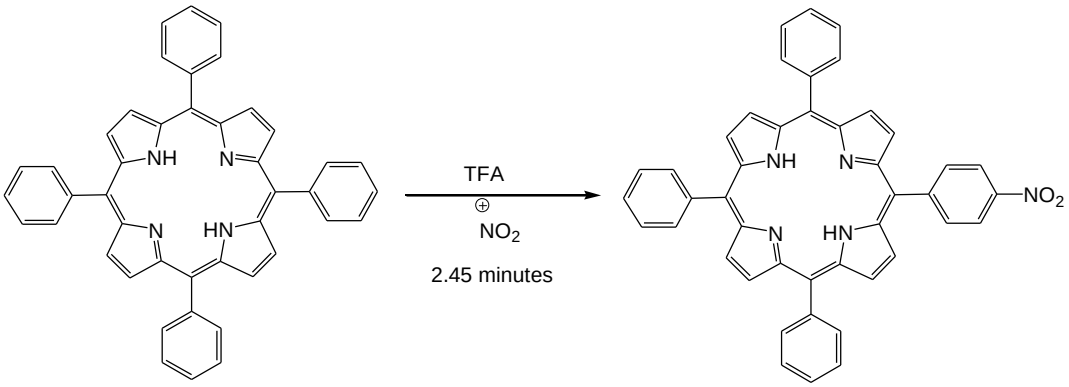

14

Scheme 3.16 Reaction scheme for nitration of TPP

Confirmation of the product was carried by ^{1}H NMR, in which the presence of two doublets at 8.66 and 8.76 ppm corresponds to the protons of the nitrated phenyl group, along with multiplets for the phenyl and pyrrolic groups at 8.25 ppm and 7.80 ppm confirming the structure. Further confirmation was carried out by mass spectroscopy, this showed a molecular peak at 660 MH^{+}.

3.6.2 Reduction of nitroporphyrin to aminoporphyrin 15

For the reduction of nitroporphyrin, **13** was dissolved in hydrochloric acid and reacted with tin(II) chloride. This reaction was stirred under nitrogen for one hour, **(Scheme 3.17)**. After an hour, dichloromethane was added and the mixture was neutralised using ammonia solution. The aqueous layer was extracted with dichloromethane and passed through celite. Then the organic layer was dried and solvent was reduced under pressure. The crude material was purified by column chromatography using alumina. Unreacted nitroporphyrin was recovered first using petroleum ether and then product **15** was eluted with dichloromethane. The purity of the product was confirmed by mass spectroscopy, in which molecular peak at 630 MH^{+} confirmed the success of reduction.

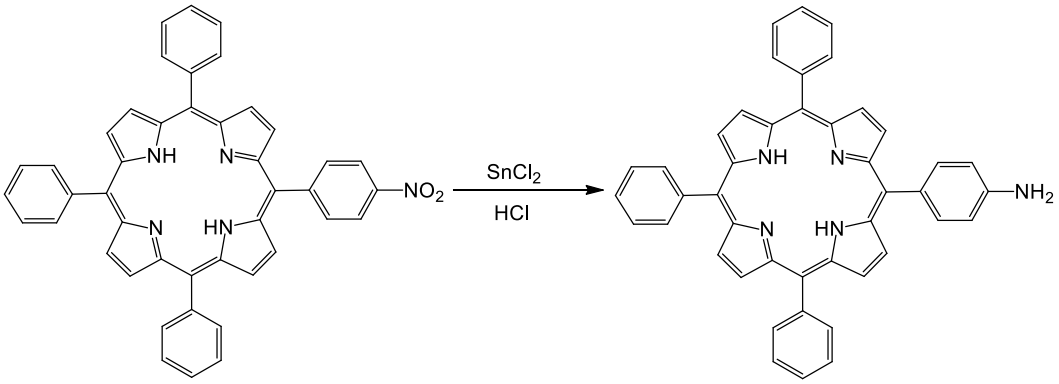

15

Scheme 3.17 - Reduction of nitroTPP

3.6.3 Synthesis of the porphyrin dimer 16

Porphyrin dimer was synthesised using the same procedure as reported by Twyman.[82] A 2:1 ratio aminoporphyrin **15**, was reacted with pyromellitic anhydride in the presence of acetic anhydride and dimethylformamide under nitrogen for eighteen hours. After eighteen hours, the dimethylformamide was removed by distillation, methanol was added and then an insoluble porphyrin was obtained via filtration. Purification of the product was performed by flash column chromatography using silica as stationary phase and 4.9/0.1 dichloromethane and methanol as mobile phase. Eluted product was collected in 7 fractions of 5 mL. Mass spectroscopy was carried out for all the fraction samples. Fractions from 3 to 5 showed desired molecular peak at 1441 MH^+. Fractions containing the desired product were collected and further confirmation was carried out using ^1H NMR, in which the presence of four internal protons at -2.75 ppm and a multiplet at 8.40 ppm, corresponds to two protons of the central aromatic phenyl, confirmed that the synthesis was a success. The amine porphyrin **15** was reacted with the linker, pyromellitic anhydride via the mechanism, shown in **(Figure 3.26)**. The lone pair of nitrogen atom of amine attacks the electrophilic carbon of pyromellitic anhydride, an amide and carboxylic acid form by opening the ring. The presence of excess acetic anhydride stopped the ring closure via the formation of acetoxy group. The next step involves the loss of acetic acid which results in the ring closure.

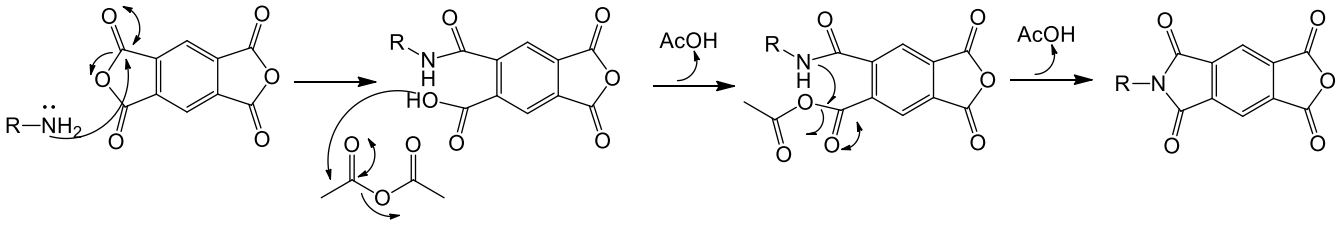

Figure 3.26 - Reaction mechanism of pyromellitic dianhydride with amine.

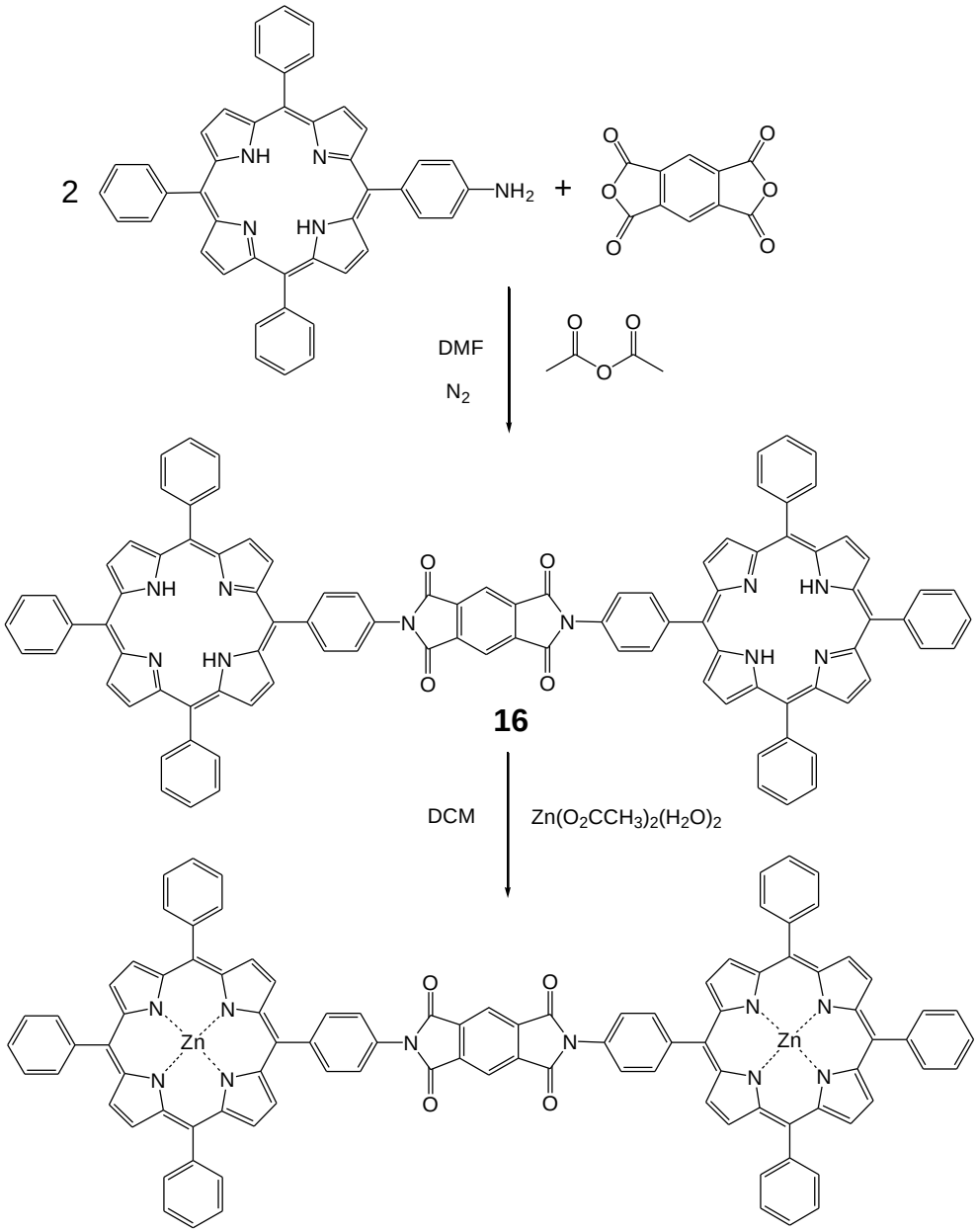

17

Scheme 3.18 - Synthesis of zinc porphyrin dimer **17**.

3.6.4 Insertion of zinc in porphyrin dimer

For the insertion of zinc, the porphyrin dimer **16** was dissolved in dichloromethane and reacted with zinc acetate dihydrate. This reaction mixture was refluxed for half an hour. Unreacted zinc acetate was removed and filtrate was reduced under pressure. Crude product was purified by flash column chromatography using silica gel and eluted with dichloromethane to give **17** as purple solid. The reaction scheme is shown in **(Scheme 3.18)**.

Confirmation of the product was carried out using ^{1}H NMR, in which disappearance of high shielded peak at -2.75 ppm corresponds to the inner four protons of porphyrin rings, which proved insertion was a success. Further confirmation of the product was provided by UV/Vis spectroscopy, where four Q bands of starting material were replaced by two Q bands. A molecular peak at 1568 also confirmed the insertion of the zinc metal in the porphyrin rings.

3.6.5 Binding of zinc porphyrin dimer with dendrons

After the successful synthesis of zinc porphyrin dimer **17**, binding experiments were carried out using UV titrations. The aim was to acquire higher binding constant values than the values obtained from dendron interactions with ZnTPP. For titrations, a stock solution of 10^{-6} M of dimer **17** was prepared in DCM. In order to maintain the same concentration of porphyrin for calculations, this stock solution of porphyrin was used to make solutions of the dendrons. After preparing the dendron solutions, these solutions were titrated into 2 mL solution of the porphyrin until the binding was saturated. The UV spectrum was recorded and the graph was plotted to get the binding constant. The same procedure was performed for the different generations of the dendrons. Binding constants for the different generations of the dendrons are shown in **(Table 3.4)**.

Dendron generations	***Binding affinities with zinc porphyrin dimer K_a/M^{-1}***	***Binding affinities with zinc tetraphenylporphyrin K_a/ M^{-1}***

G-0.5	-----	-----
G-1.5	$9x10^3$	$10x10^3$
G-2.5	$15x10^3$	$8x10^3$
G-3.5	$16x10^3$	$4x10^3$

Table 3.4 - Summary of the binding constants obtained from the interaction between the dendrons and zinc porphyrin.

The above table shows that the binding interaction values between the dendrons and zinc porphyrin dimer are lower than the binding interaction values for the zinc porphyrin. This drop in the binding interactions was unpredictable. For the confirmation of these binding interactions, it was decided to perform another UV titration experiment. For this, another batch of zinc porphyrin dimer was synthesised and the UV titration experiment was performed. These UV titration results showed really high binding constant results, as expected. Binding constant results for batch one and two are shown in **(Table 3.5)**.

Batch One binding affinities K_a	***Batch Two binding affinities*** K_a
-----	-----
$9x10^3$	$4.7x10^4$
$15x10^3$	$9.8x10^4$
$16x10^3$	$1.2x10^5$

Table 3.5 Summary of binding constants obtained from the batch one and batch two, zinc porphyrin dimer.

This raises the question as to why the same compound shows different binding interactions. To solve this, further analysis of the synthesised zinc porphyrin dimer was carried out. On analysis, the first batch was found to be pure. However, in the ^1H NMR, the second batch showed porphyrin dimer peaks along with some small minor peaks. Furthermore, the molecular ion peak at 1602 ($M+2H_2O$) was noticed for the porphyrin dimer molecular peak in the mass spectroscopy analysis. This molecular

ion peak at 1602 is probably due to the presence of the two H_2O molecules within the porphyrin dimer. This could be due to the fact that the ring has not closed i.e. it is an opened zinc dimer ring with amide and acid groups as shown in **(Figure 3.27)**. Thus, the second batch analysis indicated that this batch is the mixture of the rigid and flexible porphyrin dimer.

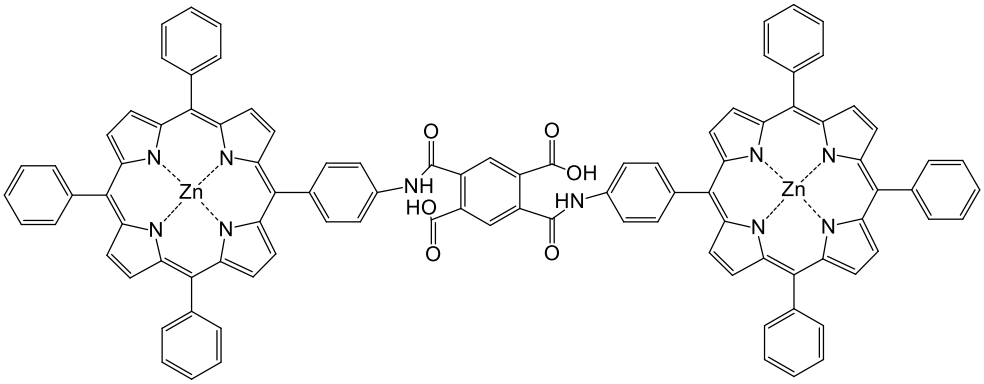

18

Figure 3.27 Represents opened zinc porphyrin dimer.

Therefore, due to the presence of the mixture of dimers, the binding interactions were more effective. The difference in the binding interactions can be ascribed to the conformational flexibility of the uncyclised dimer. For the rigid porphyrin dimer **17**, it is hard to change conformation according to the binding sites of the dendron, which resulted in the lower binding interactions. On the other hand, by changing the structural conformation easily, the flexible porphyrin dimer **18** can easily interact with the dendron binding sites. Hence, this resulted in the increased binding constants as shown in **(Table 3.5)**. The goal in this section was to increase the binding interaction by synthesising a zinc porphyrin dimer, which would introduce a cooperative effect. However, rigid porphyrin dimer **17** could not introduce cooperative effect due to the dimer structural rigidity. Although flexible dimer **18** demonstrates the advantage of flexibility, it was very hard to synthesise this dimer pure because it is contaminated with the rigid dimer. Thus, it was decided to synthesise the dimer **19**, as this was designed to be flexible and the flexible properties of the dimer were hoped to increase the binding interactions.

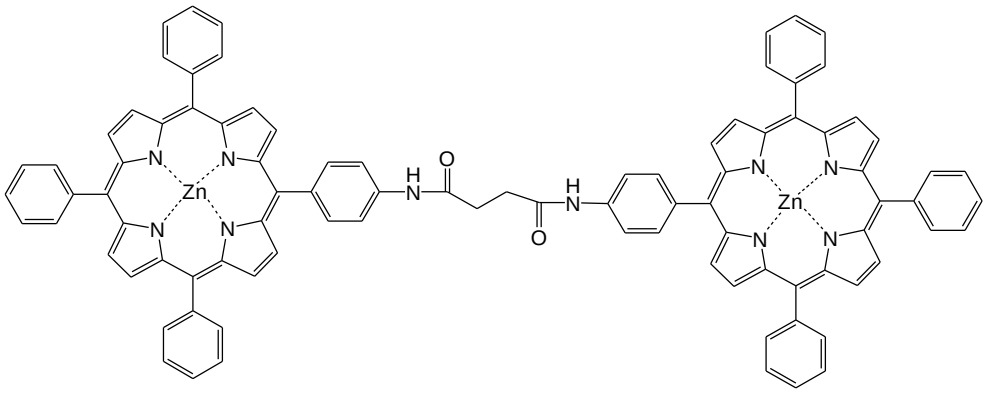

19

Figure 3.28 - Flexible porphyrin dimer.

3.7 Synthesis of flexible zinc porphyrin dimer

For the synthesis of zinc porphyrin dimer **19** the porphyrin dimer **19(a)** was needed. A 2:1 ratio of amine porphyrin was reacted with succinyl chloride in the presence of dry THF, under anhydrous conditions for 3 hours. After the removal of THF, dichloromethane was added and an organic layer was washed with the saturated solution of sodium bicarbonate and water and then dried. After filtration the product **19(a)** was purified by column chromatography using silica gel eluting with 4.5/0.5 dichloromethane/methanol solvent system. The reaction scheme for flexible porphyrin dimer **19(a)** is shown in **(Scheme 3.20)**.

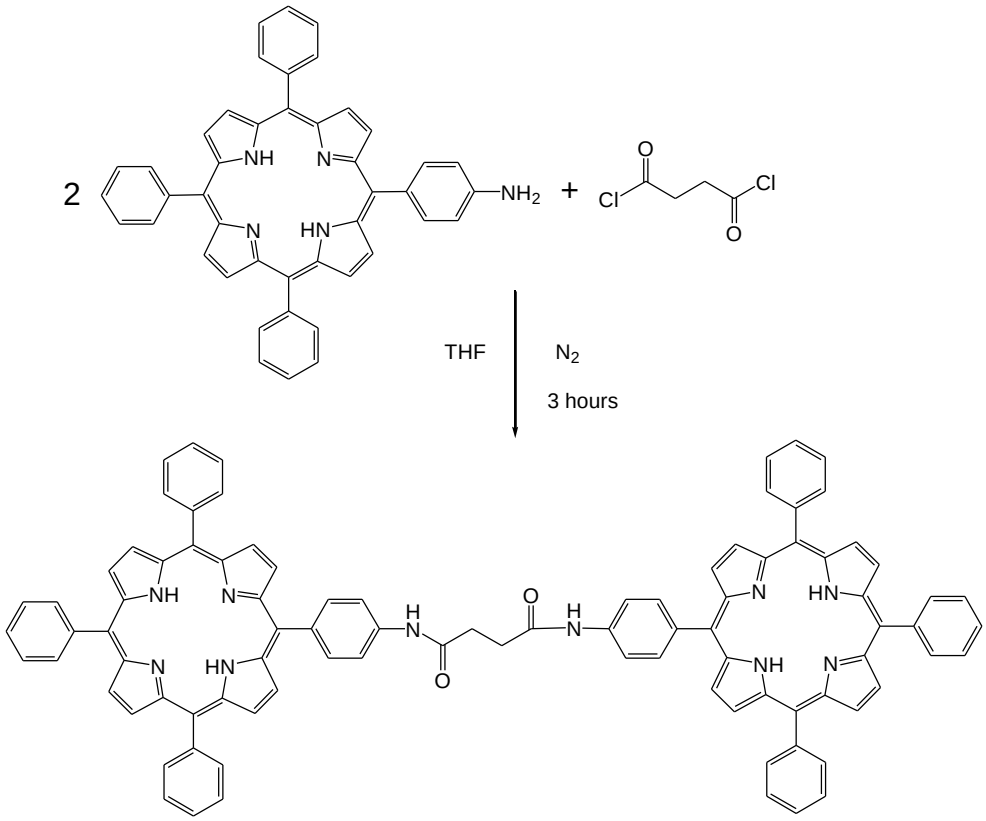

19(a)

Scheme 3.20 - Synthesis of flexible zinc porphyrin dimer **19(a)**.

The dimer synthesis was confirmed by ^{1}H NMR, which showed the presence of the internal four protons of the porphyrin ring at -2.57 ppm, along with the signal at 3.11 ppm corresponds to the methylene protons. Further confirmation was carried out using mass spectroscopy, which showed a molecular peak at 1340 MH^{+}, as desired.

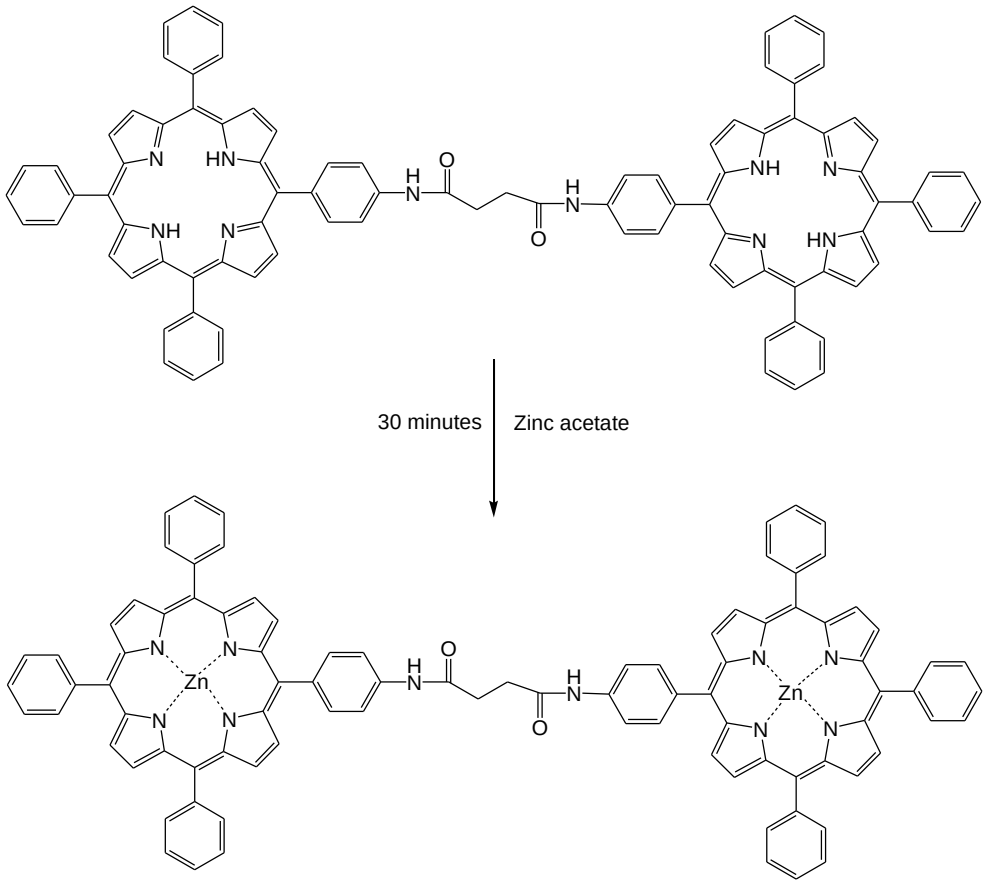

19

Scheme 3.21 - Insertion of zinc in flexible porphyrin dimer.

After the synthesis of dimer **19(a)**, next step was the insertion of zinc into the dimer. This insertion was achieved by refluxing dimer **19(a)** with zinc acetate dihydrate in DCM for half an hour. Unreacted zinc acetate was removed by filtration and the filtrate was reduced under pressure. A schematic representation of this reaction is shown in **(Scheme 3.21)**. The crude product was purified by recrystallisation using methanol. The confirmation of the product was carried out using ^{1}H NMR, mass spectroscopy and UV/Vis spectroscopy. In the ^{1}H NMR, disappearance of the high shielded peak at -2.75 ppm corresponding to the four inner, porphyrin ring protons confirmed the zinc insertion. A molecular peak at 1468 MH^{+} also confirmed the reaction success. Further confirmation of the product was provided by UV/Vis spectroscopy, where four Q bands of the starting material were replaced by two Q bands.

After the successful synthesis of flexible porphyrin dimer **19**, UV binding studies were performed by following the same procedure as explained above. Different generations of dendron solutions were titrated against the flexible porphyrin dimer. Binding constant results are shown in **(Table 3.6)**.

Dendron generations	***Binding affinities with zinc flexible porphyrin dimer K_a/M^{-1}***	***Binding affinities with zinc tetraphenylporphyrin K_a/M^{-1}***
G-0.5	-----	-----
G-1.5	1.95×10^5	10×10^3
G-2.5	1.28×10^5	8×10^3
G-3.5	1.72×10^5	4×10^3

Table 3.6 - Summary of binding constants obtained from interaction between dendrons and flexible zinc porphyrin **19** and dendrons with zinc tetraphenylpophyrin.

Thus, from the above binding constant results, it was concluded that flexible porphyrin dimer **19** increased the binding interaction by showing a cooperative effect. These binding interactions were found to be good enough to perform the light-harvesting experiment at a lower concentration range. Therefore, zinc porphyrin dimer **19** was found suitable enough to be used as a donor chromophore in our system. In the light harvesting system, the energy transfer between the donor and acceptor chromophores should obey certain requirements. The main requirement is that there should be a spectral overlapping between the donor emission spectrum and the acceptor absorption spectrum. Tin porphyrin and zinc porphyrin are absorbing and emitting between the same regions i.e. the required spectral overlapping is not possible. Although tin porphyrin was a good model compound for our preliminary binding studies, it could not be used as an acceptor chromophore in our light-harvesting system due to absorption spectrum overlap with the donor molecule. Therefore, the decision to use tin phthalocyanine as an acceptor was made. In comparison with porphyrin, phthalocyanine has a higher absorption range and this

property of phthalocyanine makes it preferable as an acceptor unit in our light-harvesting system.

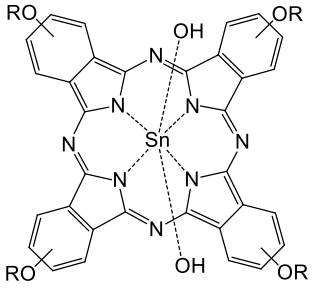

R = -$(CH_2)_4CH_3$

20

Figure 3.30 – Tin(IV) (pentyloxyphthalocyanine) dihydroxy.

Tin(IV) (pentyloxyphthalocyanine) dihydroxy **20** was synthesised as shown below:-

3.8 Synthesis of tin(IV) (pentyloxyphthalocyanine) dihydroxy $SnPc(OH)_2$ (acceptor unit)

$SnPc(OH)_2$ was synthesised from 3-penyloxy phthalonitrile shown in **(Scheme 3.22)**.

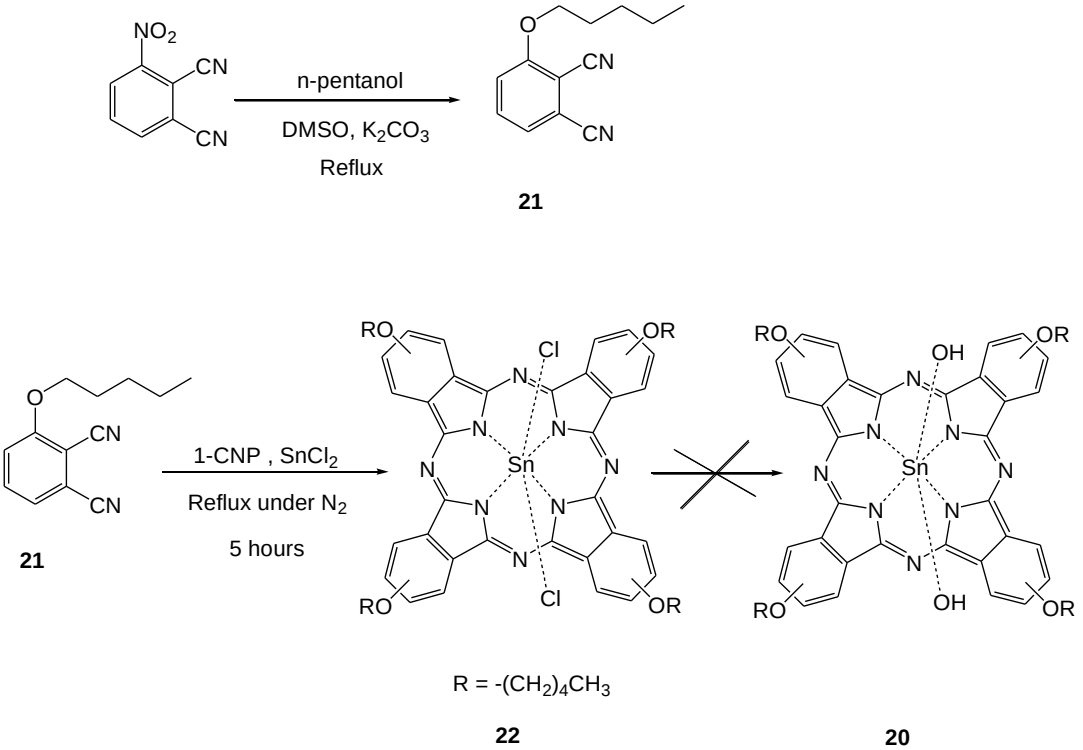

Scheme 3.22 Synthesis of tin(IV) (pentyloxyphthalocyanine) dichloride.

For the synthesis of compound tin(IV) (pentyloxyphthalocyanine) dihydroxy **20**, the first step involves the synthesis of the compound **21**. For this, 3-nitrophthalonitrile was reacted with n-pentanol in the presence of anhydrous potassium carbonate and DMSO under nitrogen. Then this reaction mixture was refluxed for 4 hours at 90°C. After 4 hours, this mixture was cooled at room temperature and water was added. After the addition of water, the reaction mixture was stirred vigorously for another 10 minutes. The resulting precipitate was collected using vacuum filtration and washed with water. Purification of the compound **21** was carried out by recrystallisation using ethanol. The purity of the product was confirmed by ^{1}H NMR, in which the presence of 3 doublets at 7.66-7.62 ppm, 7.36-7.34 and 7.25-7.35 ppm corresponds to phenyl ring protons along with multiplets at 1.89-1.92 ppm and 1.54-1.35 ppm and triplets at 4.14 ppm and 0.96 ppm of n-pentanol protons confirmed purity of the product. Further confirmation was carried out using mass spectroscopy, which showed molecular peak at 215$(MH)^{+}$.

After the successful synthesis of compound **21**, tin(IV) (pentyloxyphthalocyanine) dichloride **22** was synthesised by dissolving compound **21** in 1-CNP (1-chloronaphthalene). To this tin(II) chloride was added and then this mixture was refluxed under anhydrous conditions at 250° C for 5 hours. After 5 hours, this reaction mixture was cooled and the solution was chromatographed through a short column of silica, using hexane to remove 1-CNP. Then the column was eluted with 4/1 dichloromethane and methanol. The solvent was evaporated off. To get the final product, the crude material was washed with hot methanol. The product was characterised using a variety of analytical tools. From analysis of ^{1}H NMR, 3 sets of multiplets at 9.35-9.17 ppm, 8.32-8.24 ppm and 7.90-7.76 ppm were observed for 12 aromatic protons. Also 44 n-pentyl protons showed multiplets at 4.99-4.92, 4.79-4.72 ppm, 2.57-2.35, 1.88-1.54 ppm and 1.24-1.03 ppm. This combined with mass spectroscopy 1008$[M-Cl]^{+}$ confirmed the synthesis.

After the successful synthesis of $SnPc(Cl)_2$ **22**, the synthesis of compound **20** was carried out by following the procedure as shown in the literature.[83] The compound **22** was refluxed in the mixture of pyridine: water (1:4) for 4.5 hours. After 4.5 hours this reaction mixture was filtered and evaporated to dryness. A blue coloured product was

formed. For checking the purity of synthesised compound, ^{1}H NMR was carried out, which showed peaks related to the compound **21**. Several attempts were performed to achieve the desired product, however, compound **20** could not be synthesised. After the unsuccessful synthesis of compound **20**, the decision to use the compound **22**, as a core (acceptor unit) was made.

3.9 Self-assembly between tin(IV) (pentyloxyphthalocyanine) dichloride $SnPc(Cl)_2$ and ester terminated dendrons

The self-assembled complexes between $SnPc(Cl)_2$ **22** and different generations of the ester terminated dendrons were prepared by following a literature procedure with the little modification.[84] The self-assembled complexes are shown in **(Figure 3.31)**.

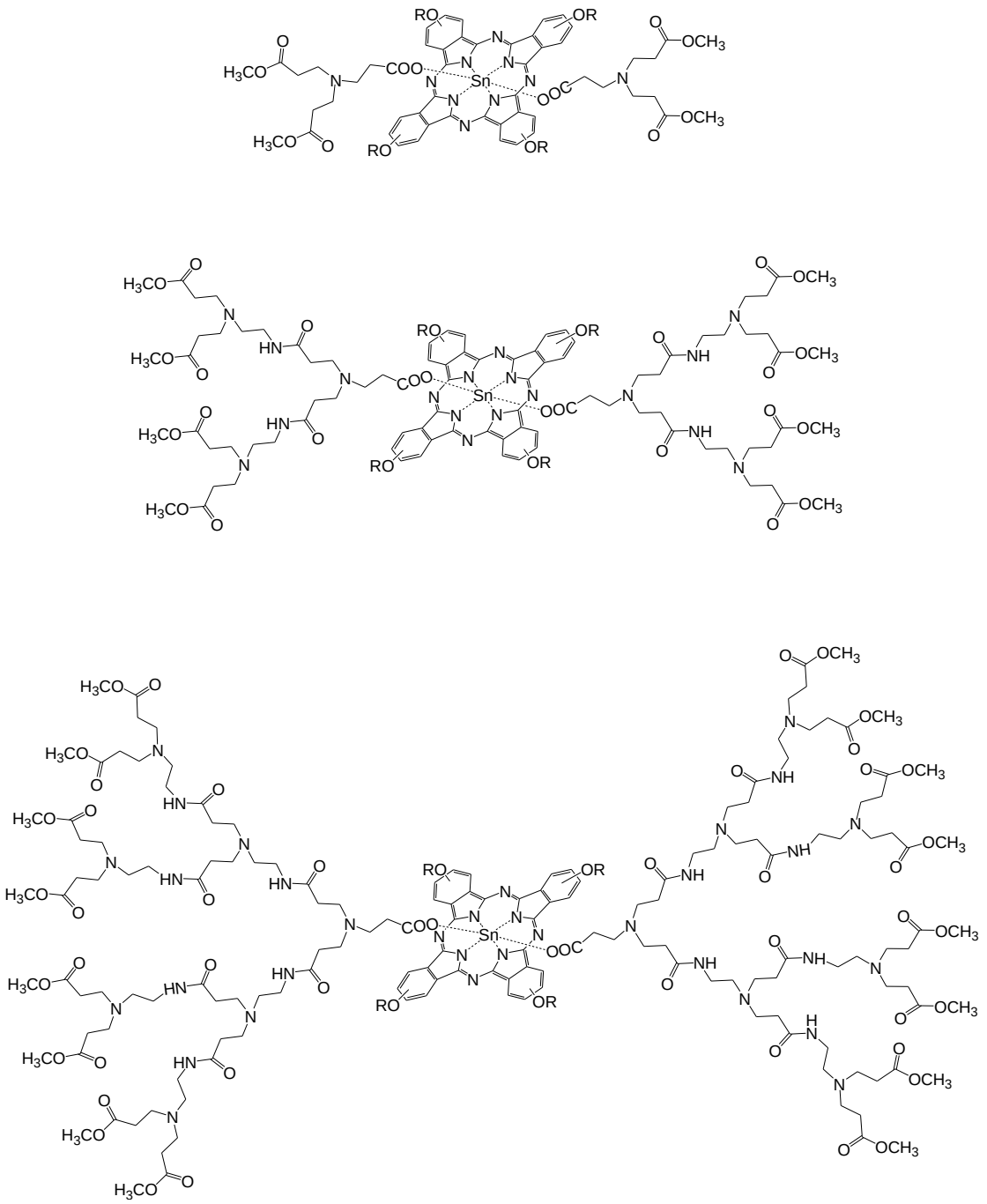

Figure 3.31 - Illustration of self-assembly between tin(IV) (pentyloxyphthalocyanine) dichloride **(22)** and different generations of ester terminated dendrons.

3.9.1 Self-assembly of tin(IV) (pentyloxyphthalocyanine) dichloride (22) with G.0.5 dendron (1)

For the self-assembly between acceptor unit **21** and dendron G- 0.5 **(1)**, the compound **22** (1 mole) and G-0.5 (2 moles) were refluxed in $CHCl_3$ for an hour. After the

removal of solvent, the green sticky product was formed. This self assembly is shown in **(Scheme 3.22)**.

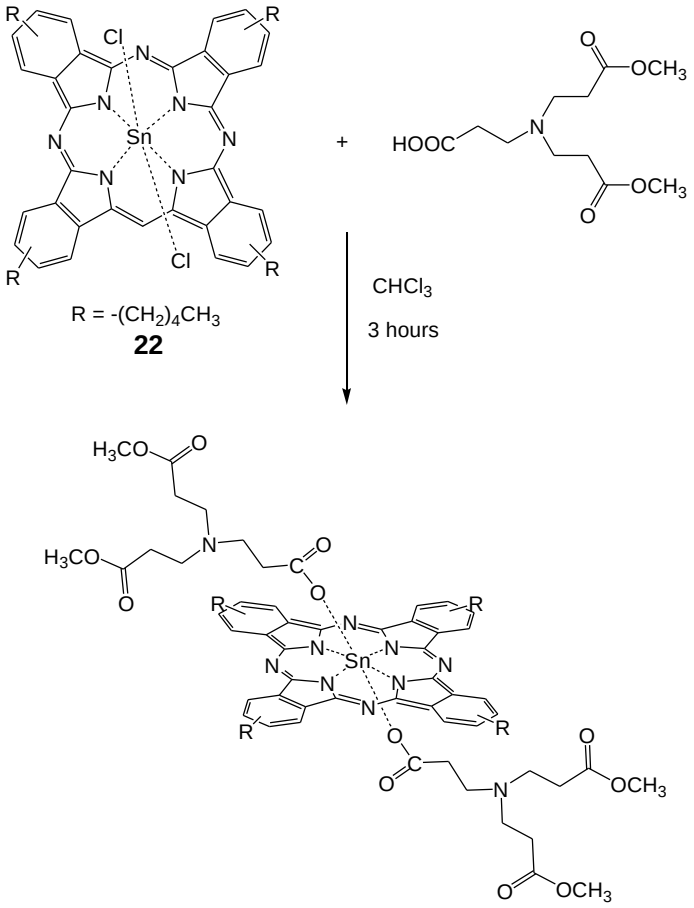

Scheme 3.22 - Schematic representation of self assembly between (**22)** and G-0.5 **(1)**.

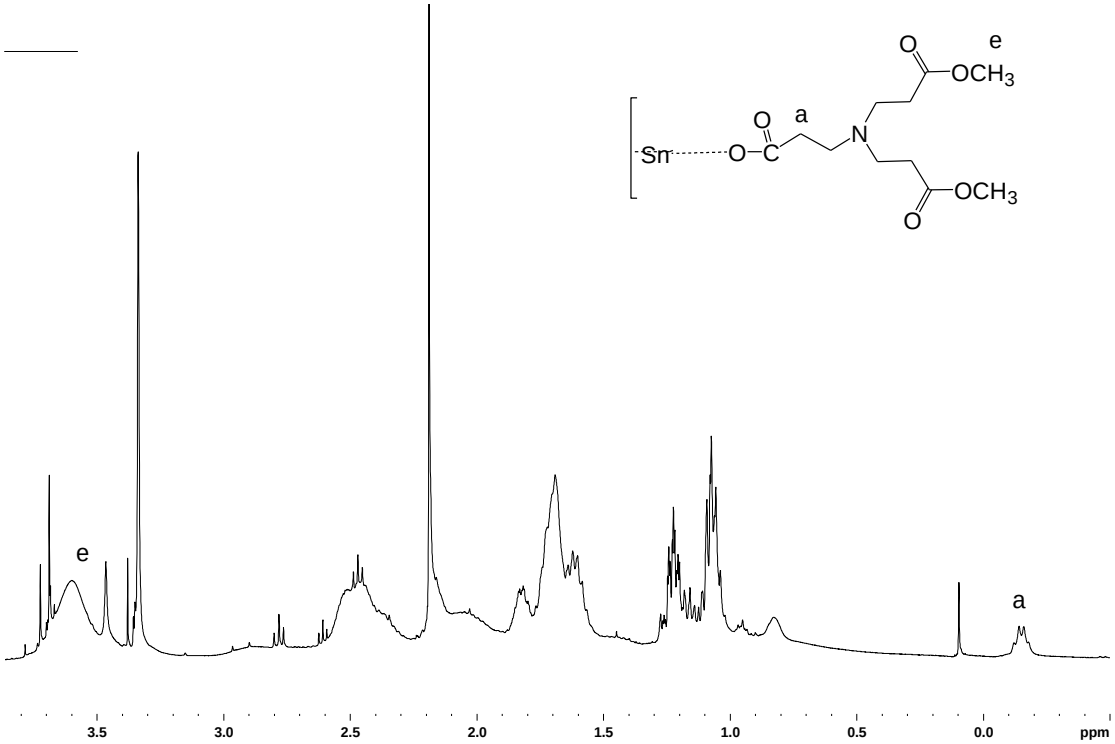

Figure 3.32 - ^{1}H NMR of self-assembled complex **22**.

This self-assembly was confirmed by ^{1}H NMR, which displayed characteristic upfield shift of dendron core methylene protons **(a)** at -0.98 ppm and broad peak at 3.61 ppm attributable to the terminal ester group protons **(e)** of the dendron as shown in **(Figure 3.32)**. In addition, 3 sets of multiplets at 7.70-7.88 ppm, 8.22-8.31 ppm and 9.14-9.35 ppm representing 12 aromatic protons of phthalocyanine were also observed. A molecular ion peak at 1237 $(M\text{-}G0.5)^{+}$ also confirmed the self-assembly between dendron and **22** was successful. This combined with the IR data, in which strong peaks 1590 cm^{-1}, 1643 cm^{-1} and 1493 cm^{-1} confirmed the binding mode of carboxylate dendron ligands to tin atom in phthalocyanine as consistent with the literature.[79]

The same procedure was followed to achieve self-assembly between the G-1.5 or G-2.5 and tin(IV) (pentyloxyphthalocyanine) dichloride.

3.9.2 Self-assembly of tin(IV) (pentyloxyphthalocyanine) dichloride, dendron and flexible zinc porphyrin dimer

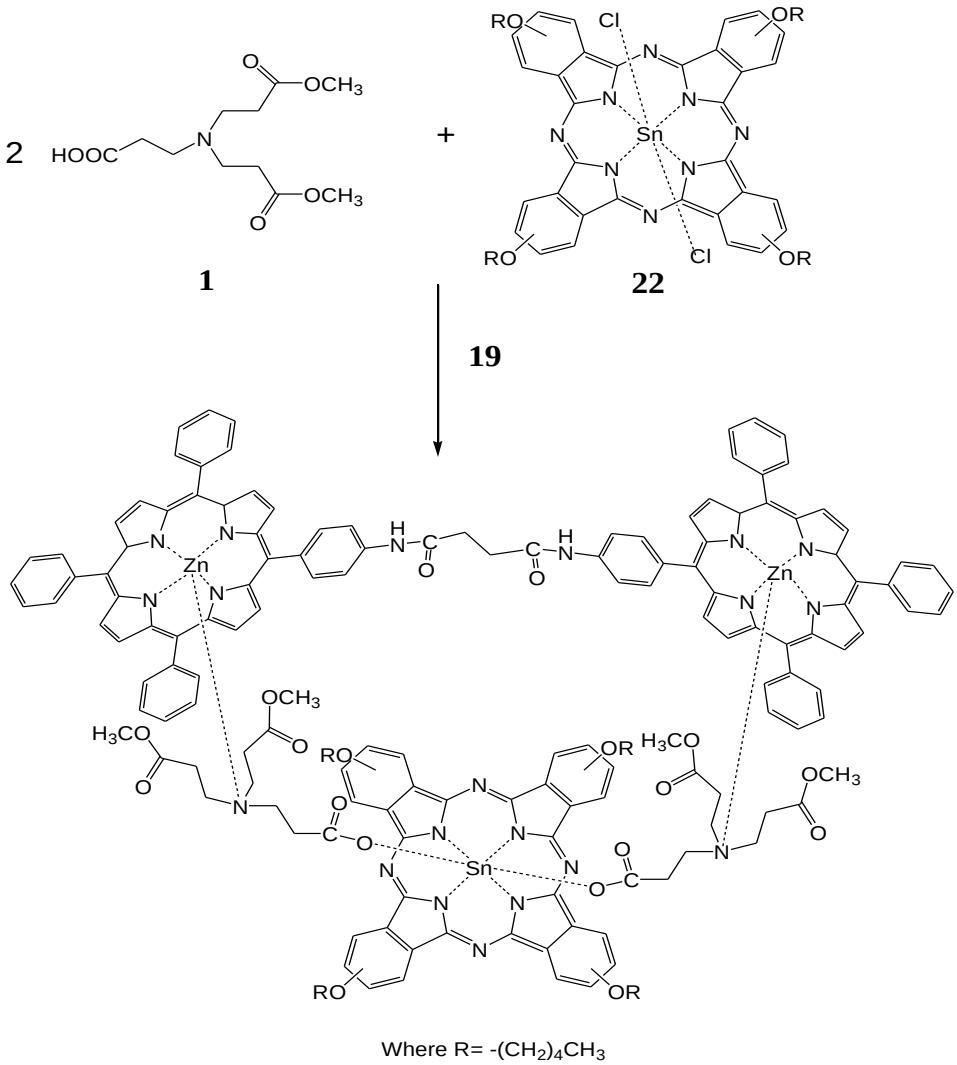

24

Scheme 3.33 - Schematic representation of self-assembly between **1**, **18** and **21.**

This self-assembly was carried out by following same steps as explained in section 3.4. Firstly, a $1x10^{-3}$M solution of acceptor unit ($SnPc(Cl)_2$) and a $2x10^{-3}$M solution of dendron G-0.5 was prepared in the deuterated chloroform and transferred into a NMR tube and the ^{1}H NMR spectrum was recorded. After this, a $1x10^{-3}$M solution of the donor unit (ZnFPD) was added in the same NMR tube and a second ^{1}H NMR spectrum was obtained. The observed ^{1}H NMRs are shown in **(Figure 3.33)**.

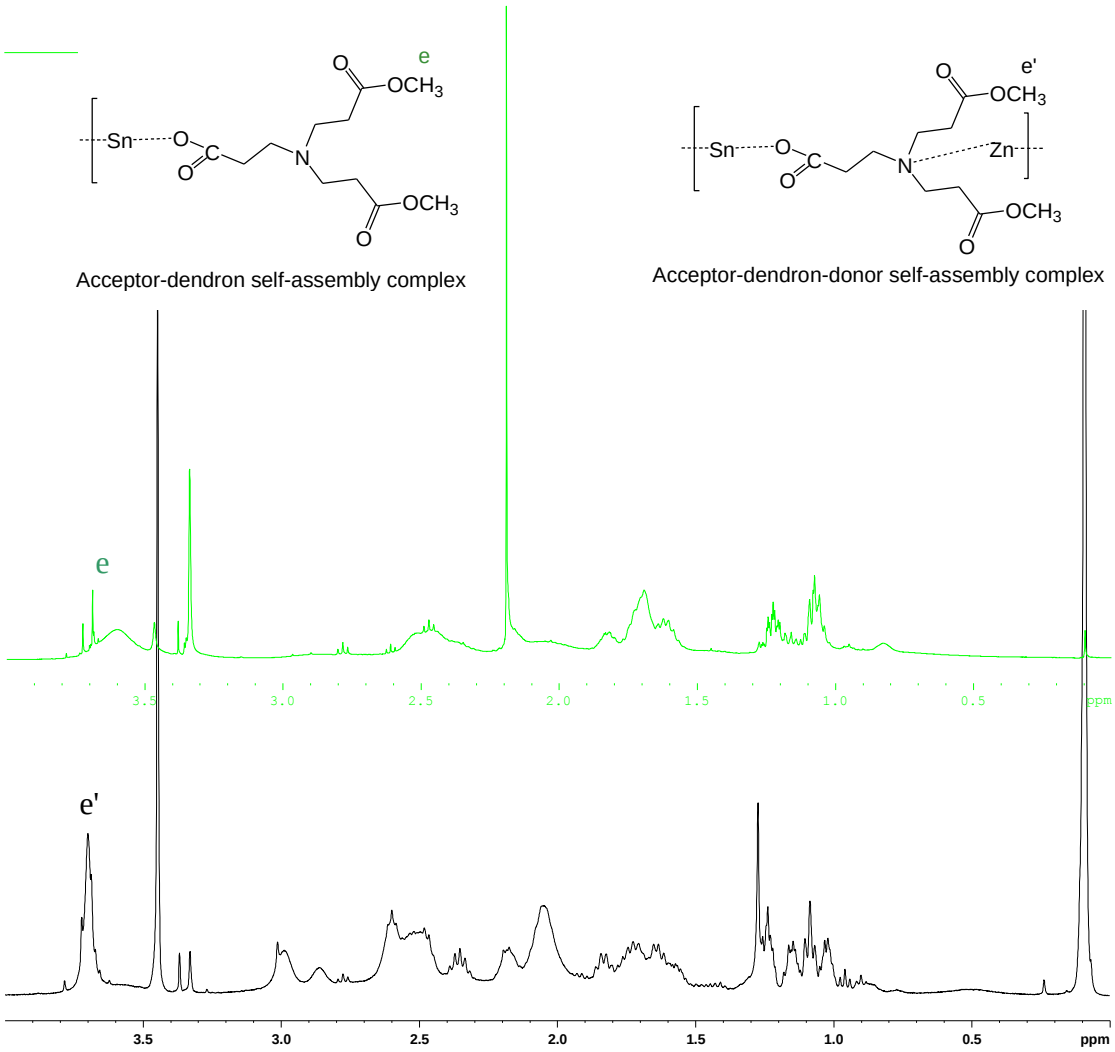

Figure 3.33 - ^{1}H NMR of self-assembled complex of SnPc(Cl)$_2$-G-0.5- ZnFPD.

Due to the extensive regions of overlap and broadened peaks from tinphthalocyanine and dendron, it was very difficult to assign specific peaks. However, self-assembly confirmation was possible by comparing the significant change in the dendron peak regions. Therefore, the self-assembly between SnPc(Cl)$_2$-G(0.5)-ZnFPD was confirmed by observing the significant change in the dendron terminal methoxy protons as these proton should show significant change after self-assembly, due to coming into the porphyrin shielded region. As shown in **Figure 3.33** dendron terminal methoxy protons (e') showed multiplet at 3.62-3.72 ppm instead of singlet, which showed the self-assembly was a success.

The self-assembly between acceptor, donor and bigger generation dendrons unit was also carried out using similar procedure and similar changes were observed for

dendron terminal methoxy protons, which confirmed the self-assembly. After observing a successful self-assembly between acceptor-dendron-donor, the next step was the light-harvesting experiment.

3.10 Light-harvesting experiments

In order to mimic the natural light-harvesting system, after the successful non-covalent self-assembly between ester terminated dendron, tin(IV) (pentyloxyphthalocyanine) dichloride and flexible zinc porphyrin dimer, it was decided to carry out the light-harvesting experiment using ester terminated dendron as scaffold to hold the suitable acceptor and the donor units. Tin(IV) (pentyloxyphthalocyanine) dichloride was chosen as an acceptor unit (core), which absorbs light at 749 nm and emits at 757 nm and flexible zinc porphyrin dimer was chosen as a donor unit, which absorbs light at 420 nm and emits at 650 nm. The main motive for choosing these compounds as an acceptor and the donor unit was the spectral overlap between the emission spectrum of the donor and the absorption spectrum of an acceptor. This overlap is the first requirement for light-harvesting. To observe the spectral overlap, the absorption spectrum of an acceptor unit i.e. **22** and the emission spectrum of the donor unit i.e. zinc flexible dimer **19** was obtained using 10^{-6} M concentration. **Figure 3.34**, shows the spectral overlap between our chosen chromophores.

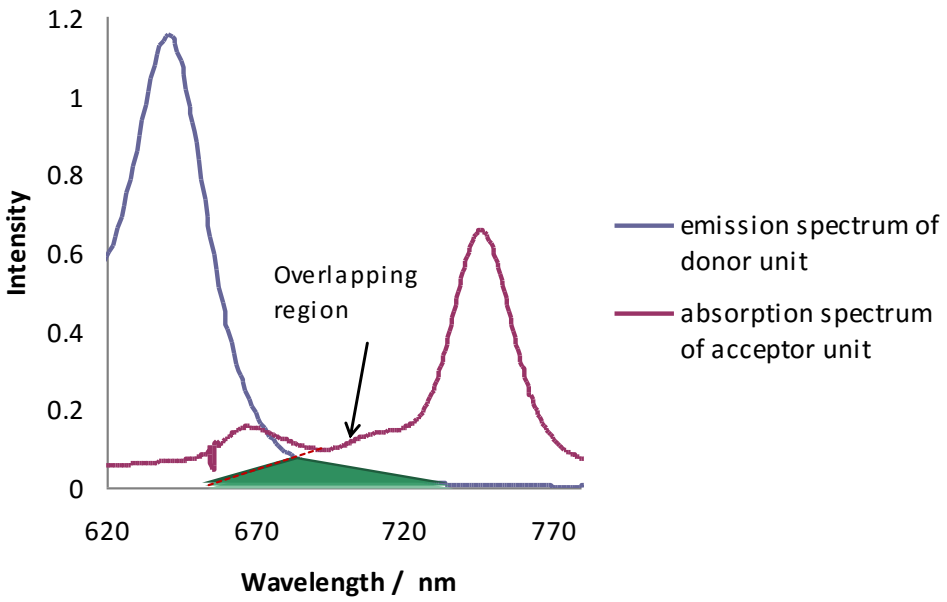

Figure 3.34 – Representation of the absorption spectrum of core and fluorescence emission spectrum of the donor unit in chloroform at room temperature.

Spectral overlap between the donor emission and the acceptor unit absorption indicated that tin(IV) (pentyloxyphthalocyanine) dichloride and flexible zinc porphyrin dimer are suitable fluorescence donor-acceptor pair for our system. By using these chromophores, there is the possibility of the light-harvesting within our non-covalent self-assembled system. After attaining the desired spectral overlap, the light-harvesting studies were carried out for the LH complexes using different generations of the dendrons.

3.10.1 Light-harvesting Studies

Light harvesting studies were carried out by observing the acceptor emission spectra after the excitation of the terminal donor units. If our self-assembled system was capable of showing light-harvesting behaviour, then the tin(IV) phthalocyanine core should emit light around 757 nm. **Figure 3.35** represents the core emission.

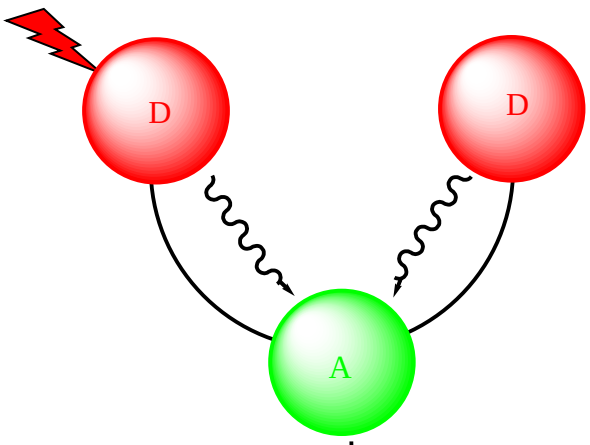

Figure 3.35 – Representation of the light-harvesting behaviour between a donor and an acceptor.

Firstly, the LH test was carried out using G-0.5 dendron as scaffold to hold the acceptor and the donor unit. The LH complex solution was prepared using 10^{-6} M concentration. This complex solution was prepared with the spectroscopic grade chloroform solution, using $1x10^{-6}$ M of tin(IV) (pentyloxyphthalocyanine) dichloride (acceptor unit), $2x10^{-6}$ M G-0.5 (polymer scaffold) and $1X10^{-6}$ M of the flexible zinc porphyrin dimer (donor unit). **Figure 3.36** showing the chemical structure of the LH complex containing tinphthalocyanine acceptor, flexible zinc porphyrin dimer as donor and the dendron scaffold G-0.5.

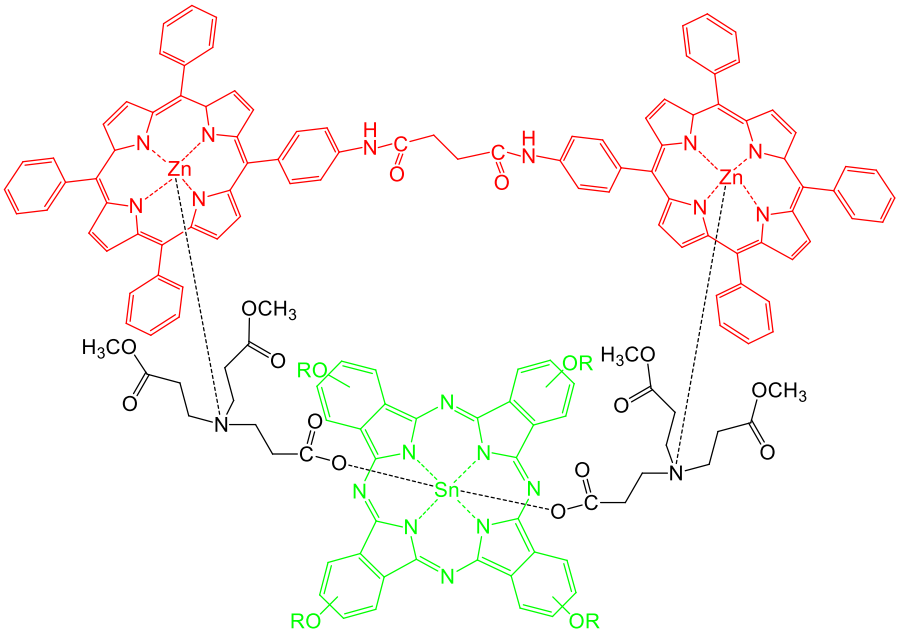

24

Figure 3.36 - The chemical structure of the G-0.5 LH complex containing tin phthalocyanine core and flexible zinc porphyrin as donor unit.

To observe the light-harvesting behaviour, the emission spectrum of the acceptor unit was observed after excitation of the zinc flexible porphyrin donor unit at 350 nm. Additionally, for comparison, the emission spectrum of the core (acceptor unit) and dendron complex, without donor units was also observed and it was expected that the core without donor units would not show any emission spectrum. However, the core without donor units showed an emission at 757 nm, this emission could probably be due to the slight absorption from the core soret band, which comes at 350 nm. In **Figure 3.37**, the dotted line shows the direct core emission without any donor unit after the excitation at 350 nm and solid line shows the emission spectrum of the LH complex core after excitation. As can be seen in **Figure 3.37,** the emission intensity of LH complex is higher than the direct core-dendron emission, it could be confirmed that the self-assembled non-covalent complex with the donor-acceptor pair was exhibiting light harvesting behaviour.

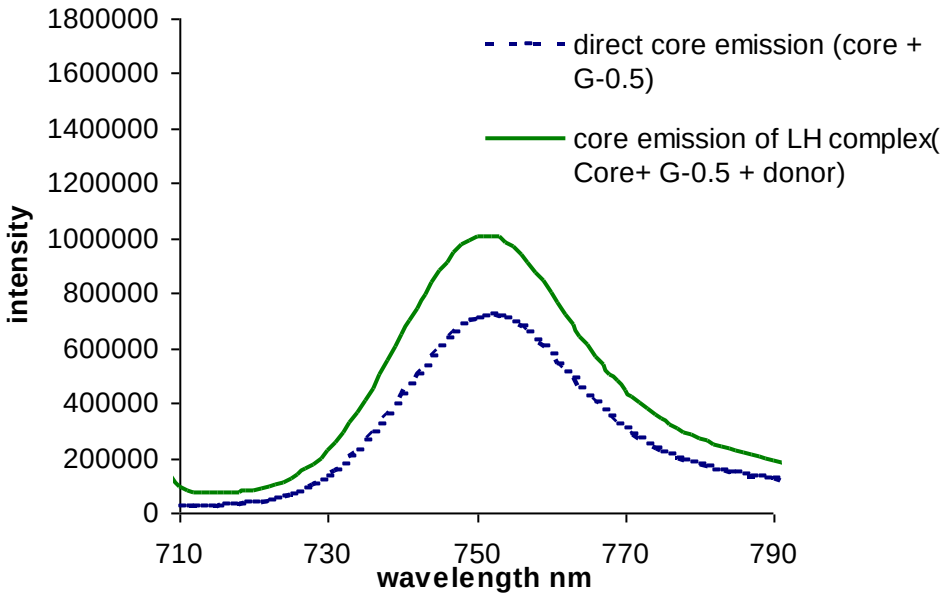

Figure 3.37-A graph showing the LH behaviour of complex **24**.

After observing the successful light-harvesting behaviour for G-0.5 dendron light-harvesting complex, the efficiency of the LH complexes was measured by calculating the quantum yield. Quantum yield is the ratio of the number of emitted photons to the number of observed photons i.e.

$$\Phi_F = \text{Number of emitted photons / number of absorbed photons} \quad \text{----------(5)}$$

The following equation was used for the calculation of the quantum yield

$$\Phi_F = \Phi_{ST}(Grad_X / Grad_{ST})(n^2_X / n^2_{ST}) \quad \text{----------(6)}$$

Where Φ is the fluorescence quantum yield, X and ST stands for standard and test respectively. Grad is the gradient from the plot of the integrated fluorescence intensity Vs absorbance and n^2 is the refractive index of the solvent used.

3.10.2 Quantum yield calculations

The quantum yield for the LH system was calculated using TPP (Φ_F = 0.11)[84] as a known sample (standard). For the quantum yield calculation, the UV/Vis absorption and emission spectrum were calculated first for the used solvent (spectroscopic grade chloroform), the absorption value was obtained at 350 nm from the absorption

spectrum and the integrated fluorescence value was obtained from the emission spectrum by exciting at 350 nm. Then, a 10^{-6}M solution of the LH complex was prepared in spectroscopic grade chloroform. From this prepared LH complex solution, 2 mL solution was transferred into a UV cuvette. After this, the absorption and emission spectrum (by exciting at 350 nm) were obtained. From these obtained spectra, the absorption and integrated fluorescence intensity values were calculated and a graph was plotted between the calculated data values of the 10^{-6}M LH complex solution and the solvent blank solution. Using the plotted graph, the gradient was calculated for the LH complex. The gradient for standard sample i.e TPP was also calculated, following the above procedure. As the same solvent was used for the standard and the LH complex sample preparation, both have same refractive index and the quantum yield $\Phi_F = 0.07$ was calculated using equation **6** and was adjusted for the background intensities.

After observing the successful light-harvesting behaviour for G-0.5 dendron, the decision to observe the light-harvesting behaviour for bigger generations of dendrons, was made. It was expected that with the increasing generations, the intensity of the core emission should also increase. When the light-harvesting test was carried out for the bigger generations, no emission was observed, even for the background emission. After studying the literature for related effects, we noticed that a similar effect was observed in photosensors.[85] It was concluded that the core emission spectrum of the bigger generation LH complexes was showing quenching. Specifically, that quenching was likely due to a inter-quenching within the LH complexes through PET (photoinduced electron transfer) process. It was assumed that the PET process was happening through a fluorophore-spacer-receptor system.[86] The assumed reason behind this inter-quenching was the tertiary amine lone pair. This lone pair was participating in the PET process by quenching the peripheral donor unit fluorophore. To confirm whether or not this quenching was caused by the lone pairs, we decided to react and remove these lone pairs by protonation using TFA (trifluoroacetic acid). The LH experiment was repeated for the higher generation dendrons by adding TFA (10^{-4} M). After the addition of TFA, the emission spectrum of the acceptor unit (core) was observed by exciting the donor units at 350 nm. It was observed that by accepting the proton from TFA, the tertiary amine nitrogen atom makes quaternary ammonium

cations and this stops the electron transfer to the periphery donor atoms and restores the emission from the periphery to the acceptor core as shown in **(Figure 3.38)**.

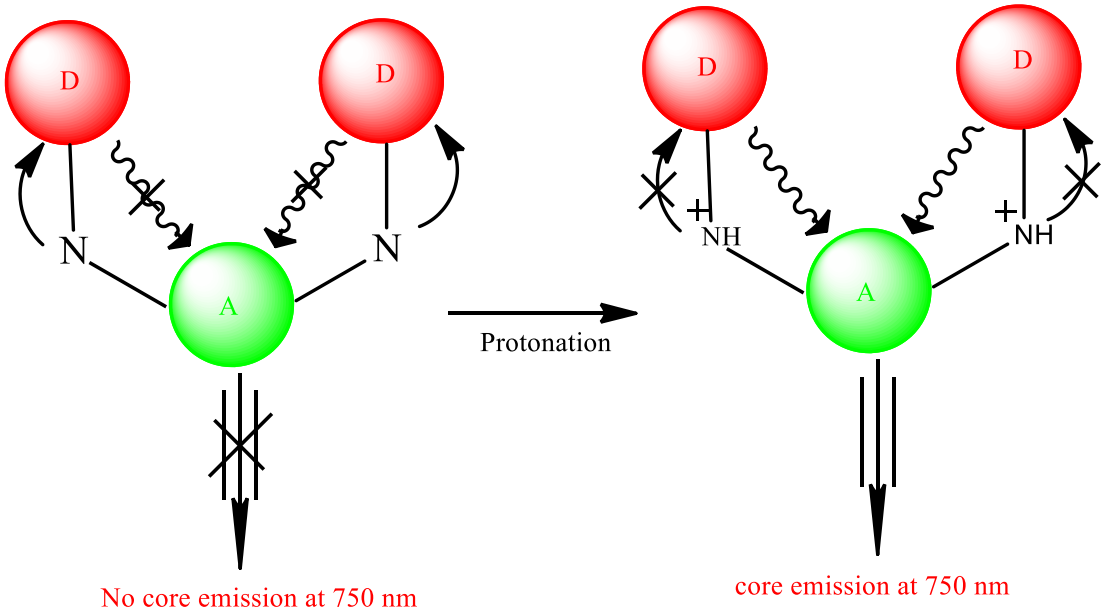

Figure 3.38 - Protonation of dendron internal tertiary amines.

Furthermore, for the comparison, the emission spectrum was also observed for the dendron and the core self-assembly without any donor units in the presence of TFA. The schematic representation of the observed core emission spectrums for the LH complexes is shown in **(Figure 3.39)**. The increased core emission intensity of the light-harvesting complex (acceptor + dendron + donor), with the increasing generations, confirmed the energy transfer in our light-harvesting system. This energy transfer confirms that our donor-acceptor pair shows the antenna effect by absorbing and channelling energy within our system. Thus, our designed acceptor-dendron-donor unit model successfully showed the light-harvesting behaviour where tin(IV) (pentyloxyphthalocyanine) dichloride acted as an acceptor and flexible zinc porphyrin dimer as donor chromophores and dendron as a scaffold.

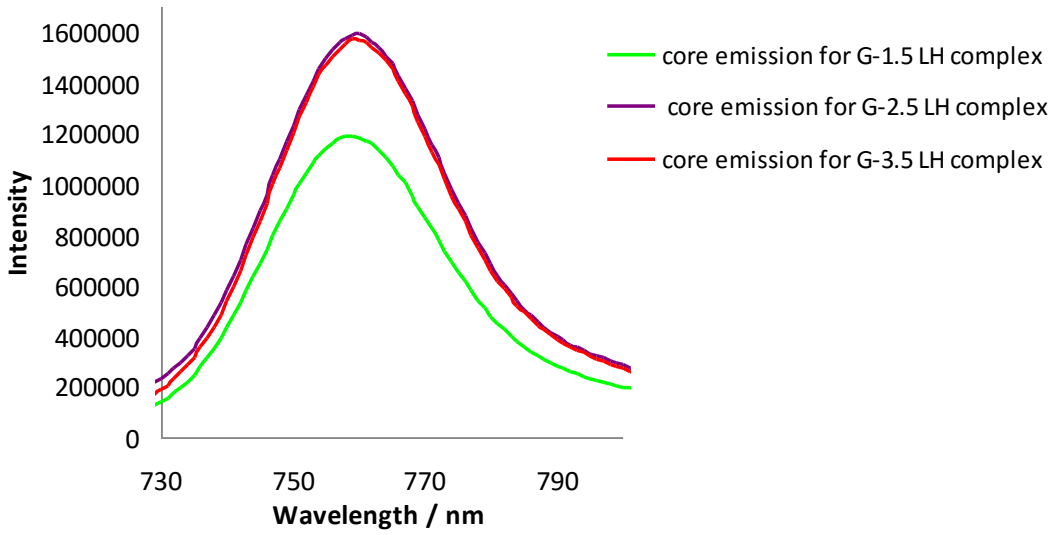

Figure 3.39 - A graph showing the core emissions for the different generation LH complexes.

After the observation of the LH behaviour in our designed system for larger generation dendrons, the quantum yields were calculated using the same procedure as described above and were adjusted for the background intensities. The calculated quantum yields for the larger generation dendron LH complexes are shown in **Table 3.7**.

LH complexes of different generation dendrons	***Calculated quantum yield***
G-0.5	0.07
G-1.5	0.05
G-2.5	0.03
G-3.5	0.01

Table 3.7 – Calculated quantum yields for LH complexes.

Chapter 4

Conclusion and Future work

The work described in this thesis involves mimicking of the natural light-harvesting systems in order to synthesise a model artificial dendrimeric light-harvesting systems. These model systems were designed as light-harvesting antenna capable of absorbing light by its periphery and efficiently transferring the energy to a single reaction centre.

The first step towards our aim was the synthesis of a dendron scaffold to hold an acceptor and the donor unit. The acid core dendrons up to generation four (G-4.0) were synthesised using two iterative steps, i.e. Michael addition and amidation. Michael addition resulted in the ester terminated dendrons (half-generation dendrons) and amidation reaction produced amine terminated dendrons (whole generation dendrons). $SnTPP(OH)_2$ and ZnTPP were used as an acceptor and the donor unit for the preliminarily studies. The ester terminated dendrons showed stronger interactions than amine terminated dendrons and a successful self-assembly between dendron containing ester terminated dendrons, acceptor and the donor units was achieved using metal-coordination supramolecular chemistry. However, this self-assembled complex was unable to achieve light-harvesting behaviour, because of the similar absorption and the emission spectrum of the acceptor and the donor. To overcome this problem, tin(IV) (5,10,15,20-tetraphenylporphyrin) dichloride i.e. $SnPc(Cl)_2$ was used as an acceptor unit. To achieve light-harvesting at a lower concentration range ZnTPP (donor unit) was not found good enough, due to the lower binding constants K_a ~ $5x10^3$ M^{-1} with the acid core ester terminated dendrons. Therefore, in order to achieve stronger interactions between the acid core dendron scaffold and the donor units, the rigid porphyrin dimer was synthesized using mono-nitrated tetraphenylporphyrin. The UV binding titration resulted in unexpected values as K_a ~ $9x10^3$ M^{-1} (G-1.5), $15x10^3$ M^{-1} (G-2.5) and $16x10^3$ M^{-1} (G-3.5). The unexpected Ka values were found due to the rigidity of the porphyrin dimer. To achieve stronger binding interactions a flexible zinc porphyrin dimer (ZnFPD) was synthesised and the K_a values found were $1.95x10^5$ M^{-1} (G-1.5), $1.28x10^5$ M^{-1} (G-2.5) and $1.72x10^5$ M^{-1} (G-3.5). Clearly, these K_a values demonstrated stronger binding interactions between dendron terminal tertiary amines and flexible porphyrin dimer. Finally, a self-assembly was carried out between ester terminated dendrons, $SnPc(Cl)_2$ and ZnFPD to synthesise a dendritic light-harvesting model system. The confirmation of this self-assembly was achieved using the NMR technique by observing significant shifts in the dendron peak regions. After the successful self-assembly, the spectral overlap between the absorption

spectrum of the acceptor i.e. $SnPc(Cl)_2$ and the emission spectrum of the donor i.e. ZnFPD was observed. Then, the light-harvesting (LH) studies were performed to observe the energy transfer between our model systems for different generations of dendrons. The G-0.5 dendron noticeably showed the LH behaviour (Φ_F = 0.07), but in the larger generation LH complexes core emission quenching was observed, due to the dendrons internal tertiary amines. To stop this quenching TFA (10^{-4} M) solution was used for the protonation of the dendron internal tertiary amines. After the addition of the TFA, the dendron LH complexes showed light-harvesting behaviours (Φ_F =0.05 for G-1.5, 0.03 for G-2.5, 0.01 for G-3.5). The efficiency of the energy transfer by observing quantum yields indicated that the phthalocyanine and ZnFPD acceptor-donor pair and dendron with an acid core focal point with ester terminals groups as scaffold to hold this pair are suitable for constructing model light-harvesting systems. Thus, we successfully designed a dendrimeric light-harvesting system, however, the efficiency of this system was not very good for the bigger generation dendrons due to the complexity of the system. Thus, the future work of this research would involve the simplification of the synthesised model by the removal of the internal nitrogen atoms in the dendron scaffold. With the removal of these internal nitrogen atoms there would be no internal quenching and our system would show higher efficiency in the energy transfer. In addition, future work would involve the investigation of light-harvesting behaviour using different acceptor and donor units. In addition, the future investigations would also involve the use of these systems for the cleavage of water into hydrogen and oxygen.

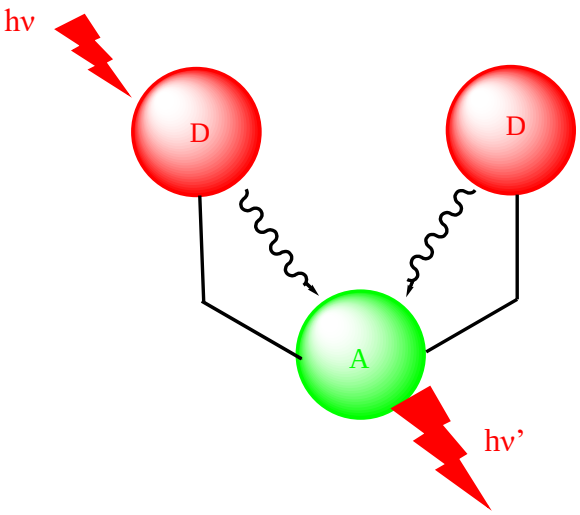

Figure 4.1 Simplified model light harvesting system.

Chapter 5

Experimental

5.1 General Experimental Conditions

Solvents & Reagents

All chemicals and reagents were obtained from commercial sources (primarily Sigma-Aldrich) and were used without further purification unless otherwise stated. Bio-Beads® SX-1 was purchased from Bio-Rad Co. Dry solvents were dispensed from the Chemistry Department Grubbs System having thoroughly dried using molecular sieves.

Infrared (IR) spectroscopy

IR spectra were recorded by using a Perkin-Elmer limited Fourier transform infrared spectrometer. Positions of peaks are started as wave numbers (cm^{-1}).

NMR Spectroscopy

All NMR samples were prepared using deuterated solvents. ^{1}H-NMR and 13C-NMR spectra were recorded by using a Bruker AV1400MHz and AV1250MHz machine. Chemical shifts were quoted using ppm, coupling constant were quoted in Hertz and anomalous impurity and solvent peaks are labelled and referenced to residual solvent signal with Tetramethylsilane δ=0 at =0 as the reference. The NMR spectra were analysed using Topspin 3.0 NMR software.

Mass Spectrometry

The form of ionisation used was dependent on the molecular weight of the sample in question. For samples of low molecular weight, an Electrospray ionisation (ES) technique was used to record spectra. The instrument used was a WATERS LCT mass spectrometer. For samples with a high molecular weight, Matrix assisted laser desorption ionisation MALDI was used. The instrumentation used was a BRUKER REFLEX III MALDI-TOF mass spectrometer.

UV/Vis Spectroscopy

The ultraviolet absorbance was recorded on an Analytik Jena AG Specord s600 UV/Vis Spectrometer and analyzed using its attached Software (WinASPECT).

UV/Vis Titrations

10^{-6}M zinc inserted porphyrins were prepared in dichloromethane; this corresponds to an absorbance of unity at λ_{max}. A solution containing a large excess of dendron ligand units was then prepared using the porphyrin stock solution to ensure a constant concentration of porphyrin throughout the titration. 2ml of the porphyrin solution (ligand free) was accurately measured into a dried cuvette and aliquots of ligand solution (between 10µl and 1000µl) were

added. UV/Vis wavelength scans were taken after each addition, monitoring the Soret band at 428nm. Solutions were made fresh and used within immediately after preparation.

Preparative Size Exclusion Chromatography

Biobead columns were conducted using SX-1 beads from Biorad. These were swelled overnight in THF. Then THF was removed with three bed volumes of DCM and loaded in to a chromatography column. It was imperative to run the column prior to loading the sample to remove any uncross-linked beads present by eluting the column with solvent. The sample was then loaded onto the column in the minimum amount of dichloromethane with the solvent flow controlled by gravity. Sample fractions were monitored with analytical GPC.

X-ray Chromatography

For the collection of crystal data a Bruker SMART4000 APEX II System was used. The structure was solved by using a programe package called WINGX.

Fluorescence Spectroscopy

Fluorescence results were obtained using a HORIBA Scientific Fluoromax-4 spectrofluorometer using its attached software (FluorEssence V3).

Fluorescence Titrations

Each 10^{-6} M solution of the LH complexes were prepared using spectroscopic grade chloroform. The LH complex solution was accurately measured (2 mL) into a quartz cuvette. Fluorescence emission solutions were made fresh and used immediately after preparation.

5.2 Synthesis Procedure

Synthesis of PAMAM dendron G-0.5 holding 2 terminal OMe terminal groups

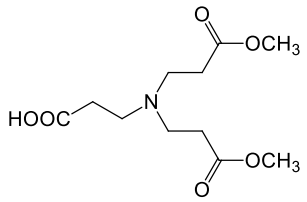

1

Methyl acrylate (11.6 g, 0.13 moles) was added dropwise to the solution of β-alanine (4 g, 0.045 moles) and potassium carbonate (6.22 g, 0.045 moles) dissolved in methanol (50 mL) at 0° C in 500 mL round bottom flask. The reaction was stirred overnight at room temperature, filtered and excess methyl acrylate was removed by evaporation and placed under high vacuum for few hours yielding viscous oil.

Yield 10 g, 85%, ^{1}HNMR(d-$CDCl_3$, 400MHz) δ_H 2.20(t, J = 7.0 Hz, 2H, $NCH_2C\underline{H}_2COOH$), 2.67(t, J = 7.3 Hz, 2H, $NC\underline{H}_2CH_2COOH$), 2.45(t, J = 7.0 Hz, 4H, $NCH_2C\underline{H}_2C{=}O$), 2.73(t, J = 7.0 Hz, 4H, $NC\underline{H}_2CH_2C{=}O$), 3.66(s, 6H, $C\underline{H}_3$); ^{13}C NMR(d-$CDCl_3$, 400MHz) δc 178.9, 175.5, 51.6, 50.9, 49.0, 35.9, 32.2; $FTIR_{\lambda max}$ (cm^{-1}) : 3240(acid OH), 2952(CH-sp^2), 2821(CH-sp^3), 1732(ester carbonyl), 1648, 1572, 1438, 1396, 1264,1176 (-C-N stretch occurs in the range of 1080-1360); ES-MS: 262 (MH+).

Synthesis of PAMAM dendron G-1.0 (holding 2 terminal NH_2 terminal groups)

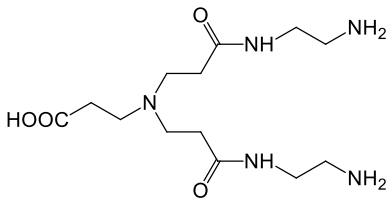

2

The ester terminated intermediate (10 g, 0.0383 moles) was dissolved in methanol (50 mL) and added dropwise to EDA (57.60 g, 0.9550 moles) in a 500 mL round bottom flask at 0° C. The reaction mixture was allowed to react for 5 days, followed by the purification of the mixture to remove excess EDA using a 9:1 azeotropic mixture of toluene: methanol followed by washing with methanol using the rotary evaporator. The mixture was then placed under high vacuum for few hours yielding a white sticky product.

Yield 8.0 g, 66%, ^{1}HNMR(D_2O, 400MHz) δ_H 2.21 (t, J = 7.0 Hz, 2H, $NCH_2C\underline{H}_2COOH$), 2.75-2.55 (m, 10H, $NCH_2CH_2C{=}ONH{+}NC\underline{H}_2CH_2COOH{+}H_2NCH_2C\underline{H}_2N$), 3.04 (t, J = 7.0 Hz, 2H, $NC\underline{H}_2CH_2COOH$), 3.10 (t, J = 7.0 Hz, 4H, $HNC\underline{H}_2CH_2NH_2$); ^{13}C NMR($D_2O$, 400MHz) δc 181.1, 49.3, 48.7, 41.2, 39.6, 34.3, 32.2; FTIR$_{\lambda max}$ (cm^{-1}) : 3263(acid OH), 3064, 2927(CH-sp^2), 2159(CH-sp^3), 1643(amide carbonyl), 1562(amide NH bend), 1557 (amine), 1465(CH_2 bend), 1384, 1315, 1232: ES-MS: 318 (MH+).

Synthesis of PAMAM dendron G-1.5 (holding 4 terminal OMe terminal groups)

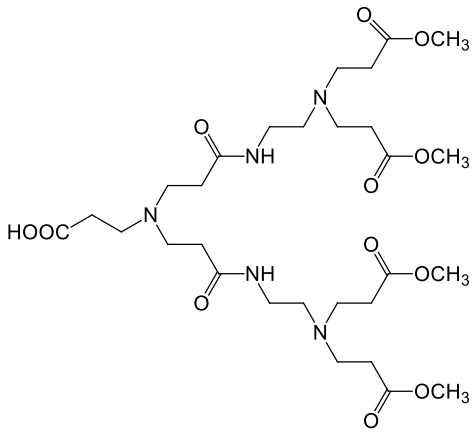

3

The diamine intermediate (6 g, 0.0189 moles) was dissolved in methanol (50ml) and added to a 500 mL round bottom flask. Methyl acrylate (8.5 g, 0.095 moles) was added dropwise to the solution over a period of 30 minutes at 0° C. The reaction was then stirred for 24 hours at room temperature until the reaction reached completion. Excess methyl acrylate was removed via rotary evaporation and placed under high vacuum for few days to remove traces of reagent yielding a honey coloured viscous oil.

Yield 10.0 g, 63%, ^{1}HNMR(d-$CDCl_3$, 400MHz) δ_H 2.21 (t, J = 7.0 Hz, 2H, $NCH_2C\underline{H}_2COOH$), 2.53 (t, J = 7.0 Hz, 6H, $NC\underline{H}_2CH_2COOH{+}NHCH_2C\underline{H}_2N$), 2.75 (t, J = 7.0 Hz, 12H, $NCH_2C\underline{H}_2C{=}OOCH_3{+}NCH_2C\underline{H}_2CONH$), 2.43 (t, J = 7.0 Hz, 8H, $NC\underline{H}_2CH_2C{=}O{+}COOHCH_2C\underline{H}_2N$), 2.36 (t, J = 7.0 Hz, 4H, $NCH_2C\underline{H}_2CONH$), 3.09-3.17 (m, 2H, $CONHC\underline{H}_2CH_2N$), 3.66 (s, 12H, $C\underline{H}_3$),; ^{13}C NMR(d-$CDCl_3$, 400MHz) δc 178.9, 175.5, 51.6, 50.9, 49.0, 35.9, 32.2; FTIR$_{\lambda max}$(cm^{-1}) 3277(acid O-H stretch), 2951(CH-sp^2), 2822(CH-sp^3), 1651(amide carbonyl stretch), 1732(ester carbonyl), 1573, 1437(acid carbonyl stretch), 1394(acid O-H bend), 1259, 1042(-C-N stretch occurs in the range of 1080-1360); ES-MS: 662(MH+) , 684(MNa+).

Synthesis of PAMAM dendron G-2.0 (holding 4 terminal NH_2 terminal groups)

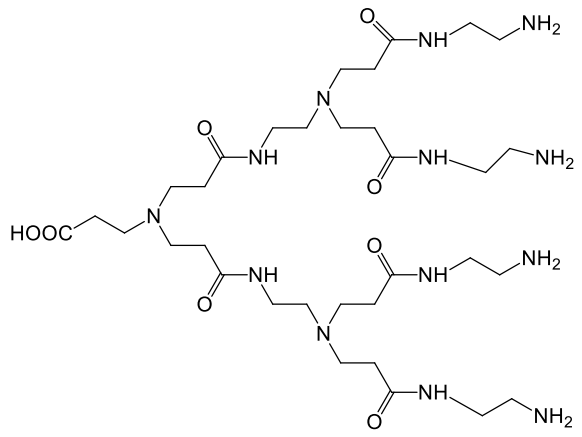

4

The ester terminated intermediate (6.0 g, 0.009 moles) was dissolved in methanol (50 mL) and added dropwise to EDA (27.31 g, 0.454 moles) in a 500 mL round bottom flask at 0° C. The reaction mixture was allowed to react for 7 days to ensure it reached completion, followed by the purification of the mixture to remove excess EDA using 9:1 azeotropic mixture of toluene: methanol followed by washing with methanol using rotary evaporator. The mixture was then placed under high vacuum for few hours yielding a white sticky product.

Yield 8.4 g, 66%, ^{1}HNMR(D_2O, 400MHz) δ_H 2.2(t, J = 7.0 Hz, 2H, $NCH_2C\underline{H}_2COOH$), 2.27(t, J = 7.0 Hz, 12H, $C\underline{H}_2CONH$), 2.46(t, J = 7.0 Hz, 4H, $CONHC\underline{H}_2CH_2N$), 2.54(t, J = 7.0 Hz, 8H, $CONHCH_2C\underline{H}_2NH_2$), 2.72-2.58(m, 14H, $NC\underline{H}_2CH_2COOH$+$NC\underline{H}_2CH_2C{=}O$), 3.07(t, J = 7.0 Hz, 8H, $CONHC\underline{H}_2CH_2NH_2$), 3.13(t, J = 7.0 Hz, 4H, $NHC\underline{H}_2CH_2N$); ^{13}C-NMR(D_2O , 400MHz) δc 181.1, 175.1, 174.8, 51.1, 49.0, 48.8, 48.6, 41.5, 39.7, 36.7, 34.3, 32.7, 32.6; FTIR$_{\lambda max}$(cm^{-1}) 3264(amide N-H stretch), 3061(acid OH), 2929(CH-sp2), 2822(CH-sp3), 1638(amide carbonyl bend), 1547(amide bend), 1434, 1394(acid O-H bend), 1197, 1030(amine C-N stretch occurs weakly in the range 1080-1360); ES-MS: 774 (MH+).

Synthesis of PAMAM dendron G-2.5 (holding 8 terminal OMe terminal groups)

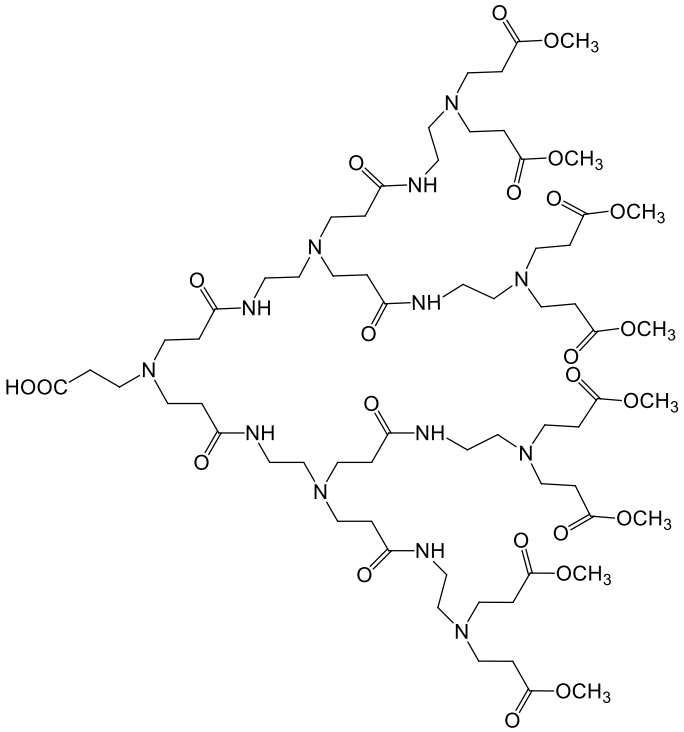

5

The amine intermediate (6.0 g, 0.0077moles) was dissolved in methanol (50 mL) and added to a 500 mL round bottom flask. Methyl acrylate (6.68 g, 0.078 moles) was added dropwise to the solution over a period of 30 minutes at 0° C. The reaction was then stirred for 2 days at room temperature until the reaction reached completion. Excess methyl acrylate was removed via rotary evaporation and placed under high vacuum for few days to remove traces of reagent yielding thick yellowish product.

Yield 4.0 g, 50%, ^{1}HNMR(d-$CDCl_3$, 400MHz) δ_H 2.2 (t, J = 7.0 Hz, 2H, $NCH_2C\underline{H}_2COOH$), 2.37-2.30 (br m, 12H, $NHCH_2C\underline{H}_2C{=}O$), 2.41 (t, J = 7.4 Hz, 16H, $C\underline{H}_2CH_2C{=}OOCH_3$), 2.77-2.48 (mm, 42H, $CH_3C{=}OCH_2C\underline{H}_2N{+}NCH_2C\underline{H}_2C{=}OOCH_3$ $+CH_2NC\underline{H}_2CH_2CONH{+}OHC{=}OCH_2C\underline{H}_2NCH_2$), 3.09-3.15(t, J = 7.0 Hz, 12H $CONHC\underline{H}_2CH_2N$), 3.66 (s, 24H, $C\underline{H}_3$), ; ^{13}CNMR (d-$CDCl_3$, 400MHz) δc 178.8, 173.1, 172.9, 172.5, 52.2, 51.6, 50.2, 49.9, 49.2, 37.3, 37.9, 33.7, 32.6; FTIR$_{\lambda max}$(cm^{-1}) 3287(acid O-H stretch), 2952(CH-sp^2), 2833(CH-sp^3), 1651(amide carbonyl stretch), 1727(ester carbonyl), 1552, 1436(acid carbonyl stretch), 1395(acid O-H bend), 1199(-C-N stretch occurs in the range of 1080-1360), 1043; ES-MS:1462(MH+).

Synthesis of PAMAM dendron G-3.0 (holding 8 terminal NH_2 terminal groups)

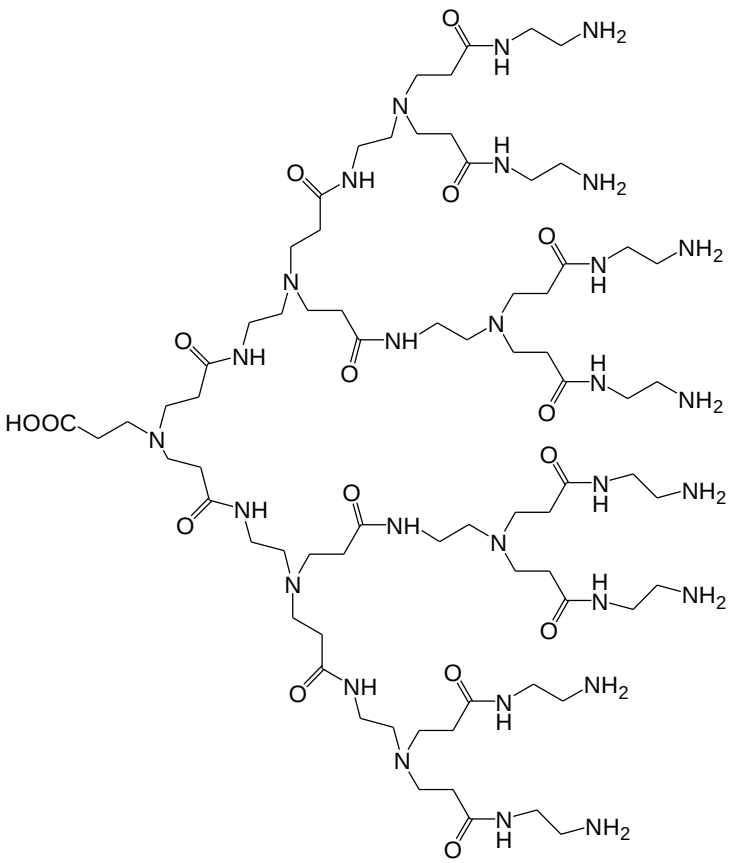

6

The ester terminated intermediate (6.1 g, 0.004 moles) was dissolved in methanol (50 mL) and added dropwise to EDA (23.0 g, 0.375 moles) in a 500 mL round bottom flask at 0° C. The reaction mixture was allowed to react for 8 days to ensure it reached completion, followed by the purification of the mixture to remove excess EDA using 9:1 azeotropic mixture of toluene: methanol followed by washing with methanol using rotary evaporator. The mixture was then placed under high vacuum for few hours yielding white a sticky product.

Yield 7.4 g, 60%, ^{1}HNMR(D_2O, 400MHz) δ_H 2.2 (t, J = 7.0 Hz, 2H, $NCH_2C\underline{H}2COOH$), 2.29 (br m, 28H, $C\underline{H}_2CONH$), 2.47 (t, J = 7.0 Hz, 12H, $CONHC\underline{H}_2CH_2N$), 2.51-2.59 (m, 16H, $CONHCH_2C\underline{H}_2NH_2$), 2.61-2.72 (m, 30H, $NC\underline{H}_2CH_2COOH$+$NC\underline{H}_2CH_2C{=}O$), 3.09 (t, J = 7.0 Hz, 16H, $CONHC\underline{H}_2CH_2NH_2$), 3.14 (12H, t, J = 7.0, $NHC\underline{H}_2CH_2N$); ^{13}C NMR(D_2O, 400MHz) δc 181.1, 175.1, 174.8, 51.1, 49.0, 48.8, 48.6, 42.4, 41.5, 40.7, 39.7, 36.7, 34.3, 32.7, 32.6; FTIR$_{\lambda max}$ (cm^{-1}) 3264(amide N-H stretch), 3061(acid OH), 2929(CH-sp^2), 2822(CH-sp^3), 1638(amide carbonyl bend), 1547(amide bend), MALDI-TOF-MS 1686(MH$^+$).

Synthesis of PAMAM dendron G-3.5 (holding 16 terminal OMe terminal groups)

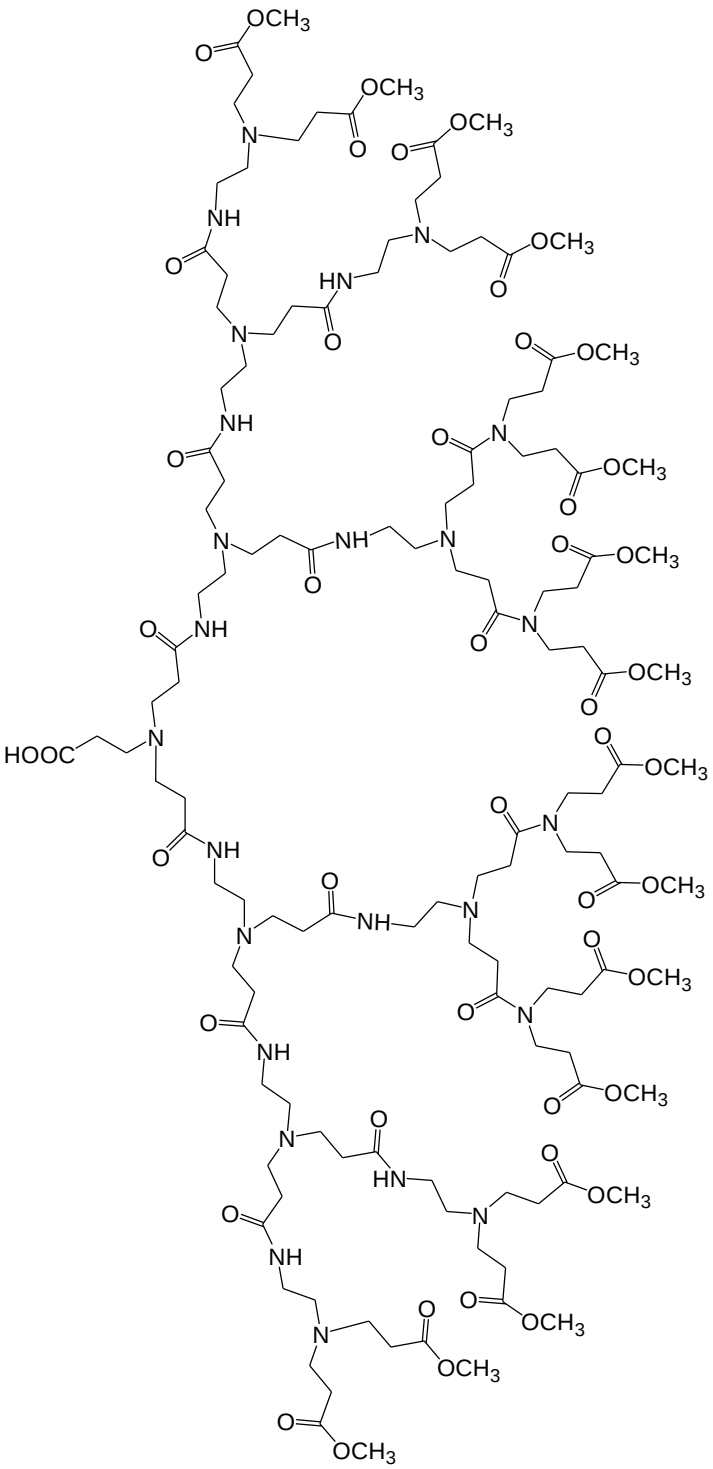

7

The amine intermediate (5.0 g, 0.003moles) was dissolved in methanol (50 mL) and added to a 500 mL round bottom flask. Methyl acrylate (5.11 g, 0.061 moles) was added dropwise to the solution over a period of 30 minutes at 0° C. The reaction was then stirred for 2 days at room temperature until the reaction reached completion. Excess methyl acrylate was removed

via rotary evaporation and placed under high vacuum for few days to remove traces of reagent yielding a thick yellowish product.

Yield 7.6 g, 50%, ^{1}HNMR(d-$CDCl_3$, 400MHz) δ_H 2.20-2.35 (br m, 2H, $NCH_2C\underline{H}_2COOH$), 2.37-2.30 (br m,32H, $NHCH_2C\underline{H}_2C{=}O$), 2.41 (t, J = 7.0 Hz 32H, $NC\underline{H}_2CH_2C{=}OOCH_3$), 2.77-2.48(m, 42H, $CH_3C{=}OCH_2C\underline{H}_2N+NCH_2C\underline{H}_2C{=}OOCH_3+CH_2NC\underline{H}_2CH_2CONH+OHC{=}OCH_2C\underline{H}_2NCH_2$), 3.09-3.15(m, 12H, $CONHC\underline{H}_2CH_2N$), 3.66(s, 48H, $C\underline{H}_3$); ^{13}C NMR(d-$CDCl_3$, 400MHz) δc 178.8, 173.1, 172.9, 172.5, 52.2, 51.6, 50.2, 49.9, 49.2, 37.3, 37.9, 33.7, 32.6; FTIR$_{\lambda max}$(cm^{-1}) 3287(acid O-H stretch), 2952(CH-sp^2), 2833(CH-sp^3), 1651(amide carbonyl stretch), 1727(ester carbonyl), 1552, 1436(acid carbonyl stretch), 1395(acid O-H bend), 1199(-C-N stretch occurs in the range of 1080-1360), 1043; ES-MS: 2890(MH^+).

Synthesis of PAMAM dendron G-4.0 (holding 16 terminal NH_2 groups)

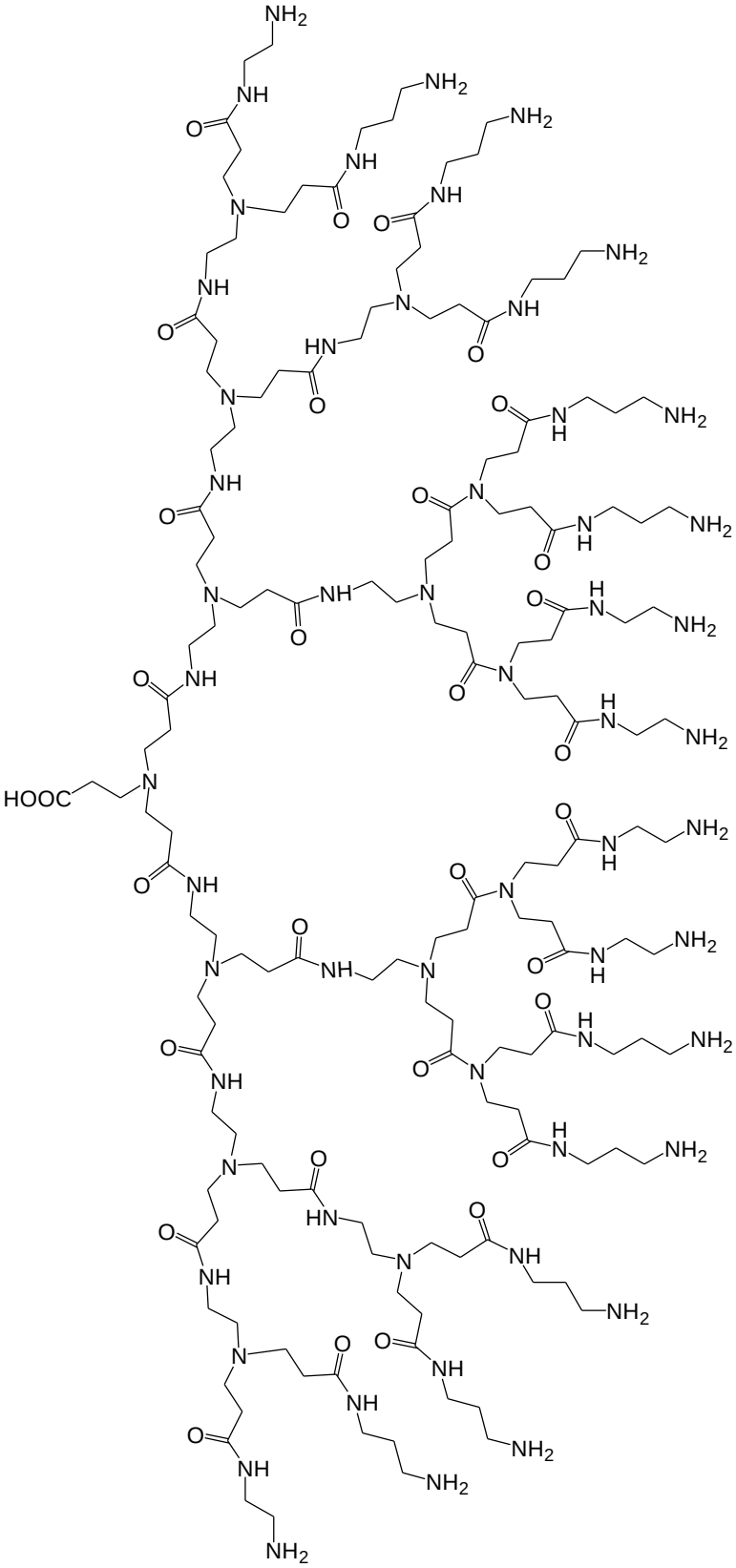

The ester terminated intermediate (5.6 g, 0.0018 moles) was dissolved in methanol (50 mL) and added drop wise to EDA (19.8 g, 0.328 moles) in a 500 mL round bottom flask at 0° C.

The reaction mixture was allowed to react for 10 days to ensure it reached completion, followed by the purification of the mixture to remove excess EDA using 9:1 azeotropic mixture of toluene: methanol followed by washing with methanol using rotary evaporator. The mixture was then placed under high vacuum for few hours yielding white sticky product.

Yield 5.0 g 45% ^{1}HNMR(D_2O, 400MHz) δ_H 2.20-2.23 (br m, 2H, $NCH_2C\underline{H}_2COOH$), 2.23-2.29 (m, 60H, $C\underline{H}_2CONH$), 2.45-2.59 (m, 28H, $CONHC\underline{H}_2CH_2N$), 2.50-260 (m, 32H, $CONHCH_2C\underline{H}_2NH_2$), 2.61-2.72 (m, 62H, $NC\underline{H}_2CH_2COOH$+$NC\underline{H}_2CH_2C{=}O$), 3.06-3.19 (m, 60H, $CONHC\underline{H}_2CH_2\ NH_2$+$NHC\underline{H}_2CH_2N$); ^{13}C-NMR ($D_2O$, 400MHz) δc 181.1, 175.1, 174.8, 53.1, 51.1, 49.0, 48.8, 48.6, 42.4, 41.5, 40.7, 39.7, 36.7, 34.3, 32.7, 32.6; FTIR$_{\lambda max}$ (cm^{-1}) 3264(amide stretch), 3061(acid OH), 2929(CH-sp^2), 2822(CH-sp^3), 1638(amide carbonyl bend), 1547(amide bend), MALDI-TOF-MS 3511(MH$^+$).

Synthesis of Tetraphenylporphyrin

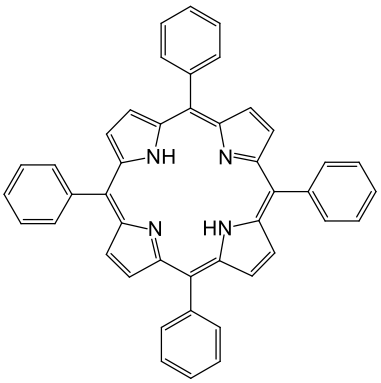

8

Freshly distilled pyrrole (5.54 mL, 80 mol) and benzaldehyde (13.13 g, 80 mmol) were added to refluxing propionic acid (300 mL). The mixture was refluxed for 30 minutes and then allowed to cool at room temperature. The reaction mixture was filtered, washed thoroughly with methanol, hot distilled water and then methanol once again. The final purple product was oven dried.

Yield 2.50 g, 50%, ^{1}HNMR (d-$CDCl_3$, 400MHz) δ_H -2.73(s, 2H, N-H), 8.89(s, 8H, pyrrolic βH), 8.25(d, J=9.0 Hz, 8H, phenolic o-CH), 7.80(d, J=2.0 Hz, 12H, phenyl m,p-CH); ^{13}C-NMR(d-$CDCl_3$, 400MHz) δc 142.1, 134.5, 127.7, 126.1; FTIR$_{\lambda max}$: 2923(s), 2854(s), 1463, 1377(w), 1173(w); UV/Vis Spectroscopy 419(soret band), 516, 549, 590, 647; ES-MS: 615(MH+).

Synthesis of tin(1V) (5,10,15,20-tetraphenyporphyrin) dihydroxy

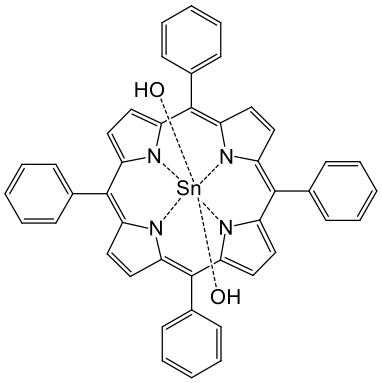

9

Tetraphenylporphyrin (250 mg) and powdered tin(11) chloride dihydrate (200 mg) were dissolved in pyridine (25 mL) stirred and refluxed for one hour. The solution was cooled at 50° C and then concentrated ammonia NH_3 (12.5 mL) was added very carefully, heating and stirring were continued for another hour. After one hour water (150 mL) was added and solid collected by vacuum filtration, washed with water and dried by suction. The filter cake was digested with chloroform (60 mL), which dissolved the purple product, leaving a brown residue of tin salts. The filtrate was dried with anhydrous Na_2SO_4 and concentrated to 10 mL on a rotary evaporator. The concentrate was passed through a short column of neutral alumina (50 g) in chloroform. The product was eluted with $CHCl_3$ and the purple band was concentrated to ~3ml. Hexane (50 mL) was carefully layered on top of the $CHCl_3$ solution, the flask stoppered, and the mixture left to crystalline for 2 days. The purple crystals were filtered, washed with hexane and dried in the vacuum desiccator.

Yield 0.15 g, 47%, ^{1}HNMR(d-$CDCl_3$, 400MHz) δ_H -6.97 (br s, 2H, OH), 7.80-7.86 (m, 12H, meta and para Ar-H), 8.30-8.39 (m, 8H, ortho Ar-H), 9.20 (s, 8H, pyrrol β-H); ^{13}C NMR(d-$CDCl_3$, 400MHz) δc 146.7, 141.3, 135.1, 132.5, 128.2, 126.9, 121.2; FTIR$_{\lambda max}$(cm^{-1}): 3646, 3109, 2921, 2158; UV/Vis Spectroscopy: 427, 518.5, 560, 600; MALDI-TOF-MS; expected (764) obtained 749(M-OH)$^{+}$.

Synthesis of tin(1V) (5,10,15,20-tetraphenyporphyrin) diacetoxy

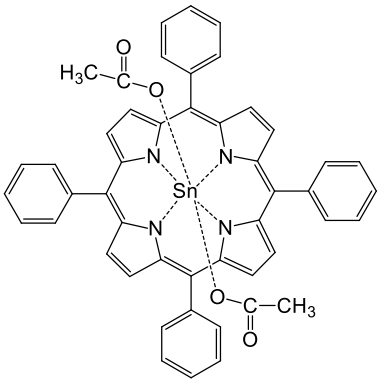

10

Tin(1V) (5,10,15,20-tetraphenyporphyrin) dihydroxy (38 mg, 0.05 mmol) was dissolved in $CHCl_3$ (5 mL) in a 100ml round bottom flask. Acetic acid (12.01 mg, 0.2 mmol) was added and mixture was stirred magnetically for 20 minutes. Anhydrous Na_2SO_4 (0.25 g) was added and then stirring was continued for another 15 minutes. The solution was filtered through a cotton wool plug in a disposable pipette into a small round bottom flask. The solvent was removed by rotary evaporator. The purple crystals formed were recrystallised using hexane

.

Yield 30 mg, 70%**,** ^{1}H NMR(d-$CDCl_3$, 400MHz) δ_H -1.01(s, 6H, C<u>H</u>$_3$), 7.80-7.89(m, 12H, Ar-H), 8.32-8.36(m, 8H, Ar-H), 9.2(s, 8H, pyrrol β-<u>H</u>); ^{13}C-NMR(d-$CDCl_3$, 400MHz) δc 168.3, 146.7, 141.3, 135.1, 132.5, 128.2, 126.9, 121.2; FTIR$_{\lambda max}$(cm^{-1}): 1660(s), 1279(s), 1469, 1360, 1309; UV/Vis spectroscopy: 424, 521, 558.5, 598; MALDI-TOF-MS; expected (850) obtained 790(M-CH_3COO)$^+$.

Synthesis of tin(1V) (5,10,15,20-tetraphenyporphyrin) dibenzoxy

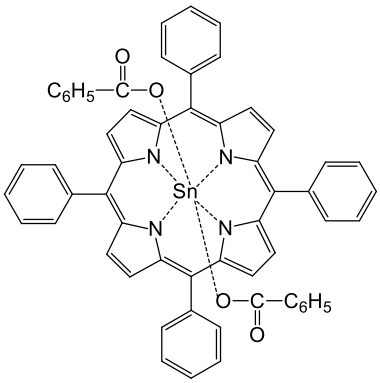

11

Tin(1V) (5,10,15,20-tetraphenyporphyrin) dihydroxy (77 mg, 0.1mmol) was dissolved in $CHCl_3$ (5 mL) in a 100 mL round bottom flask. Benzoic acid (30 mg, 0.24 mmol) was added and mixture was stirred magnetically for 20 minutes. Anhydrous Na_2SO_4 (0.25 g) was added and then stirring was continued for another 15 minutes. The solution was filtered through a cotton wool plug in a disposable pipette into a small round bottom flask. The solvent was removed by rotary evaporator. The purple powder formed was recrystallised using hexane.

Yield 50 mg, 51%**.** ^{1}HNMR(d-$CDCl_3$, 400MHz) δ_H 4.87-4.93(m, 4H, Ar- H_o), 6.67-6.71(m, 2H, Ar-H_p), 6.32-6.38(m, 4H, Ar-H), 7.79-7.88(m, 12H, Ar-H), 8.32-8.36(m, 8H, Ar-H), 9.14(s, 8H, pyrrol β-H); ^{13}C-NMR(d-$CDCl_3$, 400MHz) δc 162.8, 146.7, 141.3, 135.1, 132.5, 128.2, 126.9, 121.2; FTIR$_{\lambda max}$(cm^{-1}): 1651(s), 1312(s), 1296 (carboxylate). UV/Vis spectroscopy (nm): 423, 517, 556, 596. MALDI-TOF-MS; expected (974) obtained 853(M-$C_6H_5COO)^+$.

Self-assembly of PAMAM dendron holding 2 terminal OMe terminal groups (G-0.5) with tin(1V) (5,10,15,20-tetraphenyporphyrin) dihydroxy

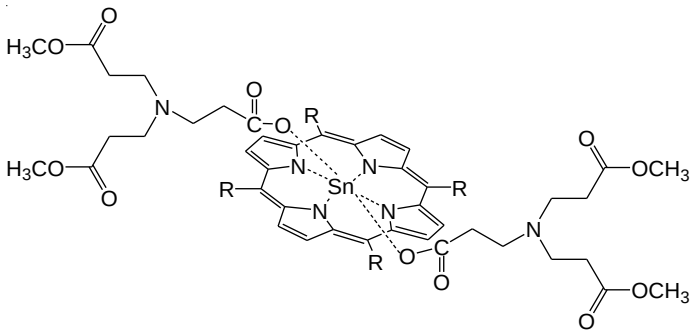

Where R = -C_6H_5

12

Dendron G-0.5 holding 2 terminal OMe terminal groups (50 mg, 0.16 mmol) and $TPPSn(OH)_2$ (60 mg, 0.08 mmol) were dissolved in $CHCl_3$ (5 mL) and stirred magnetically for an hour. The mixture was passed through a small plug of anhydrous Na_2SO_4 (0.25 g) into a round bottom flask. The solvent was removed by rotary evaporator. The purple coloured product formed.

Yield 90 mg, ^{1}H NMR(d-$CDCl_3$, 400MHz) δ_H -(0.74-0.69) (m, 1H, HOOCC$\underline{H}_2$CH$_2$), -(0.39-0.34) (m, 1H, HOOCC$\underline{H}_2$), 0.85-0.94 (m, 2H, HOOCCH$_2$C$\underline{H}_2$), 1.54-1.66(m, 4H, CH$_2$C$\underline{H}_2$N), 2.28(br s, 2H, C$\underline{H}_2$COOCH$_3$), 2.48(t, J = 7.0 Hz, 6H, C$\underline{H}_2$COOCH$_3$), 2.65- 2.77(m, 8H, NC$\underline{H}_2$CH$_2$), 3.68(s, 12H, C$\underline{H}_3$), 7.80-7.91(m, 14H, m, p- Ar-H), 8.25-8.44(m, 8H, o- Ar-H),

9.14-9.26(m, 8H, pyrrol β H); ^{13}C-NMR(d-$CDCl_3$, 250MHz) δc 173.0, 168.7, 146.7, 141.3, 135.1, 132.5, 128.2, 126.9, 121.2, 51.6, 48.9, 47.6, 32.2, 31.8, 29.7, 21.3; UV/Vis spectroscopy (nm); 424, 518, 559, 598; MALDI-TOF-MS: 1261(expected), 991(M-G-0.5)$^+$ (obtained).

Self-assembly of PAMAM dendron holding 4 terminal OMe groups (G-1.5) with tin(IV) (5,10,15,20-tetraphenylporphyrin) dihydroxy

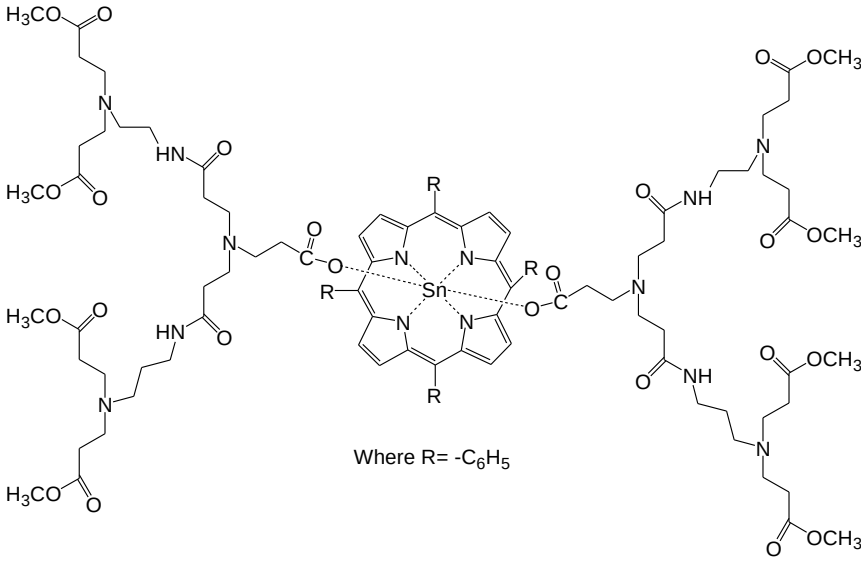

Dendron G-1.5 holding 4 terminal OMe groups (103.6 mg, 0.16 mmol), TPPSn(OH)$_2$ (60 mg, 0.08 mmol) were dissolved in $CHCl_3$ (5 mL) and stirred magnetically for an hour. Then the mixture was passed through a small plug of anhydrous Na_2SO_4 (0.25 g) into a round bottom flask. The solvent was removed by rotary evaporator. The purple coloured product formed.

Yield 130 mg, 97%, ^{1}H NMR(d-$CDCl_3$, 400 MHz) δ_H -(0.69-0.74)(m, 1H, C=OC$\underline{H}_2$CH$_2$), -(0.34-0.39)(m, 1H, C=OC$\underline{H}_2$CH$_2$), 0.94-0.85(m, 1H, C$\underline{H}_2$), 1.56(t, J = 6.9 Hz, 4H), 2.26(t, J = 6.8 Hz, 6H, C$\underline{H}_2$NCH$_2$+NC$\underline{H}_2$CH$_2$CO), 2.83-2.45(m, 38H, NC$\underline{H}_2$CH$_2$COOH+NHCH$_2$C$\underline{H}_2$N+NC$\underline{H}_2$CH$_2$COCH$_3$+NCH$_2$C$\underline{H}_2$COCH$_3$), 2.2(t, J = 7.2 Hz, 4H, CH$_2$C$\underline{H}_2$CONH+CH$_2$NC$\underline{H}_2$), 2.42(t, J = 6.9 Hz, 4H, NCH$_2$C$\underline{H}_2$CONH), 3.32-2.91(mm, 8H, CH$_2$NHC$\underline{H}_2$), 3.70(s, 24H, C$\underline{H}_3$), 7.80-7.91(m, 12H, meta and para Ar-H), 8.20-8.41(m, 8H, ortho Ar-H), 9.24(s, 8H, pyrrol β-H); ^{13}C-NMR(d-$CDCl_3$, 250MHz) δc 173.0, 168.7, 146.7, 141.3, 135.1, 132.5, 128.2, 126.9, 121.2, 51.6, 48.9, 47.6, 32.2, 31.8, 29.7, 21.3; UV/Vis Spectroscopy(nm); 424, 518, 559, 598; MALDI-TOF-MS: 2051(expected), 1392(M-G-1.5)$^+$(obtained).

Self-assembly of PAMAM dendron holding 8 terminal OMe (G-2.5) groups with tin(IV) (5,10,15,20-tetraphenylporphyrin) dihydroxy

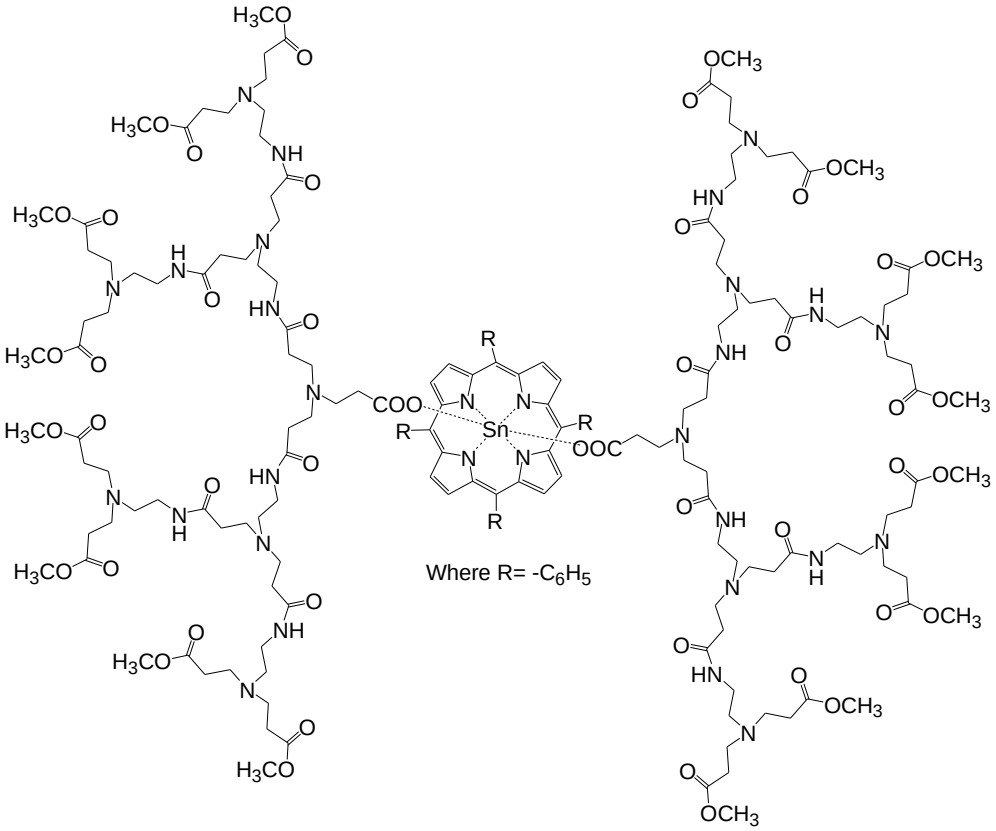

Dendron G-2.5 holding 8 OMe terminal groups (229.20 mg, 0.16 mmol), $TPPSn(OH)_2$ (60 mg, 0.08 mmol) were dissolved in $CHCl_3$ (5 mL) and stirred magnetically for an hour. Then the mixture was passed through a small plug of anhydrous Na_2SO_4 (0.25 g) into a round bottom flask. The solvent was removed by rotary evaporator. The purple coloured product formed.

Yield 190 mg, 90%, ^{1}HNMR(d-$CDCl_3$, 400MHz) δ_H 3.64(s, 48H, C<u>H</u>$_3$), -0.90(t, J = 7.0 Hz, 1H), -0.30(t, J = 7.8 Hz, 1H), 1.32(t, J = 7.4 Hz, 2H), 1.47(t, J = 7.0 Hz, 2H), 2.06-2.14(6H, m,), 2.22-2.44(mm, 54H), 2.48-2.58(m, 26H), 2.48-2.79(m, 76H), 3.06-3.11(m, 6H), 3.19-3.27(m, 16H), 7.80-7.91(m, 12H, meta and para Ar-H), 8.20-8.41(m, 8H, ortho Ar-H), 9.09-9.18(m, 8H, pyrrol β-H); ^{13}C-NMR(d-$CDCl_3$, 250MHz) δc 173.02, 168.77, 146.71, 141.35, 135.15, 132.58, 128.23, 126.99, 121.21, 51.62, 48.98, 47.64, 32.23, 31.88, 29,74, 21.35; UV/Vis Spectroscopy (nm); 424, 518, 559, 598; MALDI-TOF-MS: 3685(expected), 2194(M-G0.5) (obtained).

Synthesis of zinc 5,10,15,20-tetraphenylporphyrin (TPP)

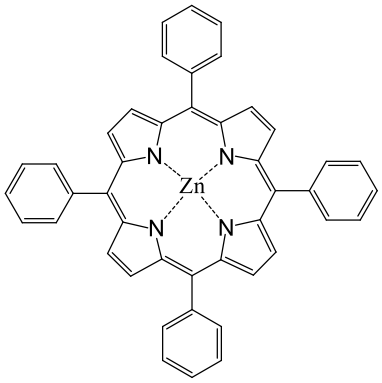

13

Tetraphenylporphyrin (TPP) (500 mg) was dissolved in chloroform. Zinc acetate (1.5 g) was added to the stirring solution of TPP at 50˚C. The reaction mixture was left for stirring for 20 minutes for the completion of reaction. Then the reaction mixture was filtered to remove zinc acetate. Removal of solvent by rotary evaporator gave the purple shiny crystals.

Yield 0.57 g, 90% , ^{1}HNMR(d-$CDCl_3$, 400MHz) δ_H 8.89(s, 8H pyrrolic βH), 8.25(d, J = 7.9 Hz, 8H phenyl o-CH), 7.80(d, J = 8.3 Hz, 12H, phenyl m,p-CH); ^{13}CNMR(d-$CDCl_3$, 400MHz) δc 150.20, 142.81, 134.45, 132.03, 127.51, 126.57, 121.16; FTIR$_{\lambda max}$: 2923(s), 2854(s), 1463, 1377(w), 1173(w); UV/Vis Spectroscopy (nm): 418, 546; ES-MS: 677 (MH+).

Synthesis of compound B

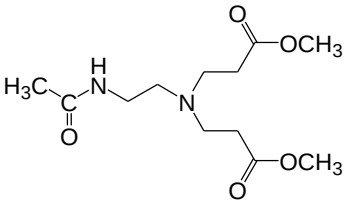

B

N-Acetylethylenediamine (0.5 g, 0.0049 moles) was dissolved in methanol (30 mL) and added to a 250 mL round bottom flask. Methyl acrylate (1.26 g, 0.015 moles) was added, drop wise, to the solution over a period of 30 minutes at 0° C. The reaction was then stirred for 12 hours at room temperature until the reaction reached completion. Excess methyl acrylate was removed via rotary evaporation and placed under high vacuum for few days to remove traces of reagent yielding a thick white product.

Yield 0.3 g, 85%, ^{1}H NMR(d-$CDCl_3$, 400MHz) δ_H 1.99(s, 3H, C$\underline{H}_3$CONH), 2.42(t, J = 6.4 Hz, 4H, $NCH_2C\underline{H}_2COOCH_3$), 2.52(t, J = 5.5 Hz, 2H, $NHCH_2C\underline{H}_2N$), 2.72(t, J = 6.4, 4H, $NC\underline{H}_2CH_2C{=}OOCH_3$) 3.28-3.32(q, 2H, $NHC\underline{H}_2CH_2N$), 3.66(s, 6H, C$\underline{H}_3$); ^{13}C-NMR(d-$CDCl_3$, 400MHz) δc 173.1, 52.9, 51.6, 49.2, 37.0, 32.8, 23.0; FTIR$_{\lambda max}$ (cm^{-1}): 2952(CH-sp2), 2821(CH-sp3), 1732(ester carbonyl), 1648, 1572, 1438, 1396, 1264,1176 (-C-N stretch occurs in the range of 1080-1360); ES-MS: 275 (MH^+).

Self-assembly of tin(IV) (5,10,15,20-tetraphenylporphyrin) dihydroxy, dendron G-0.5 and zinc 5,10,15,20-tetraphenylporphyrin

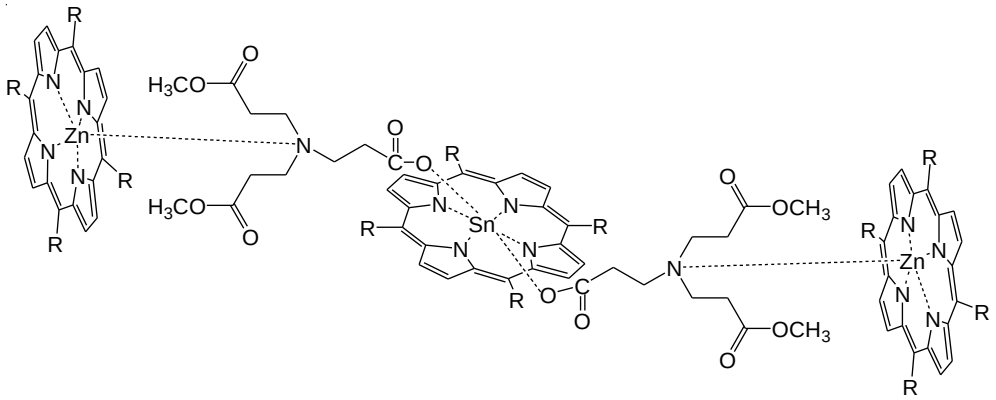

Dendron G-0.5 containing 2 terminal OMe groups (0.002 mg, 0.002 moles), tin(IV) (5,10,15,20-tetraphenylporphyrin) dihydroxy (0.002 mg, 0.001 moles) and ZnTPP (0.004 mg, 0.002 moles) was dissolved in 3 mL of $CDCl_3$. This reaction mixture was stirred for 5 minutes.

Yield ^{1}H NMR (d-$CDCl_3$, 400MHz) δ_H –0.75 (t, J =7.2 Hz, 1H), -0.45 (t, J = 7.4 Hz, 1H), 1.52-1.66 (m, 6H), 2.27-2.63 (mm, 18H), 3.58(s, 8H), 7.72-7.92 (m, 26H), 8.14-8.50 (m, 17H), 8.90 (s, 5H); ^{13}C-NMR(d-$CDCl_3$, 400MHz) δc 172.3, 171.9, 168.3, 148.7, 145.7, 141.8, 140.0, 139.9, 143.1, 134.09, 133.6, 133.4, 131.5, 131.4, 130.5, 127.2, 127.1, 126.2, 125.9, 125.8, 125.3, 119.5, 119.9, 120.1, 50.4, 50.1, 47.7, 46.8, 31.0, 30.6.

Self-assembly of tin(IV) (5,10,15,20-tetraphenylporphyrin) dihydroxy, dendron G-1.5 and zinc 5,10,15,20-tetraphenylporphyrin

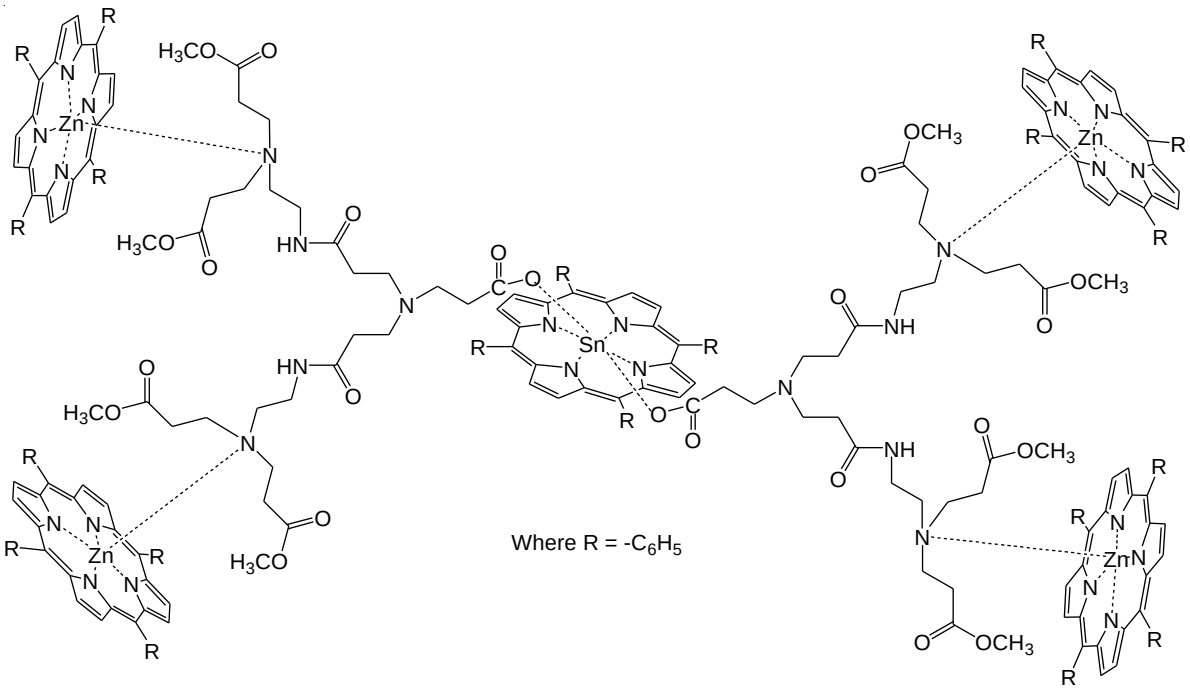

Dendron G-1.5 containing 4 terminal OMe groups (0.001 mg, 0.002 moles), tin(IV) (5,10,15,20-tetraphenylporphyrin) dihydroxy (0.001 mg, 0.001 moles) and ZnTPP (0.003 mg, 0.004 moles) was dissolved in 1 mL of $CDCl_3$. This reaction mixture was stirred for 5 minutes.

Yield ^{1}H NMR (d-$CDCl_3$, 400MHz) δ_H –0.87 (t, J =7.0 Hz, 1H), -0.75 (t, J = 6.8 Hz,1H), -1.19 (t, J = 7.5 Hz, 1H), 0.10 (t, J = 7.0 Hz,1H), 1.30-1.60(mm, 16H), 2.12-2.32 (m, 18H), 2.36-2.65 (mm, 28H), 2.65-2.93(m,16H), 3.66-3.70 (m,14H), 7.68-7.92 (m, 23H), 8.15-8.43 (m, 23H), 8.90 (s, 3H); ^{13}C-NMR(d-$CDCl_3$, 400MHz) δc 173.1, 173. 0, 172.8, 171.6, 168.7, 149.9, 147.0, 147.0, 146.9, 146.6, 143.2, 141.2, 140.7, 135.1, 134.8, 134.7, 134.5, 133.0, 132.7, 131.6, 128.4, 128.2, 127.2, 127.1, 127.0, 126.3, 121.7, 121.5, 120.6, 53.0, 52.8, 52.6, 51.7, 51.6, 51.5, 51.4, 49.2, 49.0, 48.5, 46.9, 37.0, 36.8, 36.7, 32.8, 32.7, 32.4, 32.3, 29.7.

Self-assembly of tin(IV) (5,10,15,20-tetraphenylporphyrin) dihydroxy, dendron G-2.5 and zinc 5,10,15,20-tetraphenylporphyrin

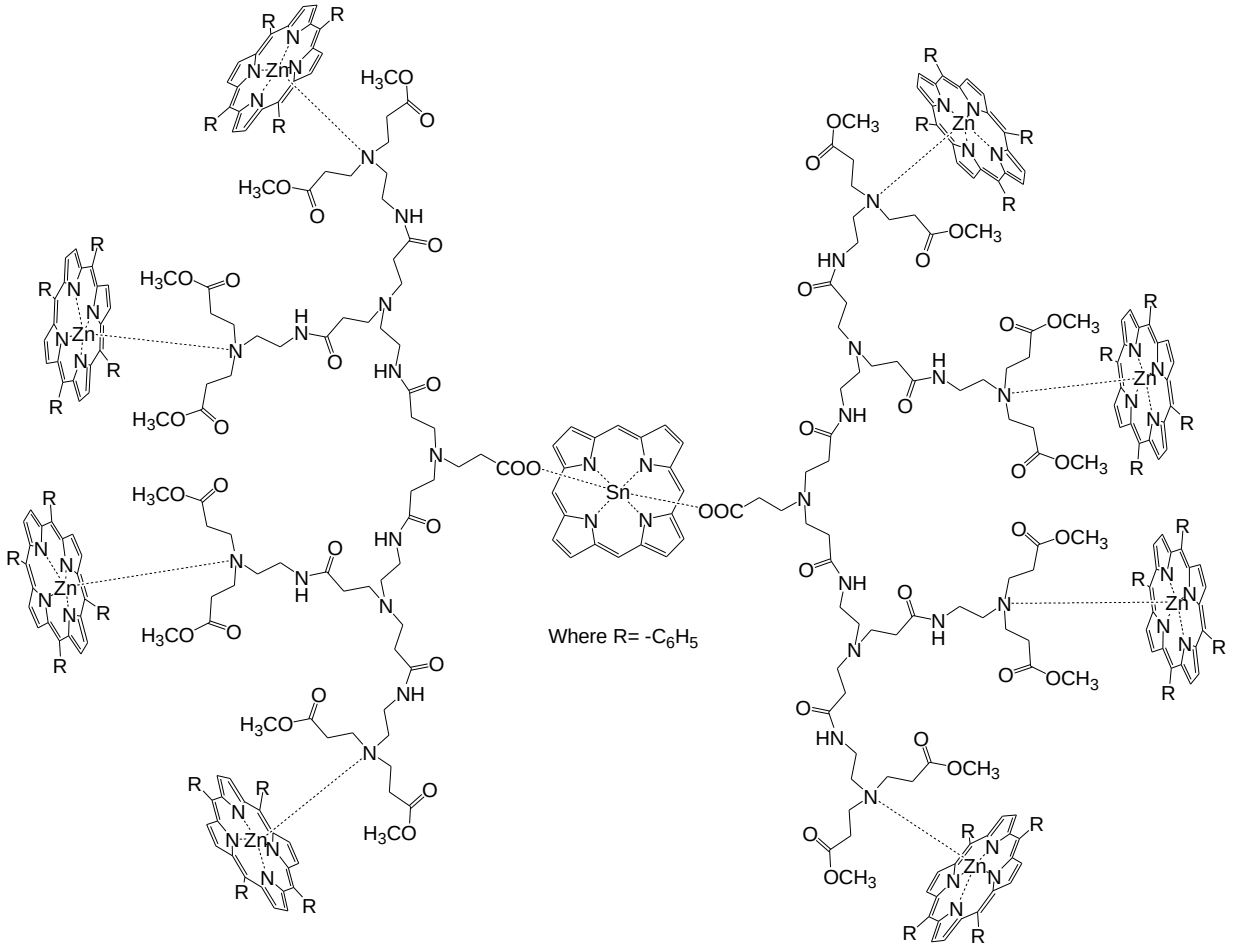

Dendron G-2.5 containing 8 terminal OMe groups (0.003 mg, 0.002 moles), tin(IV) (5,10,15,20-tetraphenylporphyrin) dihydroxy (0.001 mg, 0.001 moles) and ZnTPP (0.005 mg, 0.008 moles) was dissolved in 1 mL of $CDCl_3$. this reaction mixture was stirred for 5 minutes.

Yield ^{1}H NMR (d-$CDCl_3$, 400MHz) δ_H 0.89-0.96(m, 4H), 1.13-2.14(mm, 59H), 2.27-2.40(m, 32H), 2.43-2.46(t, J = 7.1 Hz, 14H), 2.56-2.73(m, 23H), 2.75-2.79(t, J = 7.1 Hz, 6H), 2.83-2.90(br s, 12H), 3.58-3.68(m, 38H), 7.73-7.89(m, 26H), 8.21-8.22(d, J = 8.3 Hz, 15H), 8.33-8.34(d, J = 6.5 Hz, 2H), 8.94(s, 10H), 9.13(s, 2H); 173.0, 169.7, 149.2, 146.4, 142.8, 134.4, 132.3, 128.3, 126.9, 127.5, 126.5, 121.2, 51.6, 48.9, 47.6, 32.2, 31.8, 29.8, 21.3

Synthesis of 5-(4-Nitrophenyl)-10, 15, 20-triphenylporphyrin

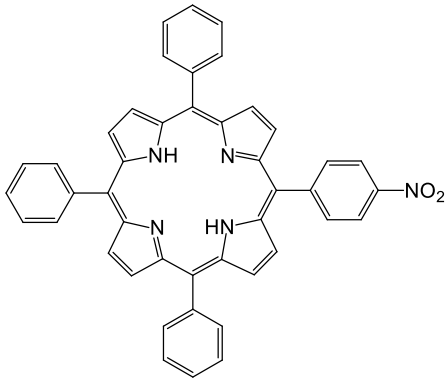

14

5,10,15,20-tetraphenylporphyrin (TPP) (2 g, 3.2 mmol) was dissolved in the minimum volume of trifluoroacetic acid (50 mL) to which sodium nitrite (0.41 g, 5.9 mmol) was added. The reaction mixture was stirred for 2 minutes 45 seconds at room temperature and then quenched by pouring into water (100 mL). The crude product was partitioned into dichloromethane (200 mL) and was filtered through celite to aid separation of the aqueous layer. The organic layer was washed with saturated sodium hydrogen carbonate (200 mL) and water before being dried over magnesium sulphate. After filtration the crude product was reduced and purified by silica column with 1/1 dichloromethane/ petroleum ether. Unreacted TPP was recovered first followed by the product which eluted as the second spot.

Yield 1.09 g, 52 % ^{1}HNMR(d-$CDCl_3$, 400MHz) δ_H -2.76(s, 2H, NH), 7.80(m, 9H phenyl m,p-CH), 8.25(m, 6H pyrrolic βH), 8.42(d, J = 8.5 Hz, 2H pyrrolic), 8.66(d, J = 8.5 Hz, 2H) 8.76(d, J = 5.0 Hz, 2H, C<u>H</u>NO_2), 8.90(m, 6H phenyl o-CH); ^{13}C-NMR(d-$CDCl_3$, 400MHz) δc 145.7, 135.7, 134.4, 132.4, 128.4, 127.5, 124.9, 115.0; FTIR$_{\lambda max}$ (cm)$^{-1}$: 3303 (w), 3025 (s), 1519 (m), 1446 (m), 1350 (s), 1267 (s); UV/Vis Spectroscopy(nm); 418(soret band), 515, 550, 590, 645(Q band); ES-MS: 660(MH^+).

Synthesis of 5-(4-Aminophenyl)-10,15,20-triphenylporphyrin

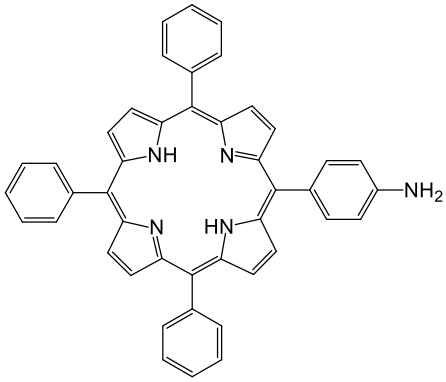

15

5-(4-Nitrophenyl)-10,15,20-triphenylporphyrin **14** (1.09 g, 1.65 mmol) was dissolved in 50 mL of HCl, to this was added tin(II) chloride (0.50 g, 3.44 mmol). The whole reaction mixture was stirred under N_2 for 1 hour at 65◦ C. Dichloromethane (100 mL) was added and the solution was neutralised with ammonium hydroxide. The aqueous layer was extracted with 3 further dichloromethane washes (100 mL) and washed through celite to aid separation. The organic layer was dried over magnesium sulphate and purified by flash column chromatography through alumina. Unreacted starting material was eluted with petroleum ether followed by product which was eluted with dichloromethane and recrystallised with hot ethanol to give a purple solid.

Yield 0.33 g, 32 % ^{1}H NMR(d-$CDCl_3$, 400MHz) δ_H -2.76(s, 2H, NH), 4.04(s, 2H, NH_2), 7.09(d, J = 8.0 Hz, 2H phenyl m-$CHNH_2$), 7.78(m, 9H phenyl, p-CH), 8.02(d, J = 8.0 Hz, 2H phenyl o-CH), 8.24(m, 6H phenyl o-CH), 8.86(m, 6H, pyrrolic), 8.97(s, 2H, pyrrolic); ^{13}C-NMR(d-$CDCl_3$, 400MHz) δc 147.6, 142.2, 135.7, 134.5, 132.4, 127.6, 126.7, 119.9, 113.4; FTIR$_{\lambda max}$(cm)$^{-1}$: 3299 (br w), 3057 (m), 1592 (w), 1425 (m), 1266 (s); UV/Vis Spectroscopy(nm); 419(soret band), 517, 551, 592, 648(Q band); ES-MS: 630(MH^+).

Synthesis of porphyrin dimer

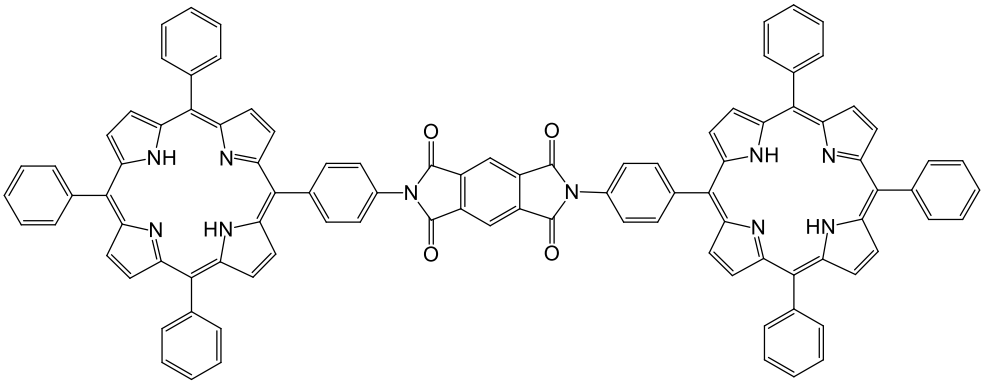

16

5-(4-Aminophenyl)-10,15,20-triphenylporphyrin (50 mg, 0.08 mmol) and pyromellitic dianhydride (9 mg, 0.04 mmol) were added to 15 mL of anhydrous dimethylformamide contained in the dry round bottom flask under nitrogen. An excess of acetic anhydride was added (5 mL) and the reaction was refluxed for 18 hours. After that dimethylformamide was removed by distillation, methanol was added and insoluble porphyrin obtained by filtration, washing with methanol. Purification was achieved by flash column chromatography with silica gel eluting with 4.7/0.3 chloroform /methanol. Second band was collected and solvent was removed by reduced pressure. Purple product was obtained after recrystallisation with dichloromethane and methanol.

Yield 33 mg, 32 % ^{1}H NMR (d-$CDCl_3$, 400MHz) δ_H -2.76(s, 4H, NH), 7.78(m, 24H), 8.31-8.10(m, 16H), 8.40(m, 2H), 9.09-8.83(m, 16H); UV spectroscopy(nm); 421(soret band), 553, 591, 648(Q band); MS (MALDI) : 1441(MH^+).

Synthesis of zinc porphyrin dimer

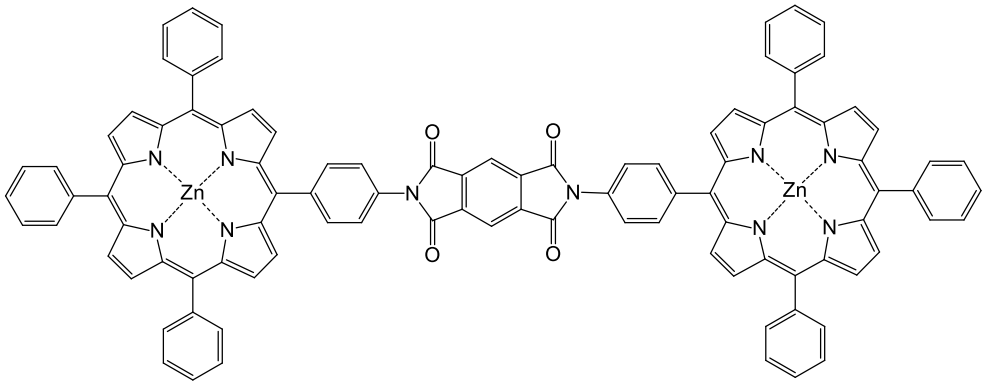

17

Porphyrin dimer (40 mg, 0.028 mmol) was dissolved in 15 mL of dichloromethane with stirring, zinc acetate dihydrate (18 mg, 0.084 mmol) was added and the solution heated to reflux for 30 minutes. After filtration a dark purple solid was obtained.

Yield 37 mg, 85 % ^{1}H NMR (d-$CDCl_3$, 400MHz) δ_H 7.78(m, 24H), 8.31-8.10(m, 16H), 8.40(m, 2H), 9.09-8.83(m, 16H); FTIR$_{\lambda max}$: 2923(s), 2854(s), 1463, 1377(w), 1173(w); UV spectroscopy(nm); 421(soret band), 551(Q band); MS(MALDI): 1568(MH^+).

Synthesis of flexible porphyrin dimer

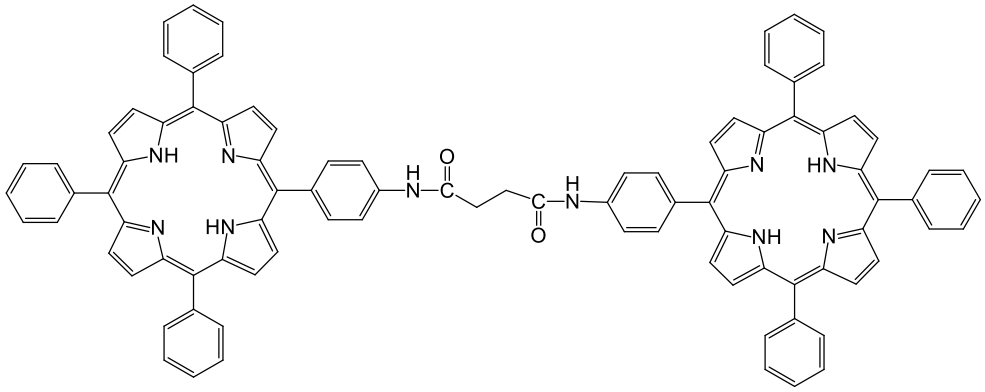

19(a)

5-(4-Aminophenyl)-10,15,20-triphenylporphyrin (150 mg, 0.24 mmol) and succinyl chloride (.013 mL, 0.48 mmol) were added to 45 mL of dry THF contained in a dry round bottom flask under nitrogen and the reaction was refluxed for 2 hours. THF was removed then product was dissolved in chloroform 50 mL and washed with saturated with saturated sodium bicarbonate 100 mL followed by washing with distilled water 100 mL. The organic layer was dried with sodium sulphate. After removal of solvent the crude was recrystallised using chloroform and methanol which gave purple product.

Yield 70 mg, 54% ^{1}H NMR(d-$CDCl_3$, 400MHz) δ_H -2.77(s, 4H, NH), 3.14(s, 4H, NHCOC$\underline{H}_2$), 7.76(m, 18H), 8.03(d, J = 8.7 Hz, 4H), 8.23(m, 16H), 8.93-8.83(m, 16H); FTIR$_{\lambda max}$: (cm^{-1}) 3315, 1556 (N-H stretch and bend), 1594 (amide C=O), 1508, 1471, 1440; Uv/Vis Spectroscopy(nm); 421(soret band), 517, 551, 592, 648(Q band); MS(MALDI) : 1340(MH^+).

Synthesis of flexible zinc porphyrin dimer

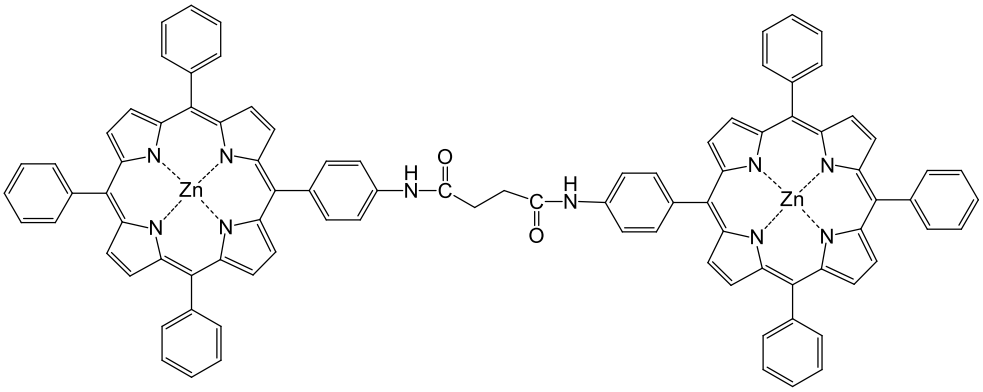

19

Flexible porphyrin dimer (110 mg, .082 mmol) **19(a)** was dissolved in 30 mL of THF with stirring, zinc acetate dihydrate (40 mg, 0.164 mmol) was added and the solution heated to reflux for 30 minutes. After filtration a dark purple solid was obtained.

Yield 70 mg, 54% ^{1}HNMR(d-$CDCl_3$, 400MHz) δ_H -2.77(s, 4H, NH), 3.14(s, 4H, NHCOC<u>H</u>$_2$), 7.76(m, 20H), 8.23-8.40 (m, 18H), 8.93-8.83(m, 16H); FTIR$_{\lambda max}$: (cm^{-1}) 3315, 1556(N-H stretch and bend), 1594 (amide C=O), 1508, 1471, 1440; UV/Vis Spectroscopy(nm); 428(soret band), 550(Q band). MS(MALDI) : 1468(MH$^+$).

Synthesis of 3-pentyloxy-1,2-dicyanobenzene

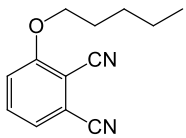

21

3-Nitrophthalonitrile (1 g, 5.77 mmol) and 1-pentanol (1.25 mL, 11.54 mmol) were added to 12 mL of DMSO contained in the dry round bottom flask under nitrogen. After 5 minutes of stirring potassium carbonate (1.6 g, 11.54 mmol) was added and reaction mixture refluxed for 4 hours at 90° C. After 4 hours the reaction mixture was cooled at room temperature and water (150 mL) was added, stirred vigorously for 15 minutes at room temperature. The resulting precipitate was filtered by vacuum and washed with water. The crude product was recrystallised with ethanol.

Yield 0.330 g, 33%, ^{1}H NMR (d-$CDCl_3$, 400MHz) δ_H 7.66-7.62(m, 1H), 7.36-7.34(d, J =7.8 Hz, 1H), 7.25-7.35(m, 1H), 4.14(t, 2H, J = 6.5 Hz, $OC\underline{H}_2$), 1.89-1.92(m, 2H, $OCH_2C\underline{H}_2$), 1.54-1.35(m, 3H, $CH_2C\underline{H}_2CH_3$), 0.96(t, 2H, J = 7.2 Hz, $CH_2C\underline{H}_3$); ^{13}C-NMR(d-$CDCl_3$, 400MHz) δc 161.5, 134.4, 130.0, 124.8, 117.5, 115.3, 113.0, 104.9, 69.9, 28.4, 27.8, 22.2, 13.9; FTIR$_{\lambda max}$(cm)$^{-1}$: 3088(s), 2959(s), 2934(alkyl H-C-H stretch), 2237, 2226(-CN- stretch), 1579, 1398, 1472(alkane bend), 1072(ester stretch), 795(aromatic bend); ES-MS: 215(MH^+).

Synthesis of tin(IV) pentyloxyphthalocyanine dichloride

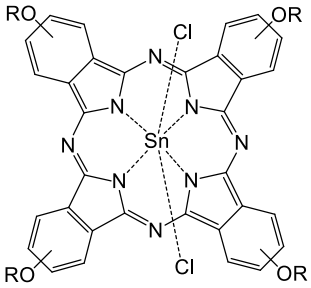

R = -$(CH_2)_4CH_3$

22

3-Pentyloxy-1,2-dicyanobenzene (428.5 mg 4 mmol) was dissolved in 5 mL 1-chloronaphthalene (1-CNP). Tin(II) chloride (189.62 mg 1 mmol) was added and the reaction mixture was refluxed at 250° C for 5 hours under nitrogen. After cooling, the solution was chromatographed with hexane to remove 1-CNP. The column was then eluted with 4/1 dichloromethane and methanol. The solvent was evaporated off and crude product was obtained and washed with hot methanol to give a green product.

Yield 0.20 g, 25%, ^{1}H NMR(d-$CDCl_3$, 400MHz) δ_H 1.24-1.03(dm, 12H), 1.88-1.54(m, 16H), 2.57-2.35(m, 8H), 4.99-4.72(dm, 8H), 7.90-7.76(m, 4H), 8.32-8.24 (m, 4H), 9.35-9.17(m, 4H); ^{13}C-NMR(d-$CDCl_3$, 400MHz) δc 157.9, 157.7, 149.6, 132.6, 116.6, 115.9, 114.4, 70.9, 69.5, 53.4, 29.8, 29.0, 28.9, 28.2, 23.0, 22.7, 14.3, 14.2; FTIR$_{\lambda max}$(cm)$^{-1}$; 2858(w), 2119(s), 1582(s), 1488, 1463, 1335, 1265, 1228, 1115, 1075, 872; Uv/Vis Spectroscopy(nm); 347, 749, 760; ESI-MS: 1044 (calculated) ,1008$(M-Cl)^+$ (obtained).

Self-assembly of dendron G-0.5 with tin(IV) (pentyloxyphthalocyanine) dichloride

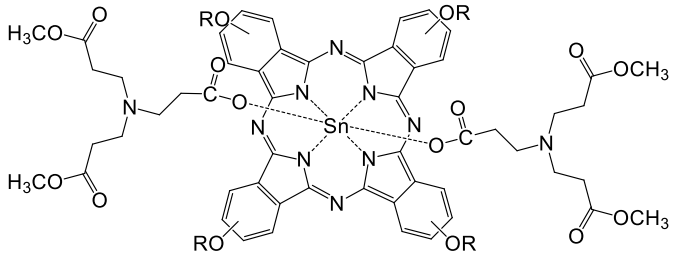

23

Dendron with 2 terminal OMe terminal groups (2.5 mg, 0.010 mmol) and $SnPc(Cl)_2$ (5 mg, 0.005 mmol) were dissolved in $CHCl_3$ (5 mL) and stirred magnetically for an hour. Then the mixture was passed through a small plug of anhydrous Na_2SO_4 (0.25 g) into a round bottom flask. The solvent was removed by rotary evaporator. The green coloured product formed.

^{1}H NMR(d-$CDCl_3$, 400MHz) δ_H -(0.19-0.10) (m, 1H), 0.77-0.86 (br s, 2H), 0.99-1.28 (mm, 16H), 1.54-2.10 (m, 27H), 2.17(s, 4H), 2.29-2.62 (m, 13H), 3.68 (s, 11H), 4.68-5.10 (m, 6H), 7.70-7.88 (m, 4H), 8.22-8.31(m, 4H), 9.14-9.35(m, 3H). ^{13}C-NMR(d-$CDCl_3$, 400MHz) δc 172.3, 157.8, 149.6, 132.8, 116.8, 114.1, 70.6, 69.5, 51.5, 51.3, 49.2, 48.3, 47.8, 31.4, 30.9, 29.8, 28.9, 28.3, 28.1, 23.0, 22.7, 14.2. $FTIR_{\lambda max}(cm)^{-1}$: 2853, 2825(w), 1731(s), 1643, 1590(s), 1537, 1493, 1435; MALDI-TOF-MS: 1497(calculated), 1237$(M\text{-}G0.5)^+$ (obtained).

Self-assembly of dendron G-1.5 with tin(IV) (pentyloxyphthalocyanine) dichloride

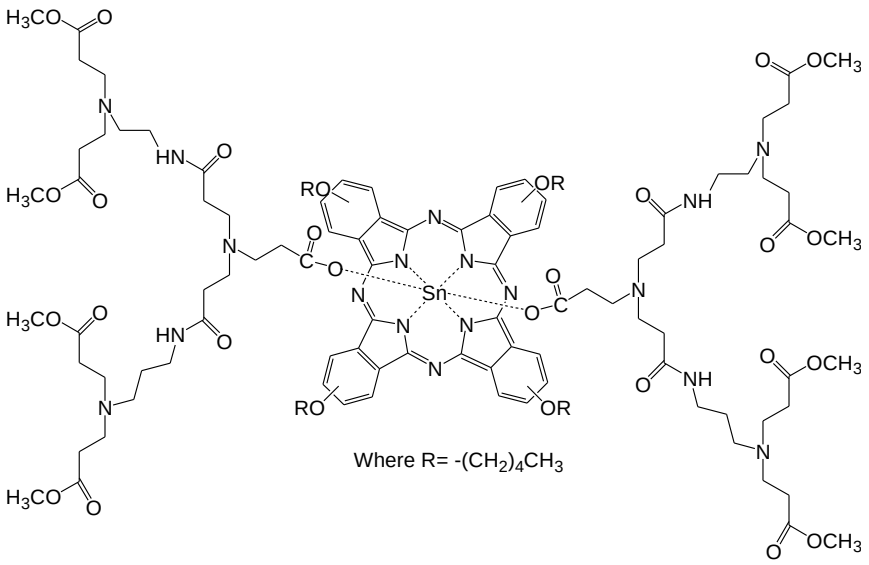

Dendron with 4 terminal OMe terminal groups (6.6 mg, 0.010 mmol) and $SnPc(Cl)_2$ (5 mg, 0.005 mmol) were dissolved in $CHCl_3$ (5 mL) and stirred magnetically for an hour. Then, the solvent was removed by rotary evaporator. The green coloured product formed.

^{1}H NMR(d-$CDCl_3$, 400MHz) δ_H -(0.25-0.17) (m, 3H), 0.84-0.17 (m, 18H), 1.54-1.87 (m, 24H), 2.13-2.20 (m, 20H), 2.28-2.56 (m, 36H), 2.62-293 (m, 18H), 3.60 (s, 18H), 4.68-5.10 (m, 6H), 7.70-7.88 (m, 4H), 8.22-8.31 (m, 4H), 9.14-9.35 (m, 4H); ^{13}C-NMR(d-$CDCl_3$, 400MHz) δc 172.9, 172.8, 171.7, 157.8, 157.5, 157.0, 153.5, 132.9, 132.0, 131.7, 116.1, 115.6, 70.8, 70.4, 69.5, 52.7, 51.6, 51.4, 49.7, 49.2, 48.3, 46.8, 36.9, 36.8, 33.0, 32.7, 32.6, 32.4, 30.5, 29.8, 28.8, 28.2, 28.1, 23.0, 22.7, 14.2; FTIR$_{\lambda max}$(cm)$^{-1}$: 2853, 2825(w), 1731(s), 1643, 1590(s), 1537, 1493, 1435; MALDI-TOF-MS: 2296(calculated), 1636(M-G1.5)$^+$ (obtained).

Self-assembly of dendron G-2.5 with tin(IV) (pentyloxyphthalocyanine) dichloride

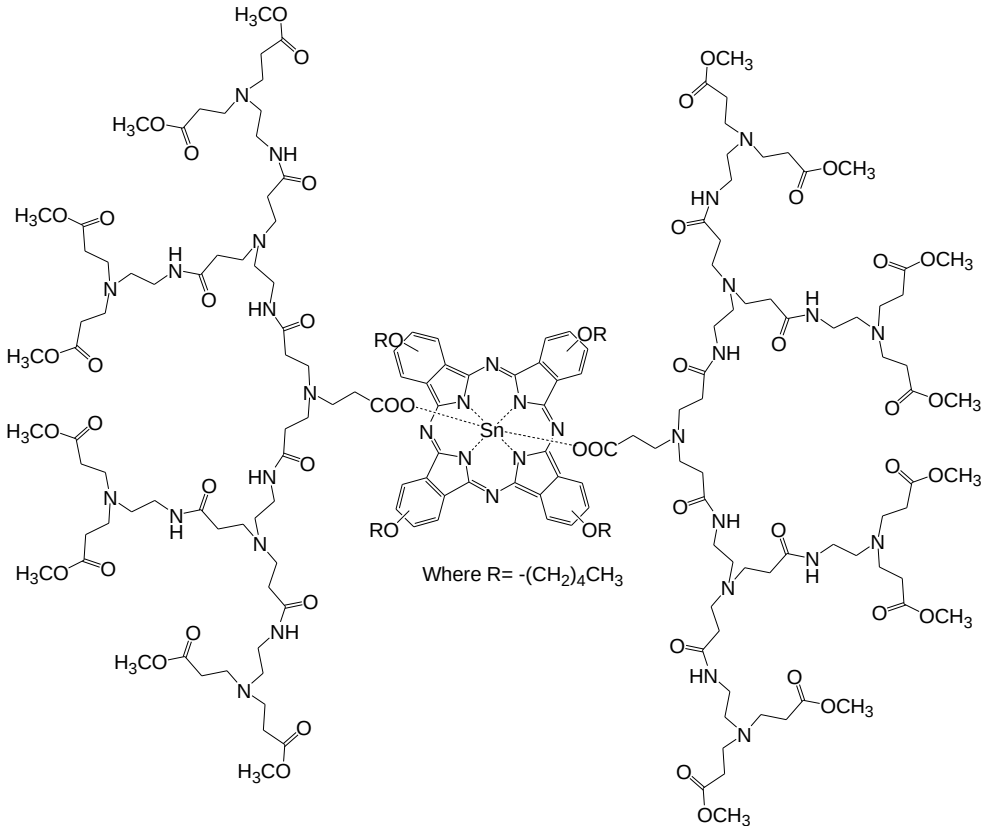

Dendron with 8 terminal OMe terminal groups (10.4 mg, 0.010 mmol) and $SnPc(Cl)_2$ (5 mg, 0.005 mmol) were dissolved in $CHCl_3$ (5 mL) and stirred magnetically for an hour. Then, the solvent was removed by rotary evaporator. The green coloured product formed.

^{1}H NMR (d-$CDCl_3$, 400MHz) δ_H 0.64-0.83 (m, 4H), 0.85-0.132 (m, 6H), 1.50-2.22 (m, 22H), 2.24-2.90 (mm, 117H), 3.05-3.52 (m, 28H), 3.56-3.66 (m, 35H), 4.51-5.01 (m, 6H), 7.70-7.88 (m, 4H), 8.22-8.31 (m, 4H), 8.92-8.85 (m, 4H); ^{13}C-NMR (d-$CDCl_3$, 400MHz) δc 172.9, 172.8, 171.7, 157.8, 157.5, 157.0, 153.5, 132.9, 132.0, 131.7, 116.1, 115.6, 70.8, 70.4, 69.5, 52.7, 51.6, 51.4, 49.7, 49.2, 48.3, 46.8, 36.9, 36.8, 33.0, 32.7, 32.6, 32.4, 30.5, 29.8, 28.8, 28.2, 28.1, 23.0, 22.7, 14.2; $FTIR_{\lambda max}(cm)^{-1}$: 2853, 2825(w), 1731(s), 1643, 1590(s), 1537, 1493, 1435; MALDI-TOF-MS: 4898(calculated), 2436(M-2.5)(obtained).

Self-assembly of tin(IV) (pentyloxyphthalocyanine) dichloride, dendron G-0.5 and flexible zinc porphyrin dimer (FPD)

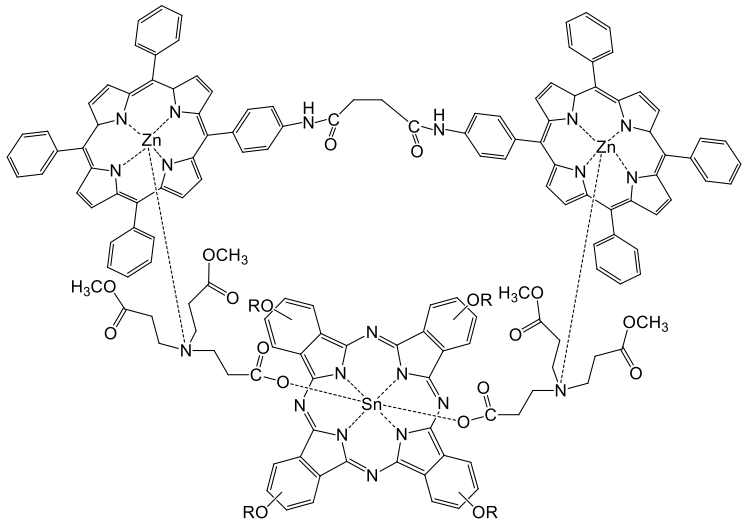

24

Dendron G-0.5 containing 2 terminal OMe groups (0.001 mg, 0.002 moles), tin(phthalocyanato)dichloride (0.002 mg, 0.001 moles) and ZnFPD (0.002 mg, 0.001 moles) was dissolved in 2 mL of $CDCl_3$. this reaction mixture was stirred for 5 minutes.

^{1}H NMR (d-$CDCl_3$, 400MHz) δ_H: –(0.22-0.15) (m, 9H), 0.76-0.97 (tm, J = 7.0 Hz, 3H), 1.01-1.18 (mtm, J = 7.2 Hz, 12H), 1.20-1.32 (m, 9H), 1.53-1.89 (m, 21H), 2.01-2.90 (br m, 25H), 2.92-3.08 (m, 7H), 3.64-3.76 (m, 9H), 4.60-5.10 (m, 6H), 7.50-7.90 (m, 12H), 8.01-8.33 (m, 10H), 8.85-8.99 (m, 4H), 9.12-9.33 (m, 4H).

Self-assembly of tin(IV) (pentyloxyphthalocyanine) dichloride, dendron G-1.5 and flexible zinc porphyrin dimer (FPD)

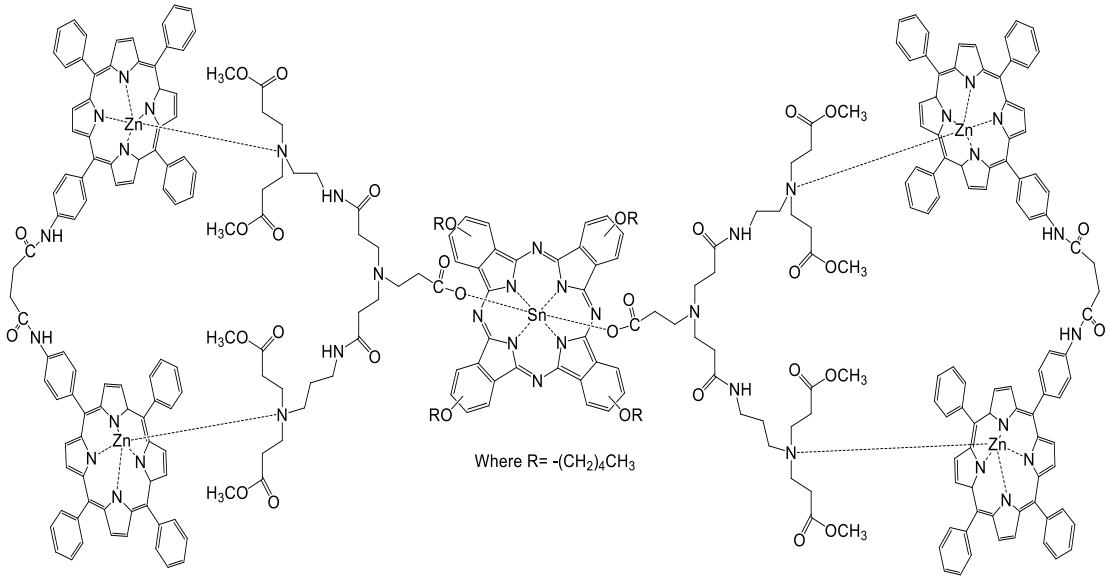

Dendron G-1.5 containing 4 terminal OMe groups (0.003 mg, 0.002 moles), tin(phthalocyanato)dichloride (0.002 mg, 0.001 moles) and ZnFPD (0.006 mg, 0.002 moles) was dissolved in 2 mL of $CDCl_3$. This reaction mixture was stirred for 5 minutes.

^{1}H NMR(d-$CDCl_3$, 400MHz) δ_H -(0.53-0.44) (m, 1H), 0.86-1.20(m, 12H), 1.22-2.10 (mm, 88H), 2.42-3.40 (mm, 58H), 3.63-3.69 (m, 16H), 4.12-4.25 (m, 4H), 7.21-7.80 (m, 12H), 8.10-8.35 (m, 5H), 8.82-9.05 (m, 5H).

Self-assembly of tin(IV) (pentyloxyphthalocyanine) dichloride, dendron G-2.5 and flexible zinc porphyrin dimer (FPD)

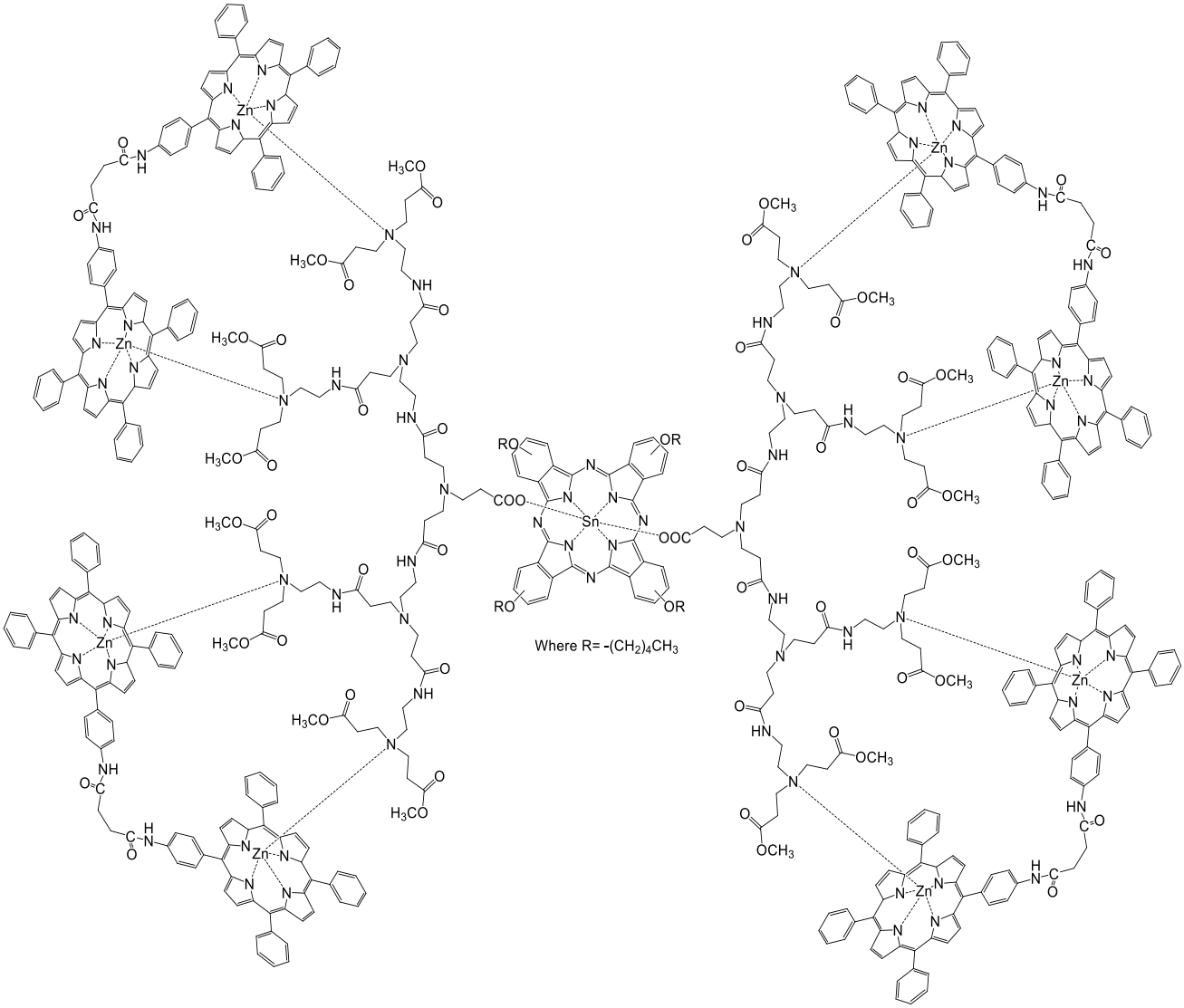

Dendron G-2.5 containing 8 terminal OMe groups (0.003 mg, 0.002 moles), tin(phthalocyanato)dichloride (0.001 mg, 0.001 moles) and ZnFPD (0.006 mg, 0.002 moles) was dissolved in 1 mL of $CDCl_3$. this reaction mixture was stirred for 5 minutes.

^{1}H NMR(d-$CDCl_3$, 400MHz) δ_H: -(0.50-0.45) (m, 1H), 0.87-1.20 (m, 8H), 1.22-1.65 (mm, 21H), 1.89-2.89 (mm, 175H), 3.08-3.30 (m, 6H), 3.60-3.69 (m, 35H), 4.12-4.28 (m, 6H), 7.50-7.85 (m, 14H), 8.05-8.39 (m,10H), 8.80-9.10 (m, 7H).

Chapter-6

References

References:-

1. Tomalia, D. A; Baker, H; Dewald, J; Hall, M; Kallos, G; Martin, S; Ryder, J; Smith, P. ***Polym. J.***, 1985, 17, 117-132.
2. Grayson, S. M; Frechet, J. M. J. ***Chem. Rev.,*** (Washington, D. C.), 2001, 101, 3819-3868.
3. Gao, C; Yan, D; ***Prog. Polym. Sci.***, 2004, 29,183-275.
4. Yates, C. R; Hayes, W; ***Eur. Polym. J.***, 2004, 40, 1257-1281.
5. Voit, B; ***J. Polym. Sci., Part-A: Polym. Chem.***, 2000, 38, 2505-2525.
6. Bosman, A. W; Janseen, H. M; Meijer, E. W. ***Chem. Rev.***, 1999, 99, 1665-1688.
7. Tomalia, D. A; Dewald, J. R.; Hall, M. J.; Martin, S. J.; Smith, P. B.; preprints of the Ist SPSJ International Polymer Conference, ***The Society of Polymer Science(Japan)***, 1984, 65.
8. Tomalia, D. A.; Dendrimer Molecules, ***Sci. Amer.***, 1995, 272, 62-66.
9. Tomalia, D. A.; ***Spektrum Der Wissenchraft***, 1995, 6179, 42-47.
10. Buhleier, E; Wehner, W; Vogtle, F.; ***Synthesis,*** 1978, 2, 155-158.
11. Inoue, K.; ***Prog. Polym. Sci***., 2000, 25, 453-571.
12. Cloninger, M. J; ***Curr. Opin. Chem. Biol.***, 2002, 6, 742-748.
13. Odian, G.; ***Principles of Polymerization***, 1970, New York, Mcgraw-Hill.
14. De Genes, P. G.; Hervet, H. J.; ***Phys. Lett.***, 1983, 44, 351-360.
15. (a) Choi, M. S.; Adia, T.; Yamazaki, T.; Yamazaki, I.; ***Chem. Eur. J.***, 2002, 8, No 12, 2668-2678. (b) Balzani, V.; Ceroni, P.; Maestri, M.; Vicinelli, V.; ***Curr. Opin. Chem. Biol.***, 2003, **7**, 657-665.
16. Thayumanayan, S.; Bharathi, P.; Sivanandan, K.; Rao Vutukuri, D.; ***Comp. Rend. Chim.***, 2003, 6, 767-778.
17. Hecht, S.; Frechet, J. M. J.; ***Angew. Chem. Int. Ed.***, 2001, 40, 74-91.
18. Esfand, R.; Tomalia, D. A.; ***Drug Discovery Today***, 2001, 6, 427-436.
19. Voit, B.; Beyerlein, D.; Eichhorn, K. J.; Grundke, K.; Schmaljohann, D.; Loontjens, T.; ***Chemie Ingenieur Technik***, 2001, 73, 1592-1596.
20. Mezzenga, R.; Boogh, L.; Manson, J. A. E.; ***Compos. Sci. Technol.***, 2001, 61, 787-795.

21. Ma, H.; Jen, A. K. Y.; ***Adv. Mater. (Weinheim Germany)***, 2001, 13, 1201-1205.
22. (a) Rodlert, M.; Plummer, C. J. G.; Garamszegi, L.; Leterrier, Y.; Grunbauruer, H. J. M.; Manson, J. A. E.; ***Polymer***, 2004, 45, 949-960. (b) Ratna, D.; Becker, O.; Krishnamurthy, R.; Simon, G. P.; Varley, R. J.; ***Polymer***, 2003, 44, 7449-7457.
23. (a) Arshady, R.; ***Microspheres, Microcapsules & Liposomes***, 2002, 5, 1-29. (b) Esumi, K.; ***Shikizai Kyokaishi***, 2001, 74, 512-517.
24. (a) Boas, U.; Heegaard, P. M. H.; ***Chem. Soc. Rev.,*** 2004, 33, 43-63. (b) Cloninger M. J.; ***Curr. Opin. Chem. Biol.***, 2002, 6, 742-748. (c) Dennig, J.; Duncan, E.; ***J. Biotechnol.***, 2002, 90, 339-347. (d) Gao, C.; Xu, Y.; Yan, D.; Chen, W.; ***Biomacromolecules***, 2003, 4, 704-712. (e) Uhrich, K.; ***Trends Polym. Sci.*** (Cambridge, United Kingdom), 1997, 5, 388-393. (f) Liu, H.; Uhrich, K. E.; ***Polym. Prepr. (Am. Chem. Soc., Div. Polym. Chem.)***, 1997, 38, 582-583.
25. Hawker, C. J.; Malmstrom, E.E.; Frank, C. W.; and Kamph, J. P.; ***J. Am. Chem. Soc.***, 1997, 119, 9903-9904.
26. Rathgeber, S.; Monkenbusch, M.; Kreitschmann, M.; Urban, V.; Brulet, A.; ***J. Chem. Phys.***, 2002, 117, 4047-4062.
27. Klajnert, B.; Bryszewska, M.; ***Aceta. Bio. Polonica***, 2001, 48, 199-208.
28. Jikei, M.; Kakimoto, M.; ***Prog. Polym. Sci***., 2001, 26, 1233-1285.
29. Mourey, H. T.; Turner, R. S.; Rubenstein, M.;. Frechet, J. M. J.; Hawker, J. C.; Wooley, K. L.; ***Macromolecules***, 1992, 25, 2401-2406.
30. Gramham, M. D; ***j. Chem. Tech. biotech.***, 2001, 76, 903-918.
31. Haker, C.J; Frectch, J. M. J**; *J. Am. Chem. Soc***, 1990, 112, 7638-7647.
32. Balzani, V.; Ceroni, P.; Gestermann, S.; Kuaffmann, C.; Gorka, M.; Vogtal, F.; ***Chem. Commun.***, 2000, 853-854.
33. James, T. D.; Shinmori, H.; Takeuchi, M.; Shinkai, S.; ***Chem. Commun.***, 1996, 705-706.
34. Baussanne, I.; Benito, J. M,; Mellet, C. O.; Fernandez, J. M. G.; Law, H..; Defaye, J.; ***Chem. Commun.***, 2000, 1489-1490.
35. Stiriba, S. E.; Frey, H.; and Haag, R.; ***Angew. Chem. Int. Ed.***, 2002, 41, 1329-1334.

36. Garber, S. B.; Kingsbury, J. S.; Gray, B. L.; Hoveyda, A. H.; ***J. Am. Chem. Soc***., 2000, 122, 8168-8179.
37. Devadose, C.; Bharathi, P.; Moore, J. S.; ***J. Am. Chem. Soc.***, 1996, 118, 9635-9644.
38. Adronov, A.; Gilat, S. L.; Frechet, J. M. J.; Ohta, K.; Neuwahl, F. V. R.; Fleming, G. R.; ***J. Am. Chem. Soc***., 2000, 122, 1175-1185.
39. Klajnert, B.; Bryszewska, M.; ***Acta Biochimica Polonica***, 2001, 48, 199-208.
40. Wells, M.; Crooks, R. M.; ***J. Am. Chem. Soc.***, 1996, 16, 3988-3989.
41. Mcdermott, G.; Prince, S. M.; Freer, A. A.; Hawthornthwaite-Lawless, A. M.; Papiz, M. Z.; Cogdell, R. J.; Isaacs, N. W.; ***Nature***, 1995, 374-517.
42. Miller, K.; ***Nature(London),*** 300, 53-55.
43. Walz, T.; Ghosh, R.; ***J. Mol. Biol.***, 1997, 265, 107-111.
44. Monger, T.; Parson, W.; ***Biochim. Biophys. Acta.***, 1997, 460, 393-407.
45. Van Grondelle, R.; dekker, J.; Gillbro, T.; Sundstrom, V.; ***Biochim. Biophys. Acta.***, 1994, 1187, 1-65.
46. Hu, X.; schulten, K.; ***Biophs. J.,*** 1998, 75683-694, 683-694.
47. Balzani, V.; Paola Ceroni; Mauro Maestri; Vicineilli, V.; ***Curr. Opin. Chem. Biol.***, 2003, **7**, 657-665.
48. Adronov, A.; Frechet, J. M. J.; ***Chem. Commun.***, 2000; 1701-1710.
49. Zeng, Yi.; Ying-Ying Li; Jinping Chen; Guogiang Yang; Yi Li; ***Chem. Asian. J.***, 2010, 5, 992-1005.
50. Nantalaksakul, A.; Raghunath Reddy, D.; Bardeen, C. J.; Thayumanavan, S.; ***Photosynth. Res.***, 2006, 87, 133-150.
51. Denti, G.; Campagna, S.; Serroni, S.; Venturi, M.; Ciano, M.; Balzani, V.; ***J. Am. Chem. Soc.***, 1992, 114, 2944.
52. McClenaghan, N. D.; Loiseau, F.; Puntoriero, F.; Serroni, S.; Camnagna, S.; ***Chem. Commun.***, 2001, 2643.
53. Gilat, S. L.; Adronov, A.; Frechet, J. M. J.; ***Angew. Chem.***, 1999, 111, 1519; ***Angew. Chem. Int. Ed.***, 1999, 38, 1422.
54. Gilat, S. L.; Adronov, A.; Frechet, J. M. J.; Ohta, K.; Neuwahl, F. V. R.; Fleming, G. R.; ***J. Am. Chem. Soc.***, 2000, 122, 1175-1185.
55. A. Adronov, P. R. L. Malenfant, J.M.J. Frechet, ***Chem. Mater.***, 2000, 12, 1463-1472.

56. Xu, Z. F.; Moore, J. S.; ***Angew. Chem.***, 1993, 105, 1394-1396.
57. Xu, Z. F.; Moore, J. S.; ***Angew. Chem. Int. Ed. Engl.***, 1993, 32, 1354-1357.
58. Xu, Z. F.; Moore, J. S.; ***Acta. Polym.***, 1994, 45, 83-87.
59. Devadoss, C.; Bharathi, P.; Moore, J. S.; ***J. Am. Chem. Soc.***, 1996, 118, 9635-9644.
60. Peng Z; Pan Y; Xu B; Zhang J; ***J. Am. Chem. Soc.***, 2000, 112, 6619-6623.
61. Kawa, M.; Frechet, J. M.J.; ***Chem. Mater.***, 1998, 10, 286-296.
62. Jiang, D. L.; Aida, T.; ***J. Am. Chem. Soc.***, 1998, 120, 10895-10901.
63. Qu J; Liu D; De Feyter S; Zhang J; Schryver FC; Mullen K.; ***J. Org. Chem***., 68, 9802-9808.
64. (a) Cotlet, M.; Masuo, S.; Lor, M.; Van der Auweraer, E. Fron. M.; Mullen, K.; Hofkens, J.; ***Angew. Chem. Int. Ed.***, 2004, 43, 6116-6120. (b) Cotlet, M.; Masuo, S.; Luo, G. B.; Van der Auweraer, M.; Mullen, K.; Verhoeven, J.; Xie, X. L. S.; De Schryver, F.; ***Proc. Nail. Acad. Sci., USA***, 2004, 101, 14343-14348.
65. Thomas, K. R.; Thompson, A. L.; Shivakumar, A. V.; Bardeen, C. J.; Thayumanavan, S.; ***J. Am. Chem. Soc.***, 2005, 127, 373-383.
66. Schenning, A. P. H. J.; Peeters, E.; Meijer, E. W.; ***J. Am. Chem. Soc.***, 2000, 122, 4489-4495.
67. Balzani, V.; Ceroni, P.; Gestermann, S.; Gorka, M.; Kauffmann, C.; Maesteri, M.; Vogtal, F.; ***Chem. Phys. Chem***, 2000, 1, 224-227.
68. Lewis, N. S.; ***Science***, 2007, 315, 798-810.
69. (a) Jordan, P.; Fromme, P.; Witt, H. T.; Klukas, O.; Saenger, W.; Krauss, N.; ***Nature***, 2001, 411, 909-917. (b) Green, B. R.; Parson, W. W.; Light-harvesting Antenna, in advances in Photosynthesis and respiration ***(Ed.; Govindjee)***, Kluwer Acedamic Publications, 2003, Vol 13.
70. Liu, Z.; Yan, H.; Wang, K.; Kuang, T.; Zhang, J.; Gui, L.; An, X.; Chang, W.; ***Nature***, 2004, 428, 287-292.
71. Nelson, N.; Ben-Shem, A.; ***Bioessays***, 2005, 27, 914-922.
72. Andrews, D. L.(Ed.); Energy Harvesting Materials, ***World Scientific***, Hackensack, NJ, 2005.
73. Yamaguchi, N.; Introduction to supramolecular chemistry; 1999.

74. Steed, J. W.; Turner, D. R.; Wallace, K. J.; Core concepts in supramolecular chemistry and nanochemistry, ***Wiley***, 2007.
75. Lee, J. W.; Kim, J. H.; Kim, B. K.; Shin, W. S.; Jin, S. H.; ***Tetrahedron***, 2006, 62, 9193-9200.
76. Meyer, G.; Hartmann, M.; Wohrle, D.; ***Makromol. Chem.***, 1975, 176, 1919-1927.
77. Stulz, E.; Ching Mak, C.; Sanders, J. K. M.; ***J. Chem. Soc., Dalton Trans***, 2001, 604-613.
78. Dennis, P. A.; ***J. Chem. Educ.***, 1998, 65, 1111-1112.
78. Lin, S. J.; Hong, T. N.; Tung, J. Y.; Chen, J. H.; ***Inorg. Chem.*** 1997, 36, 3886-3891.
79. Hiram, I. B.; Raquel, E.; Arturo, S.; Jose, L. S.; Herbert, H.; Victoria, B.; Norberto, F.; Monica, G. G.; Octavio, Olivares-Xometl; Luis, S. Z.; ***Inorg. Chem.***, 43, No. 12, 2004, 3555-3557.
80. Hancock, R. D.; Chelate ring size and metal ion selection, ***J. Chem. Educ.***, 1992, 69, 615-621.
81. Twyman, L. J.; King, Amy S. H.; ***Chem. Commun.***, 2002, 910-911.
82. Y. R. Peng, Y. H. Cao, P. F.Chen, X. X. Huang, ***Chin. Chem. Lett.***, 19, 2008, 273-276.
83. Beltran, H. I.; Esquivel, R.; Sosa Sanchez, A.; Sosa-Sanchez, J. L.; Hopfl, H.; Barba, V.; farfan, N.; Garcia, M. G.; Olivares-Xometl, O.; Zamudio-Rivera, L. S.; ***Inorg. Chem.***, 2004, 43, 3555-3557.
84. Gupta, I.; Ravikanth, M.; ***J. Chem. Sci.***, Vol 117, N0. 2, 2005, 161-166.
85. Georgive, N. I.; Asiri, A. M.; Alamry, K. A.; Obaid, A. Y.; Bojinov, V. B.; ***J. photochem. Photobiol., A***, ***Chemistry***, 2014, 277, 62-74.
86. De Silva, A. P.; Fox, D. B.; Moody, T. S.; Weir, S. M.; The Development of molecular fluorescent switches, ***Trends Biotechnol.***, Vol 19, No 1, 2001.
87. Luguya, R.; Jaquinod, L.; Fronczek, FR.; Vicente, MGH.; Smith, KM; synthesis and reaction of meso-(*p*-nitrophenyl)porphyrins, ***Tetrahedron***, 2004, 60, 2757-2763.

Appendix

Table-A Crystal data and structure refinement for tin(IV) (5,10,15,20-tetraphenylporphyrin) diacetoxy 10

Identification code	kuljit3	
Empirical formula	$C_{56}H_{34}N_4O_4Sn$	
Formula weight	1018.65	
Temperature	296(2) K	
Wavelength	0.71073 Å	
Crystal system	Monoclinic	
Space group	P2(1)/n	
Unit cell dimensions	a = 9.7820(6) Å	α= 90°.
	b = 11.1589(6) Å	β= 98.843(3)°.
	c = 20.2249(10) Å	γ = 90°.
Volume	2181.4(2) $Å^3$	
Z	2	
Density (calculated)	1.551 Mg/m^3	
Absorption coefficient	0.825 mm^{-1}	
F(000)	996	
Crystal size	0.3 x 0.18 x 0.03 mm^3	
Theta range for data collection	3.64 to 23.89°.	
Index ranges	-11<=h<=11, -12<=k<=12, -18<=l<=22	
Reflections collected	9576	
Independent reflections	3325 [R(int) = 0.0537]	
Completeness to theta = 23.89°	98.5 %	
Absorption correction	None	
Refinement method	Full-matrix least-squares on F^2	
Data / restraints / parameters	3325 / 6 / 275	
Goodness-of-fit on F^2	1.943	
Final R indices [I>2sigma(I)]	R1 = 0.0932, wR2 = 0.2568	
R indices (all data)	R1 = 0.1108, wR2 = 0.2694	
Largest diff. peak and hole	4.176 and -1.519 $e.Å^{-3}$	

Table 2. Atomic coordinates (x 10^4) and equivalent isotropic displacement parameters ($Å^2$x 10^3) for A. U(eq) is defined as one third of the trace of the orthogonalized U^{ij} tensor.

	x	y	z	U(eq)
Sn(1)	5000	0	10000	23(1)
N(1)	5145(8)	801(6)	9065(4)	24(2)
N(2)	6041(8)	1469(6)	10495(4)	22(2)
O(1)	2861(5)	948(5)	10004(3)	14(1)
O(2)	1914(13)	-301(11)	10433(6)	89(3)
C(1)	4633(9)	298(8)	8455(5)	23(2)
C(2)	5019(10)	1109(8)	7955(5)	25(2)
C(3)	5727(10)	2045(8)	8268(5)	27(2)
C(4)	5819(9)	1847(8)	8969(5)	24(2)
C(5)	6489(9)	2596(8)	9484(5)	25(2)
C(6)	6598(9)	2406(8)	10176(5)	24(2)
C(7)	7360(9)	3135(8)	10686(5)	25(2)
C(8)	7237(10)	2637(8)	11289(5)	28(2)
C(9)	6420(9)	1576(8)	11171(5)	23(2)
C(10)	7183(10)	3685(8)	9276(5)	23(2)
C(11)	8422(11)	3583(8)	9003(5)	32(2)
C(12)	9152(11)	4589(10)	8867(6)	39(3)
C(13)	8687(11)	5708(9)	8994(6)	37(3)
C(14)	7436(11)	5831(8)	9253(6)	37(3)
C(15)	6738(10)	4824(8)	9407(5)	27(2)
C(16)	3901(10)	-767(8)	8343(4)	23(2)
C(17)	3384(9)	-1120(8)	7631(4)	23(2)
C(18)	3840(10)	-2169(8)	7351(5)	28(2)
C(19)	3314(11)	-2495(9)	6709(5)	33(2)
C(20)	2320(11)	-1797(9)	6320(5)	33(2)
C(21)	1881(10)	-767(9)	6581(5)	33(2)
C(22)	2390(10)	-417(8)	7228(5)	27(2)
C(23)	1820(17)	799(13)	10326(12)	201(15)
C(24)	710(20)	1580(20)	9921(10)	115(7)
C(1S)	8481(12)	9661(11)	8240(7)	52(3)
Cl(1S)	10192(4)	9150(4)	8535(3)	98(2)
Cl(2S)	8515(3)	10442(3)	7489(2)	75(1)
Cl(3S)	7401(3)	8424(3)	8089(2)	52(1)

Table 3. Bond lengths [Å] and angles [°] for kuljit3.

Sn(1)-N(2)#1	2.101(7)	C(21)-C(22)	1.383(14) C(21)-H(21A)
Sn(1)-N(2)	2.101(7)	C(22)-H(22A)	0.9300
Sn(1)-N(1)#1	2.117(7)	C(23)-C(24)	1.528(3) C(24)-H(24A)
Sn(1)-N(1)	2.117(7)	(24)-H(24B)	0.9600C(24)-H(24C)
Sn(1)-O(1)#1	2.345(5)		0.9600
Sn(1)-O(1)	2.345(5)	C(1S)-Cl(3S)	1.737(12)
N(1)-C(4)	1.368(12)	C(1S)-Cl(2S)	1.755(15)
N(1)-C(1)	1.377(12)	C(1S)-Cl(1S) 1.782(12)	C(1S)-H(1SA)
N(2)-C(9)	1.364(12)		0.9800
N(2)-C(6)	1.385(12)	N(2)#1-Sn(1)-N(2)	180.0(4)
O(1)-C(23)	1.301(3)	N(2)#1-Sn(1)-N(1)#1	90.1(3)
O(2)-C(23)	1.248(3)	N(2)-Sn(1)-N(1)#1	89.9(3)
C(1)-C(16)	1.388(13)	N(2)#1-Sn(1)-N(1)	89.9(3)
C(1)-C(2)	1.449(13)	N(2)-Sn(1)-N(1)	90.1(3)
C(2)-C(3)	1.356(13)	N(1)#1-Sn(1)-N(1)	180.0(4)
C(3)-C(4)	1.423(13)	N(2)#1-Sn(1)-O(1)#1	90.8(2)
C(4)-C(5)	1.416(13)	N(2)-Sn(1)-O(1)#1	89.2(2)
C(5)-C(6)	1.402(13)	N(1)#1-Sn(1)-O(1)#1	89.7(2)
C(5)-C(10)	1.485(13)	N(1)-Sn(1)-O(1)#1	90.3(2)
C(6)-C(7)	1.430(13)	N(2)#1-Sn(1)-O(1)	89.2(2)
C(7)-C(8)	1.362(14)	N(2)-Sn(1)-O(1)	90.8(2)
C(8)-C(9)	1.428(13)	N(1)#1-Sn(1)-O(1)	90.3(2)
C(9)-C(16)#1	1.405(13)	N(1)-Sn(1)-O(1)	89.7(2)
C(10)-C(15)	1.382(13)	O(1)#1-Sn(1)-O(1)	179.999(2)
C(10)-C(11)	1.411(14)	C(4)-N(1)-C(1)	109.7(8)
C(11)-C(12)	1.381(15)	C(4)-N(1)-Sn(1)	125.9(6)
C(12)-C(13)	1.367(15)	C(1)-N(1)-Sn(1)	124.2(6)
C(13)-C(14)	1.409(15)	C(9)-N(2)-C(6)	109.6(7)
C(14)-C(15)	1.376(13)	C(9)-N(2)-Sn(1)	125.6(6)
C(16)-C(9)#1	1.405(13)	C(6)-N(2)-Sn(1)	124.3(6)
C(16)-C(17)	1.505(12)	C(23)-O(1)-Sn(1)	135.4(8)
C(17)-C(18)	1.402(13)	N(1)-C(1)-C(16)	127.0(9)
C(17)-C(22)	1.407(13)	N(1)-C(1)-C(2)	105.8(8)
C(18)-C(19)	1.371(14)	C(16)-C(1)-C(2)	127.2(9)
C(19)-C(20)	1.391(15)	C(3)-C(2)-C(1)	108.9(9)
C(20)-C(21)	1.361(14)	C(2)-C(3)-C(4)	107.2(8)

N(1)-C(4)-C(5)	125.3(8)	C(13)-C(12)-C(11)	120.5(10)
N(1)-C(4)-C(3)	108.4(8)	C(12)-C(13)-C(14)	119.5(9)
C(5)-C(4)-C(3)	126.3(8)	C(15)-C(14)-C(13)	119.6(9)
C(4)-C(5)-C(6)	126.9(8)	C(10)-C(15)-C(14)	121.7(9)
C(4)-C(5)-C(10)	117.0(8)	C(1)-C(16)-C(9)#1	127.0(9)
C(6)-C(5)-C(10)	116.1(8)	C(1)-C(16)-C(17)	118.0(8)
N(2)-C(6)-C(5)	127.2(8)	C(9)#1-C(16)-C(17)	115.1(8)
N(2)-C(6)-C(7)	106.9(8)	C(18)-C(17)-C(22)	117.8(9)
C(5)-C(6)-C(7)	125.8(8)	C(18)-C(17)-C(16)	121.5(8)
C(8)-C(7)-C(6)	107.9(8)	C(22)-C(17)-C(16)	120.6(8)
C(8)-C(7)-H(7A)	126.1	C(19)-C(18)-C(17)	120.4(9)
C(6)-C(7)-H(7A)	126.1	C(18)-C(19)-C(20)	121.1(9)
C(7)-C(8)-C(9)	108.2(9)	C(21)-C(20)-C(19)	119.2(9)
C(7)-C(8)-H(8A)	125.9	C(20)-C(21)-C(22)	121.1(10)
N(2)-C(9)-C(16)#1	126.1(8)	C(21)-C(22)-C(17)	120.4(9)
N(2)-C(9)-C(8)	107.4(8)	O(2)-C(23)-O(1)	99.8(10)
C(16)#1-C(9)-C(8)	126.5(9)	O(2)-C(23)-C(24)	133(2)
C(15)-C(10)-C(11)	117.7(8)	O(1)-C(23)-C(24)	102.0(13)
C(15)-C(10)-C(5)	121.8(8)	Cl(2S)-C(1S)-Cl(1S)	107.9(7)
C(11)-C(10)-C(5)	120.2(8)		
C(12)-C(11)-C(10)	120.9(9)		

Symmetry transformations used to generate equivalent atoms:

#1 -x+1,-y,-z+2

Table 4. Anisotropic displacement parameters ($Å^2 x 10^3$) for kuljit3. The anisotropic displacement factor exponent takes the form: $-2\pi^2[h^2 a^{*2}U^{11} + ... + 2 h k a^* b^* U^{12}]$

	U^{11}	U^{22}	U^{33}	U^{23}	U^{13}	U^{12}
Sn(1)	35(1)	11(1)	22(1)	0(1)	6(1)	-2(1)
N(1)	29(4)	17(4)	29(5)	2(3)	12(4)	2(3)
N(2)	33(4)	13(4)	24(4)	-1(3)	12(3)	-2(3)
C(1)	26(5)	12(4)	32(6)	2(4)	5(4)	7(4)
C(2)	34(5)	18(5)	21(5)	1(4)	3(4)	1(4)
C(3)	37(5)	17(5)	31(6)	5(4)	12(4)	5(4)
C(4)	31(5)	19(5)	26(5)	2(4)	13(4)	-1(4)
C(5)	30(5)	15(4)	31(6)	3(4)	9(4)	5(4)
C(6)	31(5)	13(4)	30(6)	1(4)	7(4)	0(4)
C(7)	32(5)	13(4)	29(5)	5(4)	4(4)	-3(4)
C(8)	36(5)	13(4)	34(6)	-3(4)	-1(4)	2(4)
C(9)	24(5)	24(5)	21(5)	-4(4)	4(4)	2(4)
C(10)	36(5)	15(4)	18(5)	1(4)	3(4)	0(4)
C(11)	45(6)	16(5)	37(6)	1(4)	14(5)	11(4)
C(12)	43(6)	30(6)	46(7)	-1(5)	14(5)	-6(5)
C(13)	43(6)	23(5)	47(7)	-1(5)	10(5)	-11(5)
C(14)	48(6)	11(5)	54(7)	-1(4)	18(5)	-2(4)
C(15)	31(5)	23(5)	29(6)	1(4)	11(4)	5(4)
C(16)	36(5)	19(5)	15(5)	-2(4)	8(4)	6(4)
C(17)	34(5)	14(4)	21(5)	2(4)	9(4)	-3(4)
C(18)	38(5)	17(5)	30(6)	-4(4)	9(5)	-4(4)
C(19)	45(6)	20(5)	37(6)	-7(5)	15(5)	-5(5)
C(20)	44(6)	33(6)	24(5)	-5(5)	14(5)	-12(5)
C(21)	31(5)	29(5)	38(6)	6(5)	2(5)	-4(4)
C(22)	34(5)	16(4)	30(6)	-1(4)	3(5)	-1(4)
C(1S)	42(6)	38(6)	74(10)	-15(7)	2(6)	7(6)
Cl(1S)	54(2)	84(3)	144(4)	2(3)	-23(2)	14(2)
Cl(2S)	51(2)	38(2)	140(4)	33(2)	28(2)	2(2)
Cl(3S)	59(2)	34(2)	67(2)	-1(1)	27(2)	-11(1)

Table-B Crystal data and structure refinement for tin(IV) (5,10,15,20-tetraphenylporphyrin) dibenzoxy 11.

Identification code	ilt1p-1
Empirical formula	$C_{58}H_{38}N_4O_4Sn$
Formula weight	973.61
Temperature	293(2) K
Wavelength	0.71073 Å
Crystal system	Triclinic

Space group	P-1	
Unit cell dimensions	a = 10.0641(6) Å	α= 65.578(2)°.
	b = 11.2533(7) Å	β= 67.905(2)°.
	c = 11.4717(7) Å	γ = 76.038(2)°.
Volume	1090.42(12) $Å^3$	
Z	1	
Density (calculated)	1.483 Mg/m^3	
Absorption coefficient	0.643 mm^{-1}	
F(000)	496	
Crystal size	0.32 x 0.18 x 0.03 mm^3	
Theta range for data collection	2.00 to 27.26°.	
Index ranges	-12<=h<=10, -14<=k<=13, -13<=l<=14	
Reflections collected	13949	
Independent reflections	4675 [R(int) = 0.0407]	
Completeness to theta	27.26° 95.6 %	
Absorption correction	None	
Max. and min. transmission	0.9810 and 0.8207	
Refinement method Full-matrix least-squares on	F^2	
Data / restraints / parameters	4675 / 0 / 304	
Goodness-of-fit on F^2	1.143	
Final R indices [I>2sigma(I)]	R1 = 0.0622, wR2 = 0.1663	
R indices (all data)	R1 = 0.0691, wR2 = 0.1732	
Largest diff. peak and hole	3.108 and -1.076 e.$Å^{-3}$	

Table 2. Atomic coordinates (x 10^4) and equivalent isotropic displacement parameters ($Å^2$x 10^3) for ILT1P-1. U(eq) is defined as one third of the trace of the orthogonalized U^{ij} tensor.

	x	y	z	U(eq)
Sn(1)	0	0	10000	23(1)

O(1)	1529(4)	1030(4)	8202(5)	40(1)
N(2)	-1245(4)	1736(4)	10174(4)	25(1)
N(1)	1193(4)	89(4)	11108(4)	26(1)
C(6)	-1153(5)	2390(5)	10922(5)	26(1)
C(10)	-2873(5)	1927(5)	8930(5)	27(1)
C(3)	1912(6)	653(5)	12444(5)	30(1)
C(17)	-313(5)	2866(5)	12441(5)	27(1)
C(22)	147(6)	4110(5)	11809(5)	33(1)
C(9)	-2380(5)	2335(5)	9673(5)	26(1)
C(1)	2305(5)	-813(5)	11450(5)	26(1)
C(18)	-941(6)	2396(5)	13832(5)	33(1)
C(5)	-169(5)	2045(5)	11643(5)	26(1)
C(8)	-3018(6)	3433(5)	10108(5)	29(1)
C(11)	-4068(5)	2786(5)	8392(5)	28(1)
C(15)	-4812(7)	4734(6)	6724(6)	44(1)
C(19)	-1124(6)	3161(6)	14576(6)	37(1)
C(12)	-5429(6)	2391(6)	8885(6)	40(1)
C(7)	-2284(6)	3465(5)	10864(5)	29(1)
C(20)	-675(6)	4412(5)	13928(6)	34(1)
C(4)	915(5)	987(4)	11717(5)	27(1)
O(2)	287(7)	2353(6)	6966(6)	75(2)
C(25)	2653(9)	2346(8)	4624(13)	91(4)
C(13)	-6480(7)	3178(7)	8292(8)	50(2)
C(2)	2774(6)	-436(5)	12276(5)	30(1)
C(14)	-6148(7)	4335(6)	7201(7)	46(2)
C(21)	-23(6)	4880(5)	12558(6)	37(1)
C(27)	5240(8)	1832(8)	3871(8)	61(2)
C(16)	-3769(6)	3973(5)	7332(5)	34(1)
C(24)	2854(9)	1733(7)	5974(7)	58(2)
C(26)	3974(9)	2349(8)	3510(8)	62(2)
C(28)	5240(12)	1366(10)	5113(9)	81(3)
C(23)	1452(8)	1662(8)	7217(11)	65(2)
C(29)	4091(12)	1294(10)	6164(12)	87(3)

Table 3. Bond lengths [Å] and angles [°] for ILT1P-1.

Sn(1)-N(1)	1 2.093(4)	C(10)-C(1)	1 1.417(7)
Sn(1)-N(1)	2.093(4)	C(10)-C(11)	1.505(6)
Sn(1)-N(2)	2.093(4)	C(3)-C(2)	1.360(7)
Sn(1)-N(2)	1 2.093(4)	C(3)-C(4)	1.427(7)
Sn(1)-O(1)	1 2.112(5)	C(17)-C(22)	1.386(7)
Sn(1)-O(1)	2.112(5)	C(17)-C(18)	1.389(7)
O(1)-C(23)	1.079(10)	C(17)-C(5)	1.500(7)
N(2)-C(9)	1.376(6)	C(22)-C(21)	1.397(7)
N(2)-C(6)	1.379(6)	C(9)-C(8)	1.440(6)
N(1)-C(4)	1.373(6)	C(1)-C(10)	1.417(7)
N(1)-C(1)	1.374(6)	C(1)-C(2)	1.437(7)
C(6)-C(5)	1.406(7)	C(18)-C(19)	1.384(7)
C(6)-C(7)	1.445(6)	C(5)-C(4)	1.406(7)
C(10)-C(9)	1.392(7)	C(8)-C(7)	1.348(7)

C(11)-C(12)	1.377(8)
C(11)-C(16)	1.389(7)
C(15)-C(14)	1.357(10)
C(15)-C(16)	1.395(7)
C(19)-C(20)	1.388(8)
C(12)-C(13)	1.399(8)
C(20)-C(21)	1.373(8)
O(2)-C(23)	1.301(10)
C(25)-C(26)	1.457(13)
C(25)-C(24)	1.483(14)
C(13)-C(14)	1.386(10)
C(27)-C(28)	1.298(11)
C(27)-C(26)	1.405(11)
C(24)-C(29)	1.288(13)
C(24)-C(23)	1.574(11)
C(28)-C(29)	1.309(14)

N(1)#1-Sn(1)-N(1)	180.000(1)
N(1)#1-Sn(1)-N(2)	90.10(15)
N(1)-Sn(1)-N(2)	89.90(15)
N(1)#1-Sn(1)-N(2)	1 89.90(15)
N(1)-Sn(1)-N(2)	1 90.10(15)
N(2)-Sn(1)-N(2)	1 180.0
N(1)#1-Sn(1)-O(1)	1 89.45(16)
N(1)-Sn(1)-O(1)	1 90.55(16)
N(2)-Sn(1)-O(1)	1 87.62(16)
N(2)#1-Sn(1)-O(1)	1 92.38(16)
N(1)#1-Sn(1)-O(1)	90.54(16)
N(1)-Sn(1)-O(1)	89.46(16)
N(2)-Sn(1)-O(1)	92.38(16)
N(2)#1-Sn(1)-O(1)	87.62(16)
O(1)#1-Sn(1)-O(1)	179.998(1)
C(23)-O(1)-Sn(1)	132.4(5)
C(9)-N(2)-C(6)	108.9(4)
C(9)-N(2)-Sn(1)	125.4(3)
C(6)-N(2)-Sn(1)	125.4(3)
C(4)-N(1)-C(1)	108.5(4)
C(4)-N(1)-Sn(1)	125.8(3)
C(1)-N(1)-Sn(1)	125.5(3)
N(2)-C(6)-C(5)	126.2(4)
N(2)-C(6)-C(7)	107.3(4)
C(5)-C(6)-C(7)	126.6(4)
C(9)-C(10)-C(1)	126.5(4)
C(9)-C(10)-C(11)	117.7(4)
C(1)#1-C(10)-C(11)	115.6(4)
C(2)-C(3)-C(4)	108.0(4)
C(22)-C(17)-C(18)	118.9(5)
C(22)-C(17)-C(5)	120.9(4)
C(18)-C(17)-C(5)	120.1(4)
C(17)-C(22)-C(21)	120.5(5)
N(2)-C(9)-C(10)	126.5(4)
N(2)-C(9)-C(8)	107.7(4)
C(10)-C(9)-C(8)	125.7(4)
N(1)-C(1)-C(10)	125.9(4)
N(1)-C(1)-C(2)	108.0(4)
C(10)#1-C(1)-C(2)	126.1(4)
C(19)-C(18)-C(17)	120.7(5)
C(6)-C(5)-C(4)	126.5(5)
C(6)-C(5)-C(17)	116.9(4)
C(4)-C(5)-C(17)	116.6(4)
C(7)-C(8)-C(9)	107.9(4)
C(12)-C(11)-C(16)	119.5(5)
C(12)-C(11)-C(10)	121.4(5)
C(16)-C(11)-C(10)	119.0(5)
C(14)-C(15)-C(16)	119.8(6)
C(20)-C(19)-C(18)	119.8(5)
C(11)-C(12)-C(13)	119.5(6)
C(8)-C(7)-C(6)	108.2(4)
C(21)-C(20)-C(19)	120.2(5)
N(1)-C(4)-C(5)	126.0(4)
N(1)-C(4)-C(3)	108.1(4)
C(5)-C(4)-C(3)	125.9(4)
C(26)-C(25)-C(24)	114.3(7)
C(14)-C(13)-C(12)	120.3(6)
C(3)-C(2)-C(1)	107.3(4)

C(15)-C(14)-C(13)	120.3(5)
C(20)-C(21)-C(22)	119.8(5)
C(28)-C(27)-C(26)	122.6(8)
C(11)-C(16)-C(15)	120.6(5)
C(29)-C(24)-C(25)	123.8(8)
C(29)-C(24)-C(23)	119.8(9)
C(25)-C(24)-C(23)	116.4(8)
C(27)-C(26)-C(25)	115.5(7)
C(29)-C(28)-C(27)	125.2(10)
O(1)-C(23)-O(2)	125.4(8)
O(1)-C(23)-C(24)	117.6(7)
O(2)-C(23)-C(24)	117.1(9)
C(28)-C(29)-C(24)	118.6(10)

Symmetry transformations used to generate equivalent atoms:

#1 -x,-y,-z+2

Table 4. Anisotropic displacement parameters ($Å^2 x 10^3$) for ILT1P-1. The anisotropic displacement factor exponent takes the form: $-2\pi^2[h^2 a^{*2} U^{11} + ... + 2 h k a^* b^* U^{12}]$

	U^{11}	U^{22}	U^{33}	U^{23}	U^{13}	U^{12}
Sn(1)	30(1)	19(1)	30(1)	-14(1)	-18(1)	5(1)
O(1)	43(2)	47(2)	46(2)	-31(2)	-18(2)	-2(2)
N(2)	31(2)	20(2)	31(2)	-14(2)	-18(2)	7(2)
N(1)	31(2)	22(2)	33(2)	-14(2)	-18(2)	6(2)
C(6)	32(2)	24(2)	29(2)	-15(2)	-15(2)	4(2)
C(10)	30(2)	24(2)	32(2)	-13(2)	-16(2)	4(2)
C(3)	38(3)	26(2)	40(3)	-18(2)	-22(2)	3(2)
C(17)	31(2)	26(2)	33(2)	-16(2)	-18(2)	5(2)
C(22)	42(3)	31(3)	32(3)	-16(2)	-15(2)	-1(2)
C(9)	31(2)	24(2)	30(2)	-14(2)	-17(2)	7(2)
C(1)	32(3)	24(2)	32(2)	-14(2)	-19(2)	5(2)
C(18)	43(3)	26(2)	36(3)	-13(2)	-19(2)	-1(2)
C(5)	33(3)	22(2)	28(2)	-11(2)	-12(2)	0(2)
C(8)	35(3)	25(2)	33(2)	-18(2)	-17(2)	9(2)
C(11)	30(2)	30(2)	35(3)	-21(2)	-18(2)	9(2)
C(15)	57(4)	38(3)	44(3)	-21(2)	-30(3)	19(3)
C(19)	47(3)	39(3)	32(3)	-20(2)	-17(2)	2(2)
C(12)	36(3)	37(3)	55(3)	-23(3)	-19(3)	0(2)
C(7)	38(3)	26(2)	34(3)	-18(2)	-21(2)	8(2)
C(20)	40(3)	37(3)	44(3)	-30(2)	-25(2)	10(2)
C(4)	35(3)	21(2)	32(2)	-13(2)	-18(2)	2(2)
O(2)	78(4)	68(3)	82(4)	-27(3)	-40(3)	12(3)
C(25)	53(5)	58(5)	213(12)	-79(7)	-74(6)	16(4)
C(13)	30(3)	61(4)	84(5)	-49(4)	-28(3)	10(3)
C(2)	34(3)	28(2)	37(3)	-16(2)	-21(2)	4(2)
C(14)	49(4)	48(3)	64(4)	-39(3)	-41(3)	27(3)
C(21)	45(3)	27(2)	49(3)	-19(2)	-21(3)	-1(2)
C(27)	52(4)	62(4)	53(4)	-16(3)	-5(3)	-5(3)
C(16)	36(3)	34(3)	38(3)	-20(2)	-16(2)	6(2)

C(24)	76(5)	54(4)	49(4)	-25(3)	-6(4)	-25(4)
C(26)	66(5)	75(5)	56(4)	-28(4)	-25(4)	-6(4)
C(28)	99(7)	87(6)	69(6)	-25(5)	-43(5)	-7(5)
C(23)	48(4)	47(4)	109(7)	-48(5)	-13(4)	-3(3)
C(29)	91(7)	84(7)	96(7)	-32(6)	-50(6)	7(5)